Anion-π Meets H-Bonding: Tuning Synergy Through the Flexibility to-Preorganization Transition in Anion Receptor Design

Olfa Zayene, Jun Hu, Anne Gaucher, Romain Plais, Manuel Barday, Xavier Moreau, Jean-yves Salpin, Damien Prim

Anion-π Meets H-Bonding: Tuning Synergy Through the Flexibility-to-Preorganization Transition in Anion Receptor Design

Olfa Zayene[a], Jun Hu[a,b], Anne Gaucher[a], Romain Plais[a], Manuel Barday[a], Xavier Moreau[a], Jean-Yves Salpin[b*], Damien Prim[a*]

[a] *Université Paris-Saclay, UVSQ, CNRS, Institut Lavoisier de Versailles, 78035 Versailles cedex, France*

[b] *Université Paris-Saclay, Univ Evry, CY Cergy Paris Université, CNRS, LAMBE, 91025, Evry-Courcouronnes, France*

Dedicated to Professor François Terrier, a pioneer in physical organic chemistry whose work and legacy continue to inspire.

Graphical Abstract

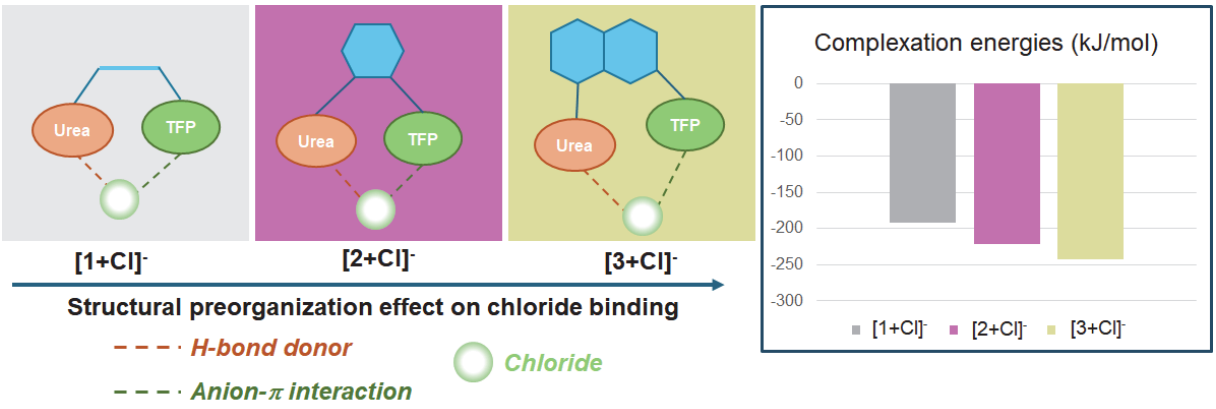

Three anion receptors combining both hydrogen bonding and anion-π interactions were synthetized, involving different spacers in order to evaluate the influence of molecular preorganization and rigidity on chloride binding. The naphthalene spacer in receptor **3** leads to more effective anion binding compared to flexible or less structured systems.

Abstract:

This study focuses on a series of receptors incorporating urea and pentafluoropyridine motifs to investigate the synergistic combination of hydrogen bonding and anion-π interactions for anion recognition. We synthesized three receptors with various spacers to evaluate the influence of molecular preorganization and rigidity on anion binding. Flexible receptor **1** and rigid receptors **2** and **3** were synthesised following a two-step protocol, involving the construction of the urea fragment from isocyanate precursors and a nucleophilic aromatic substitution to install the tetrafluoropyridine motif as key steps. Computational analyses (DFT, NCI plots), NMR spectroscopy, and mass spectrometry were employed to assess structural features and binding performance. DFT calculations revealed that all receptors allow complexation with chloride through dual urea and π-anion sites. Structural rigidity in receptor **3** showed enhanced binding efficacy due to steric strain and additional C–H···Cl^- interaction from its naphthalene core. NMR titrations provided qualitative insights into binding events, with receptor **3** exhibiting the largest shieldings for all H-bonds, in line with theoretical predictions. Mass spectrometry and collision-induced dissociation (CID) experiments confirmed receptor–anion complexation, with fragmentation patterns supporting the relative binding strengths. The overall ranking is **3**>**2**>**1**, corroborating computational and experimental data.

Introduction:

Anions are ubiquitous and play a crucial role in various fields,[1,2] including medicine, environmental science, and catalysis.[3] As a result, anion recognition has become a fundamental area of supramolecular chemistry. In this context, several types of non-covalent interactions contribute to anion binding, such as hydrogen bonding (H-bonding),[4–6] van der Waals (VDW) forces, sigma-hole interactions,[7] and anion-π interactions.[8] Combining multiple interactions within a single receptor design remains challenging, as it requires an understanding of possible synergies and how they might impact anion binding. [9]

The potential synergy between hydrogen bonding and anion–π interactions has been highlighted in both experimental and theoretical studies. Matile and co-workers have demonstrated that π-acidic naphthalenediimide (NDI) systems bearing hydrogen bond donor arms can activate anionic substrates and stabilize transition states in catalytic contexts, revealing the powerful cooperative effects at play in anion–π catalysis.[10–13] Complementary computational investigations by Alkorta et al. further emphasized the stabilizing role of such dual interactions, showing enhanced binding and charge-transfer when anions and H-bond donors act simultaneously on π-acidic surfaces.[14,15]

In this context, our study seeks to systematically examine this cooperative behavior within a series of structurally controlled receptors, enabling direct comparison between flexible and preorganized systems in order to deepen the understanding of how spatial arrangement and rigidity influence the interplay of hydrogen bonding and anion–π recognition. We disclose in this paper, the exploration of the combination of hydrogen bonding—one of the most common non-covalent interactions—with anion-π interactions, which are comparatively less studied in anion recognition. For hydrogen bonding, we chose the urea functional group because of its well-established anion-binding properties. For anion-π interactions, we have incorporated the pentafluoropyridine motif, which is known in the literature as anion-π interaction donor.[9] However, the presence and effectiveness of the latter interaction within a designed receptor family remains uncertain or at least to clarify.[16]

To investigate the synergy between these two interactions, we systematically varied the spacer unit connecting the urea and pentafluoropyridine moieties (Figure 1). The spacer plays a critical role in determining the flexibility / or pre-organisation of the receptor, which in turn affects the efficiency of anion recognition. To this end, we designed two types of spacer:

1. A flexible linear carbon chain (receptor **1**), which allows conformational adaptability in the presence of the anion.
2. Rigid aromatic spacers, including a phenyl (receptor **2**) or a naphthalene moiety (receptor **3**), which impose a pre-organised structure, creating a defined binding cavity where the relative positions of the urea and pyridine groups are fixed. The size of the cavity differs between the phenyl- and naphthalene-based receptors, affecting the spatial arrangement of the interacting sites.

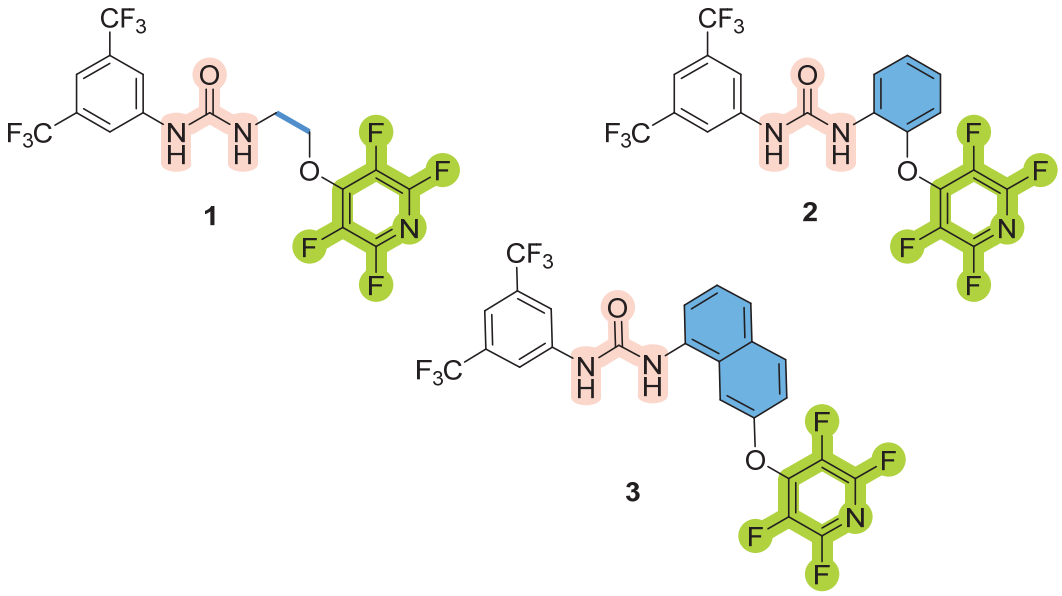

Figure 1. Target receptors **1-3**

Within this series, to assess the impact of receptor design on the synergistic effect of hydrogen bonding and anion-π interactions, we will study their complexation with chloride anions using a combination of theoretical (DFT calculations), solution (NMR spectroscopy), and gas-phase (mass spectrometry) techniques. This systematic approach will provide insights into how structural pre-organisation and interaction synergy influence anion recognition, contributing to the rational design of more efficient anion receptors.

Computational study: Geometries optimisation and binding analysis

The geometries of the three receptors were optimised using the APFD/Aug-cc-pVDZ level with the Gaussian 16 set of programs.[17] For receptor **1**, two initial conformations were considered (Figure 2). In the first conformation (**1a**), the spacer is extended, keeping the urea and pentafluoropyridine (TFP) fragments far apart, to minimise steric hindrance. In the second conformation (**1b**), the spacer is folded, bringing the urea and TFP fragments closer together, which led to stabilisation through weak intramolecular interactions. As a matter of fact, a comparison of the total energies of these two conformers, both of which converged to a local minimum with no imaginary frequencies, showed that **1b** is more stable than **1a** by 35.5 kJ/mol in relative energies (See Table S3 of the supporting Information), thereby suggesting that the receptor may naturally adopt a pre-organised structure, in which the urea and TFP fragments are already positioned to interact with the anion without requiring additional energetic cost for folding. The calculation of the NCIPlots using Multiwfn software[18] on **1a** and **1b** was consistent with the energies of the receptor, as **1b** has more intramolecular stabilising interactions (Figure 2, interactions plotted in green) than **1a.**

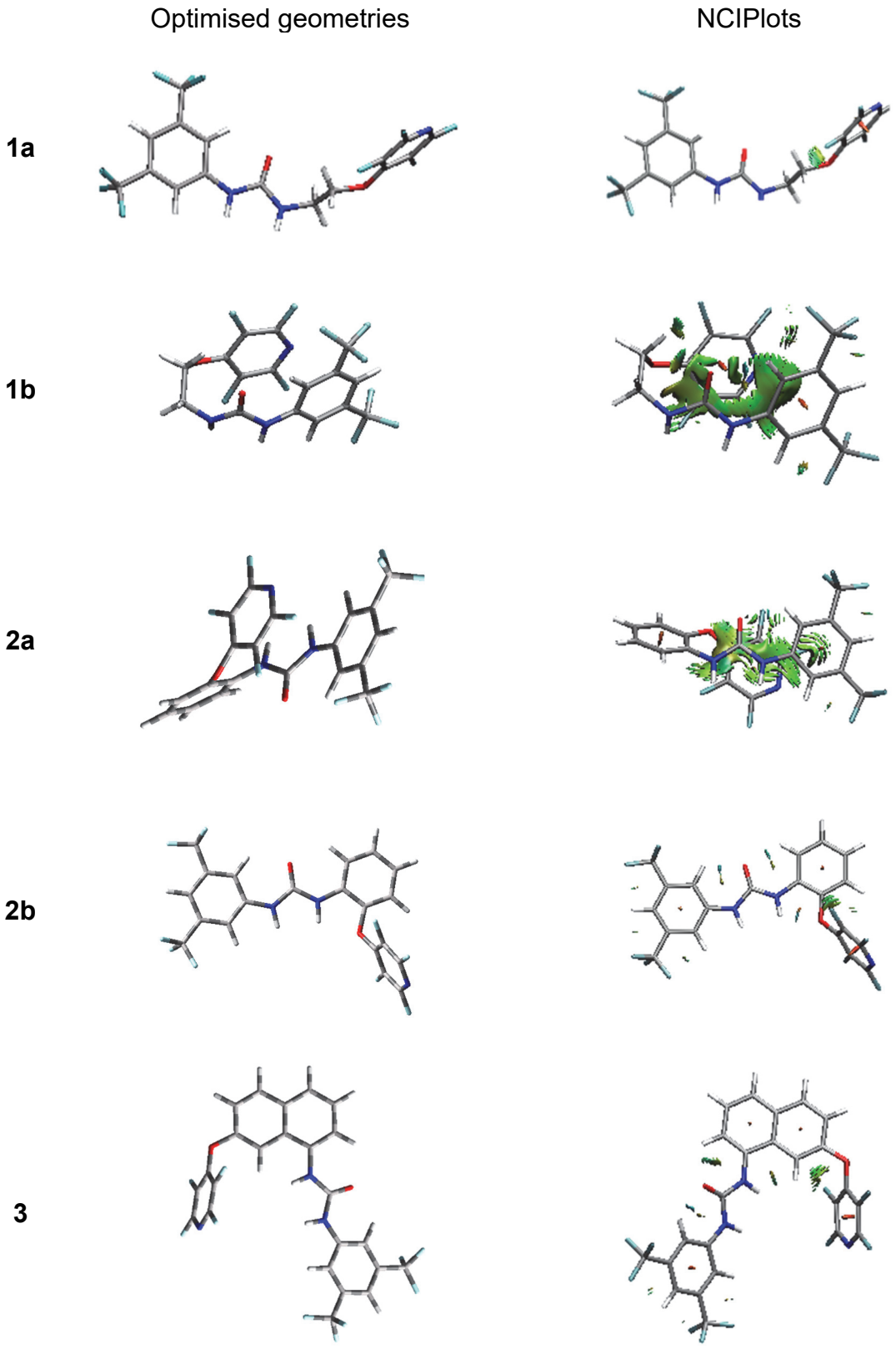

Figure 2. Computed topology of the various receptors **1** and associated NCI plots. NCI analyses were performed using Multiwfn 3.7. RDG isosurfaces were generated with an isovalue of 0.4 a.u., using the medium quality grid. The scalar field $\text{sign}(\lambda_2)\rho$ was used to color the isosurface, with a default color range of −0.05 to +0.05 a.u., corresponding respectively to attractive (blue), van der Waals (green), and repulsive (red) interactions. Density and gradient cutoffs were set to their default values in Multiwfn, namely $\rho < 0.05$ a.u. and $|\text{sign}(\lambda_2)\rho| < 0.05$ a.u.

Consequently, we focused on a pre-organised topology of the bonding cavity for receptors **2** and **3**. Indeed, the presence of a phenyl and a naphthyl rigid spacers creates defined binding cavities. For example, the initial geometry of **3** was selected so that the urea protons face the cavity and the TFP fragment, maximizing potential interactions. The choice of this 3D topology is supported by 2D NMR results (see NMR section, *vide infra*). After optimisation, both receptors reached a local minimum with no imaginary frequencies. In the particular case of receptor **2**, two forms, **2a** and **2b** of close stability are found exhibiting a slightly different folding (Table 1). **2a** turns to be slightly more stable due to a stabilising interaction between the urea motif and pentafluoropyridine ring. Remarkably, these two conformations are almost degenerate when considering relative free energies. As a consequence, both conformations will be considered for the chloride bonding study.

Upon addition of the chloride anion (Cl^-) to the optimised geometries, three anion-receptor complexes were obtained (Table 1). In all three cases, qualitative analysis using NCI plots, calculated with Multiwfn software, [18] confirmed that the anion interacted simultaneously with both the urea and TFP fragments. The blue-coloured interaction plot in the NCI analysis indicates a strong favourable interaction between the anion and the urea protons, confirming the presence of hydrogen bonding. A green-coloured interaction plot, indicating a weaker but favourable interaction, was observed between the anion and the TFP fragment, providing evidence for anion-π interactions (Figure 3). Interestingly, the nature of the anion-π interaction differed between complexes. In [**1**+Cl]$^-$and [**2a**+Cl]$^-$ it induces a η^2 interaction, whereas a η^3 and η^6 interaction is observed in complexes [**2b**+Cl]$^-$ and [**3**+Cl]$^-$, respectively. Moreover, in the case of [**3**+Cl]$^-$, a third type of non-covalent interaction is evidenced, corresponding to a C-H···Cl^- interaction between the anion and one hydrogen of the naphthalene moiety located inside the binding cavity.

To assess the complexation quantitatively, the interaction energies of the three anion-receptor complexes were calculated, yielding values ranging from -192.4 kJ/mol for [**1**+Cl]$^-$ to -243.1 kJ/mol for [**3**+Cl]$^-$ (Table S1). Thus receptor **3** presents the highest affinity for chloride and **1** the lowest. [**2a**+Cl]$^-$ and [**2b**+Cl]$^-$ exhibit intermediate values (Table S1) allowing an overall ranking **1**<**2**<**3**. Taking into account that [**2a**+Cl]$^-$ exhibits a significative lower interaction energy than [**2b**+Cl]$^-$, only the latter will be further considered. The associated BSSE (Basis Set Superposition Error) have been estimated, and are rather low (2.7-3.1 kJ/mol, see Table S1). This finding is consistent with BSSE estimated for complexes involving trifluoroterephthalonitrile-containing receptors.[19] Finally, note that for the sake of comparison, we have also carried out the computational study at the B3LYP/6-311++G(d,p) level, by including the D3 version of Grimme's dispersion with Becke-Johnson damping (GD3-BJ).[20] Results are gathered in the section 4.6 of the supplementary materials. We could deduce from this comparison that the optimized geometries of both neutral and complexes are close, and that the computed interaction energies are very similar. Consequently, the fact that

B3LYP also performed well is an important point with a view to studying systems of increasing size, because APFD calculations are slightly longer than those involving B3LYP.

Modification of interatomic distances before and after anion binding are indicative of the effective complexation with chloride. In addition, the interstitial distances between the anion and fragments capable of generating weak interactions are also worth investigating in order to establish the receptor-host relationship. To this end, selected calculated binding distances are summarized in Table 1 and deserve comments. Table 1 is organised according to the nature of the spacer and the weak interactions involved in the binding of the chloride anion.

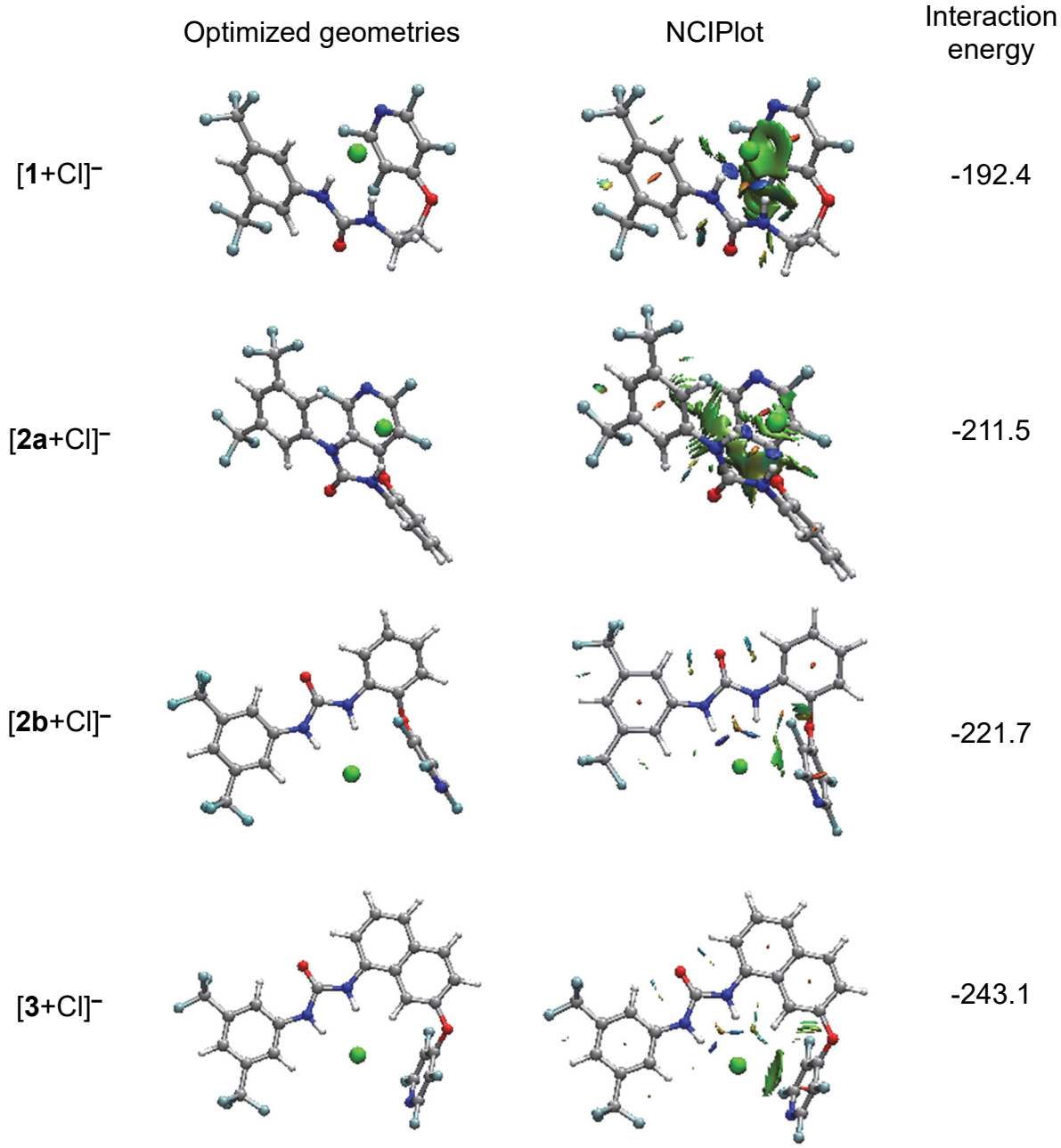

Figure 3: computed forms of the various [**receptor**+Cl]⁻ complexes and associated NCI plots.

The urea fragment and the H bond interactions were first examined (Table 1, entries 1-4). For a hydrogen bond to be considered significant, the sum of the van der Waals radii [21] of the anion and the interacting atom (2.95 Å) should be greater than the H···Cl$^-$ distance.[22] This condition was fulfilled in all observed N–H···Cl$^-$ interactions, confirming the presence of hydrogen bonding as evidenced in NCI plots.

From the receptor to the corresponding complex, the N_a-H_a and N_b-H_b distances increase. Notably, all N_a-H_a distances vary in a similar manner (1.011 to 1.044, 1.010 to 1.046, and 1.009 to 1.042), indicating an almost identical contribution to chloride complexation. The N_b-H_b distances also increase in all complexes, but to a lesser extent. It clearly highlights the influence of the 3D topology imposed by the rigid phenyl and naphthyl spacers in compounds **2b** and **3**. A more detailed study about the effect of the different functional groups onto the N-H bond lengthening is provided in section 4.3 of the supporting information.

The H_a···Cl$^-$ distances decrease from receptor **1** to receptors **2b** and **3**, suggesting a strengthening of the hydrogen bonding interaction from **1** to **2b** and **3** as suggested by computed H-bonding energies (Table 2, *vide infra*). Moreover, all H_b···Cl$^-$ distances are significantly longer than their H_a analogs, likely indicating a greater contribution of H_a to Cl$^-$ complexation. This evolution of bond distances thus seems to indicate a positive influence of the presence of rigid spacers in **2b** and **3** on the efficiency of hydrogen bonding in anion complexation.

Table 1. Comparison of selected bond distances in receptors **1**-**3** and their associated chloride complexes, computed at the APFD/aug-ccpvdz level.

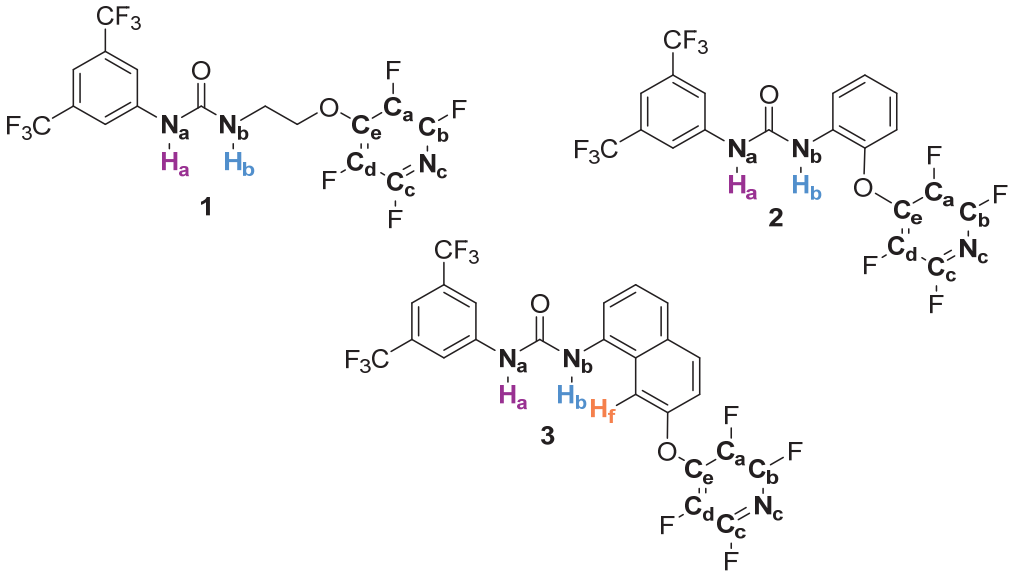

	Fragment contribution							
Entry	Urea	H-bond[a]	**1**	[**1**+Cl]$^-$	**2b**	[**2b**+Cl]$^-$	**3**	[**3**+Cl]$^-$
1		N_a-H_a	1.011	1.044	1.010	1.046	1.009	1.042
2		N_b-H_b	1.011	1.034	1.010	1.036	1.009	1.028
3		H_a···Cl	--	2.045	--	2.015	--	2.030
4		H_b···Cl	--	2.136	--	2.165	--	2.220
	Ar C-H	H-bond						
5		C-H_f	--	--	--	--	1.088	1.095
6		H_f···Cl	--	--	--	--	--	2.417
7	anion-π	Cl···centroïd	--	3.409	--	3.631	--	3.291
8		C_a···Cl	--	3.956	--	3.537	--	3.565
9		C_b···Cl	--	3.825	--	4.109	--	3.518
10		N_c···Cl	--	3.602	--	4.429	--	3.559
11		C_c···Cl	--	3.377	--	4.180	--	3.548
12		C_d···Cl	--	3.465	--	3.631	--	3.581
13		C_e···Cl	--	3.778	--	3.258	--	3.548

[a] distances in Å

From the topological analysis, we may estimate the binding energy of each hydrogen bond (HB), by using the electron density at their associated bond critical point.[23] Assuming a charged hydrogen bond towards Cl^-, the different HB binding energies are summarized in Table 2.

Table 2. HB binding energies (BE) in kJ/mol

Complex	(N_a-H_a···Cl^-)	(N_b-H_b···Cl^-)	(H_f···Cl^-)
[**1**+Cl]$^-$	-57.2	-47.9	–
[**2b**+Cl]$^-$	-60.8	-45.5	–
[**3**+Cl]$^-$	-58.4	-41.4	-30.2

One may observe that there is a very good correlation between the computed BE and the H_x···Cl distances (Figure S26). HB distances can therefore be used confidently to discuss HB strength for the various complexes. These estimates notably confirm the strengthening of the N_a-H_a···Cl HB on going from receptor **1** to receptor **3**. One can also notice that the hydrogen bonds involving H_a are systematically stronger than those involving H_b, resulting in the more pronounced lengthening of the N_a-H_a bond. This is in agreement with the stronger variation of the chemical shift of H_a upon addition of chloride during NMR experiments (*vide infra*).

The contribution of the $C_{aromatic}$-H fragment to the complexation event through hydrogen bonding was also investigated. For [**3**+Cl]$^-$, the presence of C-H···Cl^- bonding was confirmed by the lenghtening of the C-H_f distance upon anion interaction. In addition, the C-H_f···Cl^- distance being 2.417 Å, is shorter than 2.95 Å, further confirming the presence of a hydrogen bond. The computed BEs (Table 2) show that this HB remains weaker than those involving the urea motif but partly explains the weakening of the N_b-H_b···Cl HB within the [**3**+Cl]$^-$ complex. These observations support a clear positive contribution from the rigid naphthalene platform.

For anion-π interactions, the distance between the anion and the centroid of the aromatic ring should be ≤ 4 Å, same as each atom of the aromatic ring and the anion for a η^6 anion-π interaction.[24] These conditions were met for **1** and **3** (Table 1). For **2b**, only C_c···Cl, C_e···Cl and C_d···Cl were shorter than 4 Å indicating a weaker interaction with η^3 type.

Firstly, the centroid···Cl^- distance appears significantly shorter in [**3**+Cl]$^-$ compared to [**1**+Cl]$^-$ and [**2b**+Cl]$^-$, suggesting a more beneficial effect of increased steric strain in the binding cavity. It is also worth noting that all C···Cl and N···Cl bond distances in [**3**+Cl]$^-$ are approximately 3.5 Å, suggesting an η^6 coordination mode. In contrast, the C_c···Cl and C_d···Cl bond distances are shorter compared to other C···Cl bonds in **1,** indicating an η^2 coordination mode. Similarly, C_c···Cl, C_d···Cl and C_e···Cl distances are sensibly shorter in **2b** indicating an η^3 coordination mode. Overall, the bond distances are more homogeneous in **1** than in **2b**. This difference may also indicate a better adaptability of the flexible arm.

Overall, the theoretical analysis of the weak interactions involved in chloride binding highlights the significant role of hydrogen bonding and anion-π interactions in complex stabilization. Compared to receptor **1**, the presence of rigid spacers in **2** and **3** impacts the overall topology of the corresponding complexes and results in a slight enhancement of the efficiency of hydrogen bonding Ha···Cl^-. However, a decrease of the H_b···Cl^- is counterbalanced in **3** by a stronger anion-π interaction. In addition, the naphthalene platform in [**3**+Cl]$^-$ contributes positively through C-H···Cl^- interactions, further enhancing the binding capacity. Noteworthy, in [**1**+Cl]$^-$, the anion-π interaction occurs through a nearly η^2 coordination mode. In contrast, [**2b**+Cl]$^-$ displays a η^3 coordination mode while [**3**+Cl]- exhibits η^6 coordination mode. These observations highlight the interplay between structural rigidity, steric effects, and three weak interactions in optimizing chloride anion binding efficiency, making **3** the best candidate.

For gaining quick information, we have attempted to compare the above analysis with a more qualitative overview. The qualitative analysis of weak interactions can be carried out using the bond distances from Table 1 and computed H bond binding energies in Table 2. For each interaction, several contributing fragments can be considered. Each of these fragments can be assigned three levels of contribution depending on the increasing importance of their contribution to chloride ion complexation phenomenon (Table 3): - (no contribution – pink), + (weak contribution – orange), ++ moderate contribution (yellow) or +++ (enhanced contribution – green).

Table 3. Qualitative ranking of receptor abilities

Weak interaction	Fragment	[**1**+Cl]$^-$	[**2b**+Cl]$^-$	[**3**+Cl]$^-$
Urea H Bond	N_a-H_a	+++	+++	+++
	N_b-H_b	++	++	+
	H_a···Cl	+++	+++	+++
	H_b···Cl	++	++	+
C_{ar}-H-Cl	C-H_f	-	-	+
	H_f···Cl	-	-	+
π-Cl	Centroid···Cl	++	-	++
Overall ranking		**1 < 2b < 3**		

Thus, the N_a-H_a distance remains very similar regardless of the complex ([**1**+Cl]$^-$, [**2b**+Cl]$^-$, or [**3**+Cl]$^-$), indicating a comparable (strong) contribution of this fragment. On the other hand, the N_b-H_b bond is shorter for the [**3**+Cl]$^-$ complex than for its analogs **1** and **2b**, indicating a weaker contribution in **3**.

The length of the $H_a\cdots Cl$ or $H_b\cdots Cl$ bond also indicates the contribution of the urea fragment to the complexation phenomenon. In this context, the $H_b\cdots Cl$ bond is longer for [**3**+Cl]$^-$, whereas $H_a\cdots Cl$ bonds are significantly shorter (below 2.1 Å) for all the complexes, especially for [**2b**+Cl]$^-$ and [**3**+Cl]$^-$.

Thus, it appears that the rigid phenyl and naphthyl motifs have a pronounced effect on the parameters derived from the urea fragment. The C-H_f and $H_f\cdots Cl$ bonds are specific to the rigid naphthalene motif. They are only present in [**3**+Cl]$^-$ and therefore contribute exclusively to this complex.

The tetrafluoropyridine motif, which is likely to contribute through the weakest interaction, is the last fragment analysed. The Cl$\cdots$centroïd distances are significantly shorter for [**1**+Cl]$^-$ (3.409 Å) and [**3**+Cl]$^-$ (3.291 Å) compared to [**2**+Cl]$^-$ (3.631 Å). This could indicate a detrimental effect due to a sterically more constrained binding cavity. Furthermore, the C$\cdots$Cl and N$\cdots$Cl distances are homogeneous in complex [**3**+Cl]$^-$, suggesting a η^6 coordination mode. In contrast, the complexes [**1**+Cl]$^-$ and [**2b**+Cl]$^-$ exhibit differentiated C-Cl bond distances. The $C_c\cdots Cl$ and $C_d\cdots Cl$ distances appear shorter in [**1**+Cl]$^-$, likely confirming an η^2 coordination mode. In [**2b**+Cl]$^-$ the $C_c\cdots Cl$, $C_d\cdots Cl$ and $C_e\cdots Cl$ distances appear shorter, confirming an η^3 coordination mode.

From this qualitative analysis, we confirmed a significant contribution of the rigid and templating naphthalene fragment to the complexation phenomenon through the addition of H$\cdots$Cl , C_{ar}-H-Cl, and π-Cl bonds. This ranking **3** > **2** > **1** is in agreement with the calculated interaction energies.

The combination of hydrogen bonding and anion-π interactions is highly dependent on the structural nature of the spacer unit. Our study suggests that pre-organization by rigid spacers enhances anion binding by reinforcing both interactions, with larger cavities further enhancing this effect. These findings provide valuable guidance for the rational design of more efficient anion receptors.

We next concentrated our efforts in the preparation of receptors **1**, **2** and **3**, and in the analysis of complexation to chloride by mean of NMR and mass spectrometry.

Synthesis

The synthesis of the receptors follows a straightforward and mild two-step procedure (scheme 1). For **1** and **3**, a nucleophilic addition reaction is carried out at room temperature to form the urea intermediate. This is followed by a nucleophilic aromatic substitution (SN_{Ar}) to introduce the pyridine moiety.[25] Receptors **1** and **3** were obtained with respective yields of 89% and 35%. For **2**, the synthetic sequence required further optimisation and was inverted. The SN_{Ar} occurred first followed by the nucleophilic addition, leading to **2** in a yield of 75%.

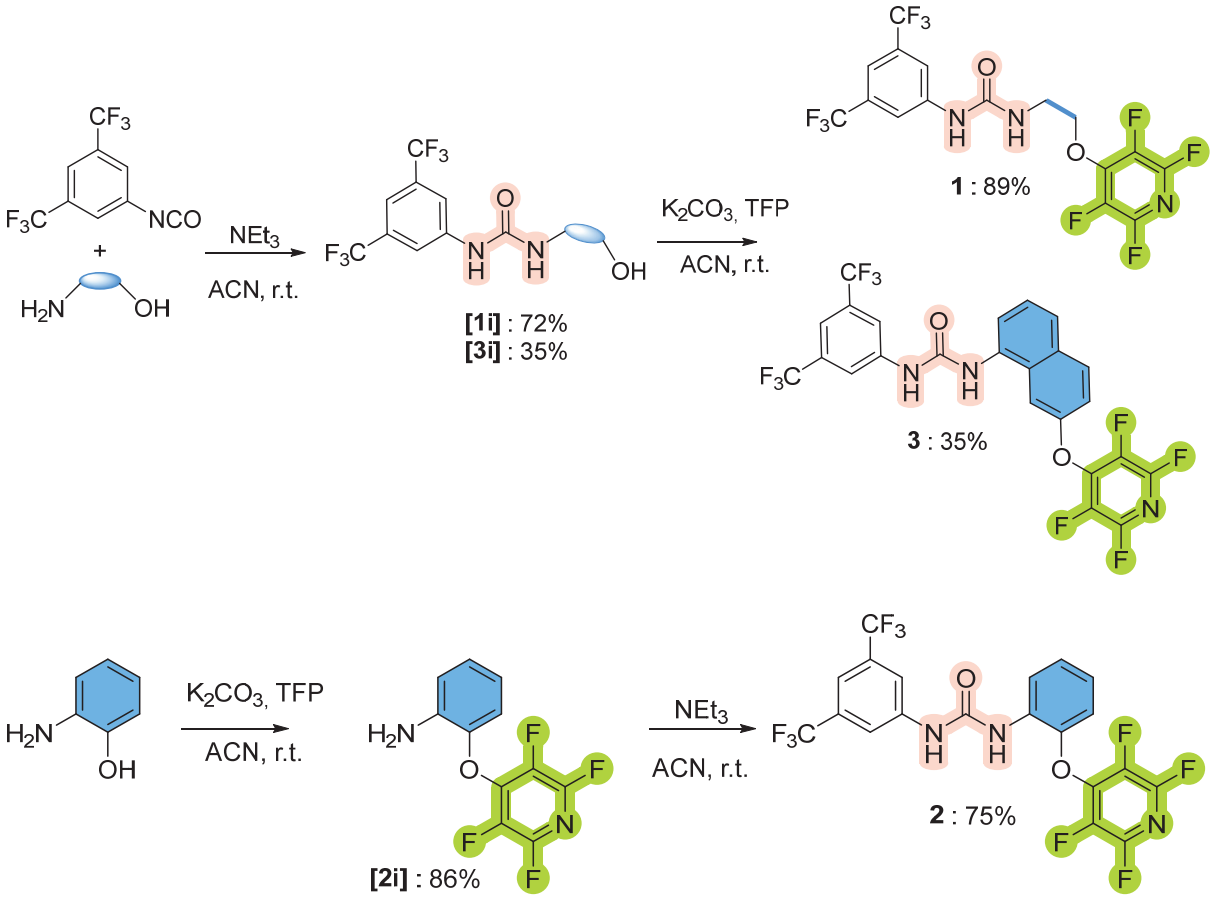

Scheme 1. Synthesis routes of **1**, **2** and **3**

For receptor **3**, a 2D NMR study confirmed the structure optimized by DFT calculations. The NOESY spectrum revealed interactions between H_a and H_b, indicating that both urea protons are in the same plane (Figure 4). In addition, the interaction between H_b and H_f suggests that the urea moiety is located within the pre-organised cavity. Furthermore, the HOESY spectrum is in complete agreement with the presence of the pyridine moiety in a plane parallel to the urea through a correlation between F_a and H_f.

^{1}H NMR qualitative insights

Unfortunately, the comparison of the association constant obtained from a ^{1}H NMR titration, between **1**-Cl (755 L/mol) and **2**- or **3**-Cl, could not be carried out. Attempts to obtain quantitative results from a formal titration of receptors **2** and **3** failed partly because of partial and rapid degradation of receptor **2** in solution (CD_3CN or CD_3COCD_3), or strong overlap of the characteristic urea and naphthalene proton signals in the naphthalene analogue **3**.

In this context, a qualitative NMR approach is presented in this paper. It will be followed by a full mass spectrometry analysis.

^{1}H NMR allows us to gain information by analysing which protons are affected by the addition of the anion. Observing the chemical shift shielding from the receptor to the corresponding complexes is a simple experimental way of qualitatively assessing the strength of H bonds, as illustrated by Figure 4.

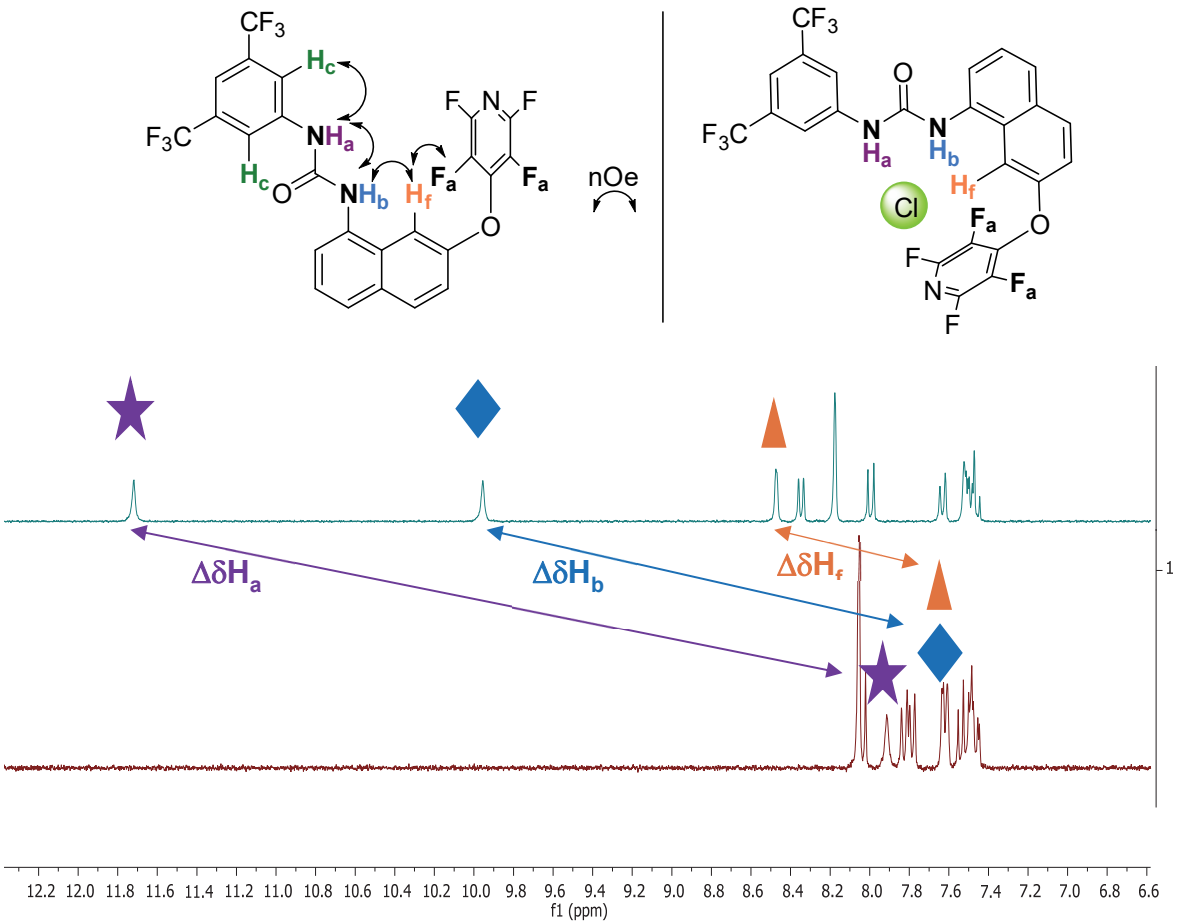

Figure 4. Overlap of ^{1}H NMR spectra (CD_3CN) of **3** (red) and **3**+25 eq of Cl^- (green)

For all three receptors, 25 equivalents of TBACl were added, and the Δδ values of H_a, H_b, and H_f were calculated. The urea protons are strongly impacted by the anion addition; in each case, the H_a proton is sensibly more affected than H_b (Table 4). Receptor **3** exhibits the largest $\Delta\delta H_a$ and $\Delta\delta H_b$ values, indicating stronger interactions compared to receptors **2** and **1**. Furthermore, the presence of an $H_f\cdots Cl^-$ interaction is also detected with a ΔδHf of 0.84 ppm, confirming an additional weak interaction in [**3**+Cl]$^-$. This qualitative analysis allows the establishment of the **3** > **2** > **1** capability ranking, which is in good agreement with both the above qualitative data and DFT results.

Table 4. Qualitative ranking of receptor abilities by ^{1}H NMR

Proton	Δδ (ppm)		
	1-Cl	**2**-Cl	**3**-Cl
H_a	3.38	3.75	3.80
	++	++	++
H_b	1.80	2.07	2.46
	+	+	++
H_f			0.84
	-	-	+
Overall	+	+	++
Ka[a]	744	nd	nd

[a] : unit in L/mol

From this NMR qualitative analysis, it turns out that receptor **3** should be the most effective. This finding is in good agreement with ranking **3**>**2**>**1** determined from the calculated interaction energies and DFT calculations.

The next step will be to compare the receptor binding abilities using mass spectrometry. This will provide further insights into their binding properties.

Mass spectrometry

Our previous studies have shown that chloride/receptors complexes described as stable species in the gas phase according to computational studies, can be easily observed experimentally when using electrospray ionization.[19,26–29] This is again the case with the present receptors. Employing electrospray ionization on equimolar solution (10^{-5}M) of **receptor**/NBu_4Cl prepared in a 90/10 ACN/water mixture, results in the formation of abundant peaks that may be ascribed to $[(\textbf{receptor})_n+Cl]^-$ ions (n=1,2), as illustrated by the Figure S21, obtained for the **1**/NBu_4Cl mixtures. Note however that in the particular case of receptor **2**, these complexes could be observed only when solutions were prepared just before the mass spectrometry experiments. It turned out that this compound rapidly degrades as soon as it is solubilized, leading to a weak complex that is impossible to study over the long term and thus to compare with **1** and **3** analogs. In spite of this peculiar behaviour, we were able to record the collision induced dissociation (CID) spectrum of the 1:1 complex for the three receptors, in order to get some insights about their structure. These spectra are gathered in Figure 5.

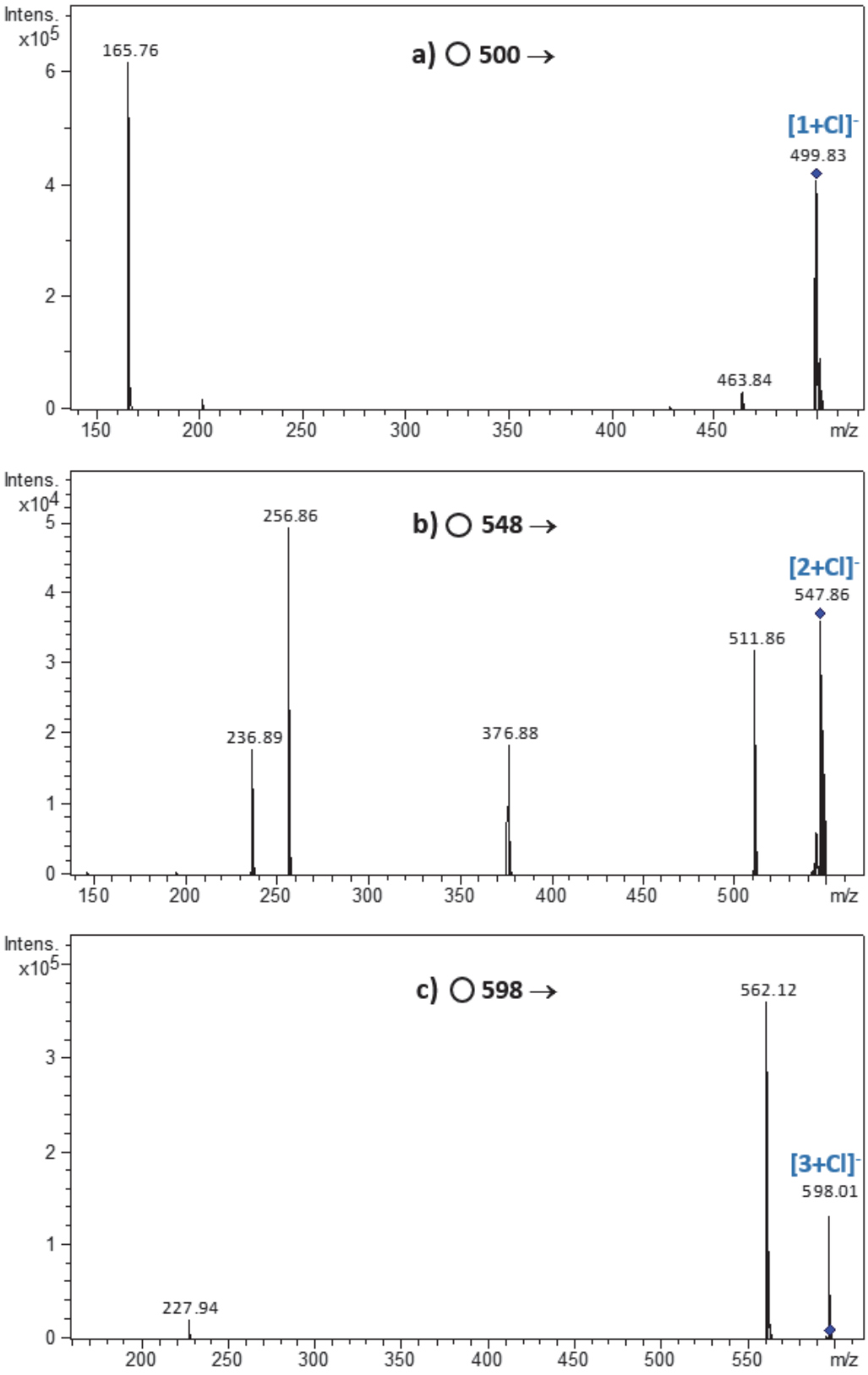

Figure 5: MS/MS spectrum of **a)** [**1** + Cl]$^-$, **b)** [**2** + Cl]$^-$ and **c)** [**3** + Cl]$^-$ recorded on a 3D quadrupole ion trap.

First, these CID spectra are characterized by 2 distinct processes: i) deprotonation of the receptor by loss of hydrogen chloride (-36u), and ii) fragment ions arising from the cleavage of covalent bonds within the receptor. As these spectra were recorded with a

3D quadrupole ion trap (Bruker Amazon Speed ETD), the low mass range by default is limited by a low mass cutoff of 27% of the precursor ion. In addition, modifying the cutoff to try to observe the *m/z* 35/37 ion resulted in the complete loss of signal. Consequently, this instrument is unable to detect the possible formation of Cl^- by elimination of the intact receptor. Therefore, we also recorded these spectra with a Q-TOF instrument which does not suffer from this limitation, and we did not observe any Cl^- ion, thereby suggesting a rather strong interaction between the anion and the receptor. Starting with [**1**+Cl]$^-$, two main product ions are observed (Figure 5a). One can see that elimination of HCl leading to deprotonated receptor [**1**-H]$^-$ is a minor process. But this process is indicative of a strong interaction of chloride with the urea motif, as formation of the [**receptor**-H]$^-$ ions probably implies removal of one of the urea proton. Implicitly, removal of the Ha proton should be more favorable as the resulting anion would be stabilized by a mesomeric effect involving the bis-CF_3 phenyl ring. This is confirmed by DFT calculations which indicate that the Ha deprotonated receptor is more ~22 kJ/mol more stable than the Hb deprotonated form (Figure S26). The dominant fragmentation process gives rise to a *m/z* 166 which certainly imply the fluorinated pyridine moiety. This ion may be obtained by a S*N*$_2$-like mechanism involving the attack of Cl^- onto the C(H_2)-O carbon and departure of the $[OC_5F_4N]^-$ ion (*m/z* 166, Figure S22). Alternatively, one may envisage deprotonation of H_a as a first step, followed by an intramolecular attack of the pyridine by an S*N*$_{Ar}$ process, and ultimately formation of *m/z* 166. This assumption is supported experimentally by the MS3 spectrum of [**1**-H]$^-$ (Figure 6a). The fact that this product ion is totally shifted by 16 mass units (*m/z* 182) when the carbonyl group (C=O) of receptor **1** is replaced by a thiocarbonyl group (C=S), also supports this assumption.[30] This process may be favoured by the folding of the receptor around Cl^- through the combination of hydrogen bonds and anion-π interactions, and may suggest the interaction of Cl^- with the pyridine motif. The behaviour upon collision of [**2**+Cl]$^-$ and [**3**+Cl]$^-$ ions is similar, and different from that of [**1**+Cl]$^-$. First, the peak associated with the deprotonation of the receptor is much more intense, and remarkably corresponds to the base peak for [**3**+Cl]$^-$. This may be due to the fact that deprotonation of both nitrogens of urea results in very stable anions strongly stabilized by mesomeric effect, either by the bis-CF_3 phenyl ring (H_a) or the aromatic spacer (H_b). DFT calculations show that with the introduction of an aromatic spacer, removal of the Hb proton becomes slightly favoured (Figure S26) over removal of Ha. We also recorded the CID spectra of both deprotonated receptors (Figure 6b and 6c). One can see that all the product ions observed in Figures 5b and 5c are also present for the deprotonated receptors. In addition, the relative intensities of *m/z* 377, 257, and 237 ions on the MS/MS spectra of [**2**+Cl]$^-$, and [**2**-H]$^-$, are strikingly similar. These data suggest a two-step process for receptors **2** and **3**: deprotonation by loss of HCl followed by dissociation of the deprotonated receptors. Possible mechanisms accounting for the formation of the various fragments are given in supporting information (Figures S23 and S24), and assume that a mixture of deprotonated forms resulting from the removal of both H_a and H_b could be at the origin of the different product ions. Finally, we also recorded a series of MS/MS/MS spectra according to the 512 → 257 → sequence, which confirm that

m/z 237 ions probably arise from *m/z* 257 by loss of hydrogen fluoride (HF). A similar dissociation is observed for *m/z* 562 (Figure 6c), leading to *m/z* 542.

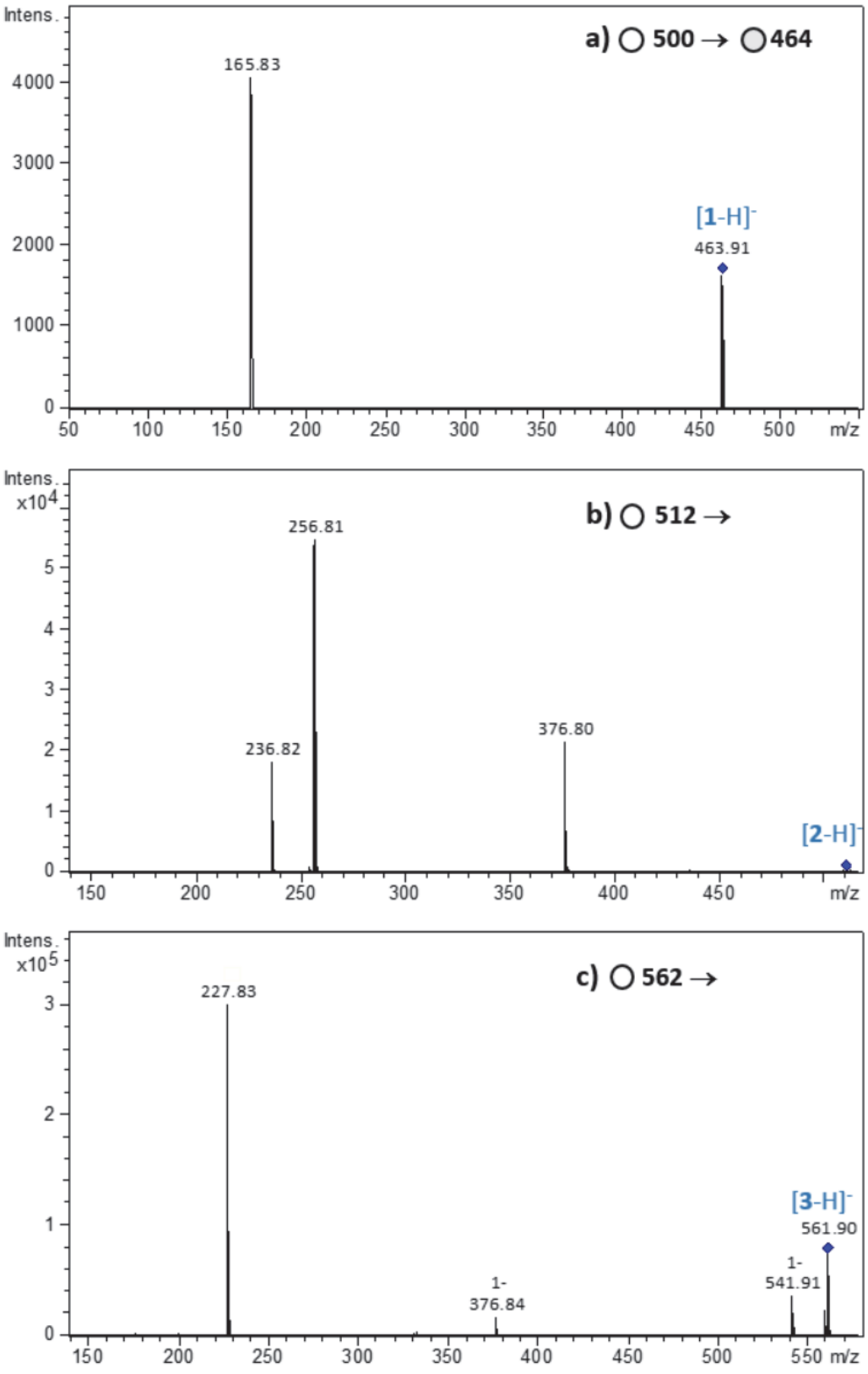

Figure 6. Low-energy **a)** MS3 spectrum of [**1** - H]⁻ (*m/z* 464) and MS2 spectra of **b)** [**2** - H]⁻ (*m/z* 512) and **c)** [**3** - H]⁻ (*m/z* 562) recorded on a 3D quadrupole ion trap. Excitation amplitude: 0.30V, 0.20V and 0.25V, respectively

Like with many receptors, the CID spectrum of [(**receptor**)$_2$+Cl]$^-$ ions (not shown) is characterized by the elimination of one intact molecule of receptor, leading to the 1:1 complex. So, we also tried to determine the relative chloride affinities of the three receptors by means of the kinetic method.[19,31,32]. This method implies the formation of heterodimers of the type [**receptor 1**+**receptor 2**+Cl]$^-$ which is then subject to a CID experiment. If weak interactions are involved within the dimer, these ions should dissociate to generate two monomers [**receptor 1**+Cl]$^-$ and [**receptor 2**+Cl]$^-$, the most intense product ion corresponding to the molecule having the highest affinity for chloride. Due to its instability in solution, it was not possible to generate heterodimers with receptor **2**. On the other hand, the [**1**+**3**+Cl]$^-$ ion could be easily generated by electrospray (*m/z* 1063) by infusing an equimolar 1:1:1 mixture of **1**/**3**/NBu$_4$Cl, and its low-energy CID spectrum is given in the Supporting Information (Figure S25). The dominant fragmentation process channel corresponds to the formation of the [**3**+Cl]$^-$ monomer, clearly indicating that receptor **3** has a higher affinity for Cl$^-$ than receptor **1** in the gas phase, therefore confirming the relative order deduced from DFT calculations and NMR experiments. The fact that the ion [**1**+Cl]$^-$ is only present in trace amounts is consistent with an important difference in computed interaction energies in favour of **3** (~50 kJ/mol).

Conclusion

Our study demonstrates that synthetic receptors designed to combine hydrogen bonding and anion-π interactions significantly enhance chloride ion recognition. Incorporating rigid, pre-organized frameworks, such as the naphthalene spacer in receptor **3**, leads to more effective anion binding compared to flexible or less structured systems. Both theoretical (DFT calculations) and experimental (NMR spectroscopy, mass spectrometry) evidence confirm that structural preorganization and the synergy of multiple weak interactions are key factors in optimizing anion recognition. Receptor **3**, in particular, exhibits superior chloride affinity due to a unique combination of N–H···Cl$^-$, C–H···Cl$^-$ and Cl···π interactions. From our data, we set the following ranking: **3**>**2**>**1**, which highlights the crucial role of molecular design, especially the use of rigid and pre-organized architectures, in achieving new-generation receptors for supramolecular anion recognition.

Acknowledgements

We are grateful to the CNRS and the Universities of Versailles Saint Quentin, Evry Val d'Essonne and Paris-Saclay. We thank the French Ministère de l'Enseignement Supérieur et de la Recherche for funding (O.Z. and J.U.). This work has been supported as part of France 2030 programme "ANR-11-IDEX-0003", awarded by the Graduate School Chemistry of the université Paris-Saclay.

Refrences

[1] P. A. Gale, E. N. W. Howe, X. Wu, M. J. Spooner, *Coord. Chem. Rev.* **2018**, *375*, 333–372.
[2] P. A. Gale, Dehaen, Wim, *Anion Recognition in Supramolecular Chemistry*, Springer, Berlin, **2010**.
[3] N. Busschaert, C. Caltagirone, W. Van Rossom, P. A. Gale, *Chem. Rev.* **2015**, *115*, 8038–8155.
[4] V. Amendola, L. Fabbrizzi, L. Mosca, *Chem. Soc. Rev.* **2010**, *39*, 3889.
[5] V. Amendola, L. Fabbrizzi, L. Mosca, F. Schmidtchen, *Chem. – Eur. J.* **2011**, *17*, 5972–5981.
[6] G. Picci, R. Montis, V. Lippolis, C. Caltagirone, *Chem. Soc. Rev.* **2024**, *53*, 3952–3975.
[7] J. Y. C. Lim, P. D. Beer, *Chem* **2018**, *4*, 731–783.
[8] A. Frontera, P. Gamez, M. Mascal, T. J. Mooibroek, J. Reedijk, *Angew. Chem. Int. Ed.* **2011**, *50*, 9564–9583.
[9] R. Plais, G. Clavier, J.-Y. Salpin, A. Gaucher, D. Prim, *Eur. J. Org. Chem.* **2023**, *26*, e202201281.
[10] Y. Zhao, Y. Domoto, E. Orentas, C. Beuchat, D. Emery, J. Mareda, N. Sakai, S. Matile, *Angew. Chem. Int. Ed.* **2013**, *52*, 9940–9943.
[11] Y. Zhao, Y. Cotelle, N. Sakai, S. Matile, *J. Am. Chem. Soc.* **2016**, *138*, 4270–4277.
[12] Y. Zhao, Y. Cotelle, A.-J. Avestro, N. Sakai, S. Matile, *J. Am. Chem. Soc.* **2015**, *137*, 11582–11585.
[13] Y. Zhao, Y. Domoto, E. Orentas, C. Beuchat, D. Emery, J. Mareda, N. Sakai, S. Matile, *Angew. Chem.* **2013**, *125*, 10124–10127.
[14] I. Alkorta, F. Blanco, P. M. Deyà, J. Elguero, C. Estarellas, A. Frontera, D. Quiñonero, *Theor. Chem. Acc.* **2010**, *126*, 1–14.
[15] I. Alkorta, F. Blanco, J. Elguero, C. Estarellas, A. Frontera, D. Quiñonero, P. M. Deyà, *J. Chem. Theory Comput.* **2009**, *5*, 1186–1194.
[16] M. Göth, F. Witte, M. Quennet, P. Jungk, G. Podolan, D. Lentz, W. Hoffmann, K. Pagel, H. Reissig, B. Paulus, C. A. Schalley, *Chem. – Eur. J.* **2018**, *24*, 12879–12889.
[17] Frisch, M.J., Trucks, G.W., Schlegel, H.B., et al. (2016) Gaussian 16, Revision B.01. Gaussian, Inc., Wallingford.
[18] T. Lu, F. Chen, *J. Comput. Chem.* **2012**, *33*, 580–592.
[19] O. Zayene, R. Plais, L. Rolhion, F. Bourdreux, G. Pieters, A. Gaucher, G. Clavier, A. Coeuret, J.-Y. Salpin, D. Prim, *ChemistrySelect* **2024**.
[20] S. Grimme, S. Ehrlich, L. Goerigk, *J. Comput. Chem.* **2011**, *32*, 1456–1465.
[21] A. Bondi, *J. Phys. Chem.* **1964**, *68*, 441–451.
[22] S. J. Grabowski, *J. Phys. Org. Chem.* **2004**, *17*, 18–31.
[23] S. Emamian, T. Lu, H. Kruse, H. Emamian, *J. Comput. Chem.* **2019**, *40*, 2868–2881.
[24] P. Gamez, *Inorg Chem Front* **2014**, *1*, 35–43.
[25] T. J. Fuhrer, M. Houck, C. A. Corley, S. T. Iacono, *J. Phys. Chem. A* **2019**, *123*, 9450–9455.
[26] O. Zayene, J. Hu, A. Damond, C. Roc, J. Marrot, A. Gaucher, J.-Y. Salpin, D. Prim, *ChemPlusChem* **2024**, *89*, e202400380.

[27] R. Plais, G. Gouarin, A. Bournier, O. Zayene, V. Mussard, F. Bourdreux, J. Marrot, A. Brosseau, A. Gaucher, G. Clavier, J.-Y. Salpin, D. Prim, *ChemPhysChem* **2023**, *24*, e202200524.
[28] R. Plais, H. Boufroura, G. Gouarin, A. Gaucher, V. Haldys, A. Brosseau, G. Clavier, J.-Y. Salpin, D. Prim, *RSC Adv.* **2021**, *11*, 9476–9487.
[29] R. Plais, G. Gouarin, A. Gaucher, V. Haldys, A. Brosseau, G. Clavier, J. Salpin, D. Prim, *ChemPhysChem* **2020**, *21*, 1249–1257.
[30] Manuscript under preparation.
[31] R. Graham Cooks, J. S. Patrick, T. Kotiaho, S. A. McLuckey, *Mass Spectrom. Rev.* **1994**, *13*, 287–339.
[32] G. Bouchoux, *Mass Spectrom. Rev.* **2007**, *26*, 775–835.

Anion-π Meets H-Bonding: Tuning Synergy Through the Flexibility-to-Preorganization Transition in Anion Receptor Design

Supplementary Information

Table of contents

1. General procedures, Material and Instrumentation

1.1 General experimental procedures and Materials

Unless otherwise noted, all starting materials were obtained from commercial suppliers and used without purifications.

Reaction progress was carried out using pre-coated TLC sheets ALUGRAM® Xtra SIL G/UV_{254} (0.20mm) from Macherey-Nagel® and visualized under 254 and 365 nm UV lamp from Fisher Bioblock Scientific®. Flash chromatography was proceeded using Silica 60M (0.04-0.063mm) for column chromatography silica gel from Macherey-Nagel®.

1.2 Instrumentation

^{1}H NMR spectra were recorded with Bruker AV-I 300MHz spectrometer at 298K, referenced to TMS signal and were calibrated using residual proton in Acetone d6 (δ=2.05ppm), according to the literature.[1] ^{19}F NMR spectra were recorded with Bruker AV-I 300MHz spectrometer at 282MHz and 298K and were calibrated using $CFCl_3$ as reference. ^{13}C NMR spectra were recorded with a Bruker AV-I 300MHz spectrometer at 75MHz and 298 K and were calibrated using Acetone d6 (δ = 29.8 ppm).[1] ^{1}H NMR spectroscopic data are reported as follow: chemical shift δ [parts per million] (multiplicity, coupling constants in Hertz, integration). Multiplicities are reported as follow: s = singlet, d = doublet, t = triplet, q = quadruplet, quint = quintuplet, sext = sextuplet, hept = heptuplet, dd = doublet of doublet, td = triplet of doublet, tt = triplet of triplet, ddd = doublet of doublet of doublet, m = multiplet. ^{13}C NMR spectroscopic data are reported in terms of chemical shifts δ [ppm] and when it is necessary multiplicity and coupling constant in Hertz.

To check the structure of the product obtained during the synthesis, high resolution mass spectra (HRMS) were obtained with a Waters Xevo QTOF instrument fitted with an electrospray ionization source (ESI-), using Leucine Enkephaline solution as internal calibrant.

Studies of the gas-phase interactions of **1**, **2** and **3** with chloride ion, were performed onto a 3D ion trap instrument (Bruker Amazon Speed ETD). Complexes were generated in the gas phase by electrospray ionization. To this end, equimolar mixtures of **2**/NBu_4Cl and **3**/NBu_4Cl were prepared. Starting from 5 10^{-2} M stock solutions of **1**, **2** and **3** and NBu_4Cl solubilized in acetonitrile (ACN) and purified water, respectively, 10^{-4} M or 10^{-5} M mixtures of **2**/ NBu_4Cl and **3**/NBu_4Cl (90/10 ACN/H_2O) were introduced in the electrospray source by a syringe pump (4-5 µL/min). Typical experimental conditions were as followed: Capillary voltage: - 4500 V; End plate offset: -500 V; Dry gas: 10 L/min / Dry gas temperature: 200 °C, Nebulizer gas: 7.3 PSI; Cap exit and Trap drive values automatically adjusted through the target mass parameter: 550 and 1025 to study the monomers and dimers, respectively.

All spectra were recorded in the “Maximum Resolution mode”
MS analysis : ICC mode : “on” (80000 ions) and acquisition time : auto.
MS^n analysis : ICC mode off / accumulation time 1 to 5 ms to reach c.a. 20000 ions for the selected precursor / Isolation window 4 to 8 Da / Fragmentation delay 40 ms/ amplitude of fragmentation : 0.20-0.6 depending on the ions / Low mass cutoff : Auto.

1.3 Molecular modelling and software

All calculations were carried out using Gaussian 16® program:

Gaussian 16, Revision B.01, M. J. Frisch, G. W. Trucks, H. B. Schlegel, G. E. Scuseria, M. A. Robb, J. R. Cheeseman, G. Scalmani, V. Barone, G. A. Petersson, H. Nakatsuji, X. Li, M. Caricato, A. V. Marenich, J. Bloino, B. G. Janesko, R. Gomperts, B. Mennucci, H. P. Hratchian, J. V. Ortiz, A. F. Izmaylov, J. L. Sonnenberg, D. Williams-Young, F. Ding, F. Lipparini, F. Egidi, J. Goings, B. Peng, A. Petrone, T. Henderson, D. Ranasinghe, V. G. Zakrzewski, J. Gao, N. Rega, G. Zheng, W. Liang, M. Hada, M. Ehara, K. Toyota, R. Fukuda, J. Hasegawa, M. Ishida, T. Nakajima, Y. Honda, O. Kitao, H. Nakai, T. Vreven, K. Throssell, J. A. Montgomery, Jr., J. E. Peralta, F. Ogliaro, M. J. Bearpark, J. J. Heyd, E. N. Brothers, K. N. Kudin, V. N. Staroverov, T. A. Keith, R. Kobayashi, J. Normand, K. Raghavachari, A. P. Rendell, J. C. Burant, S. S. Iyengar, J. Tomasi, M. Cossi, J. M. Millam, M. Klene, C. Adamo, R. Cammi, J. W. Ochterski, R. L. Martin, K. Morokuma, O. Farkas, J. B. Foresman, and D. J. Fox, Gaussian, Inc., Wallingford CT, 2016.

This work was performed using HPC resources from the “Mésocentre” computing center of CentraleSupélec and École Normale Supérieure Paris-Saclay supported by CNRS and Région Île-deFrance (http://mesocentre.centralesupelec.fr/).

Computed structures were preoptimized with a MM2 forcefield using Chem3D®. Then, optimizations were calculated at APFD/aug-cc-pVDZ calculation level using Gaussian 16® software without any solvent correction. Stationary points were verified by a harmonic vibrational frequencies calculation. None of the predicated geometry has any imaginary frequency implying that the optimized geometry of each of the molecules under study lay at a minimum local point on the potential energy surface.

NCIplots were generated from total densities using the script developed by Rzepa available on the website application of the Imperial College London.[2,3]

Distances were measured using Gaussview software on structures optimized without any solvent correction. Distances between tetrafluoropyridine centroid (defined using the six atoms of the tetrafluoropyridine rings) and chloride were measured using UCSF Chimera software.[4]

2. Synthetic procedures

Preparation of **1i** intermediate

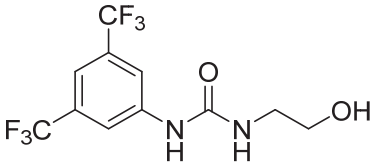

The synthesis procedure of **1i** was reported in a previous publication.[5]

Preparation of **1**

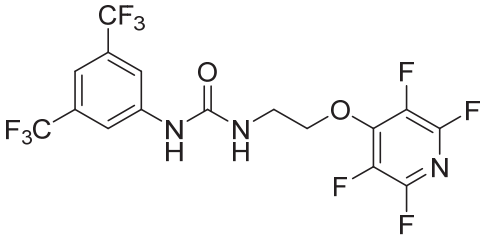

1-(3,5-bis(trifluoromethyl)phenyl)-3-(2-hydroxyethyl)urea **1i** (100mg, 0.32mmol, 1.0eq), dry K_2CO_3 (47mg, 0.34mmol, 1.05eq) and 3.5mL of dry acetonitrile were added to a round bottom flask. The mixture was stirred for 15 minutes at rt. Pentafluoropyridine (37µL, 0.34mmol, 1.05eq) was then added dropwise and the mixture was stirred at rt for 16 hours. The reaction was diluted with ethyl acetate, quenched with water and the aqueous layer was extracted three times with ethyl acetate. The combined organic layers were dried over $MgSO_4$, filtered and solvent was evaporated under reduced pressure. The crude product was purified by a flash chromatography, eluting with a gradient of solvents (Cyclohexane/EtOAc 8/2 to 0/100), giving access to 108mg of the desired 1- (3,5-bis(trifluoromethyl)phenyl)-3-(2-((perfluoropyridin-4-yl)oxy)ethyl)urea **1** as a white powder. Yield : 72%.

^{1}H NMR (300 MHz, Acetone d6, TMS): δ (ppm) 8.89 (s, 1H), 8.13 (s, 2H), 7.53 (s, 1H), 6,48 (s, 1H), 4.72 (t, 2H, $^3J_{H-H}$ = 11 Hz), (q, 2H, $^3J_{H-H}$ = 5 Hz.

^{19}F NMR (282 MHz, Acetone d6, $CFCl_3$): δ (ppm) -62.6 (s, 6F), -92.6 to -92.8 (m, 2F), -158.9 to -159.2 (m, 2F).

^{13}C NMR (75 MHz, Acetone d6, TMS): δ (ppm) 155.8 (s, 1C), 148.5-148.2 (m, 1C), 146.7-143.1 (large d, 2C, $^1J_{C-F}$ = 234 Hz), 143.4 (s, 1C), 138.1-134.3 (large d, 2C, $^1J_{C-F}$ = 254 Hz), 133.1-131.8 (q, 2C, $^2J_{C-F}$ = 32 Hz), 129.9-119.1 (q, 2C, $^1J_{C-F}$ = 270 Hz), 118.5 (m, 2C), 115.1-114.9 (quint, 1C, $^2J_{C-F}$ = 4 Hz), 74.7 (t, 1C $^4J_{C-F}$ = 5 Hz), 40.6 (s, 1C).

HRMS (ESI+- TOF) m/z [M+H]+: calculated for $C_{16}H_{10}N_3O_2F_{10}$ 466.0613, found 466.0621.

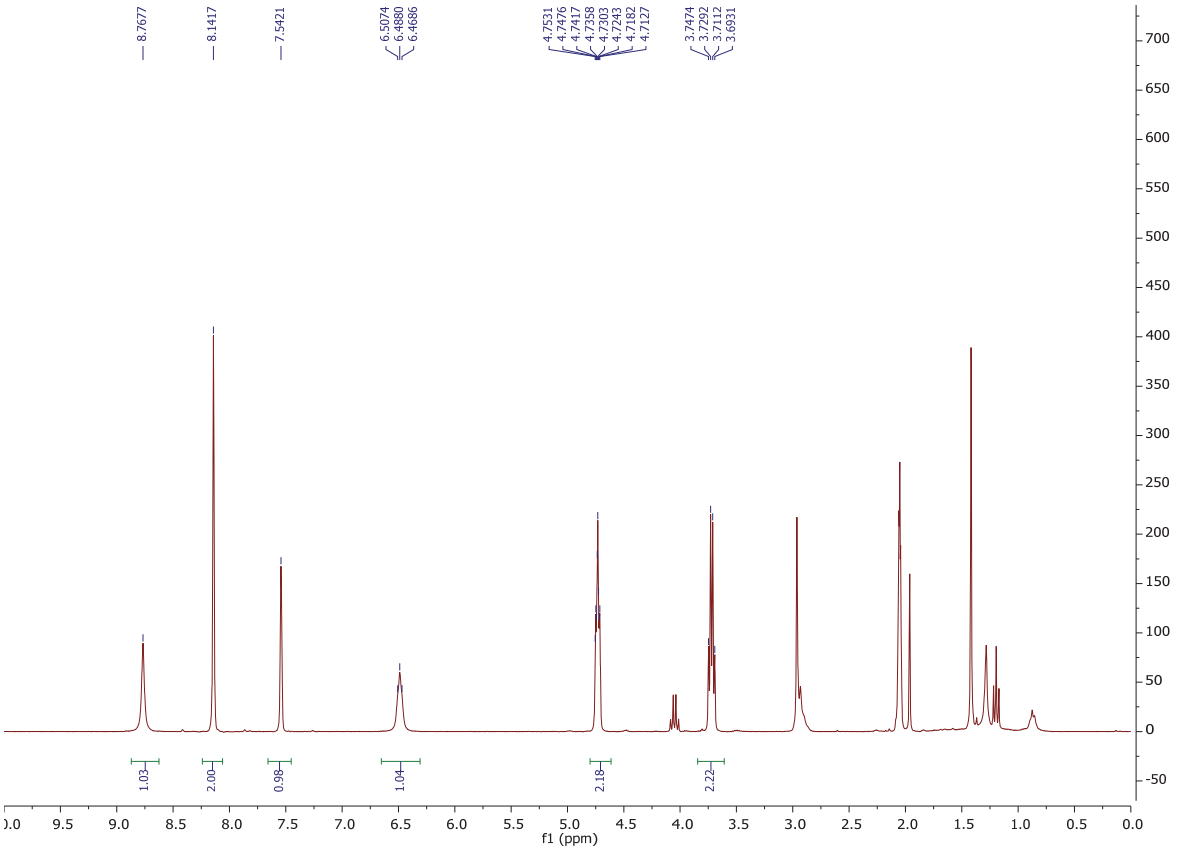

*Figure S1 ^{1}H NMR spectrum of **1***

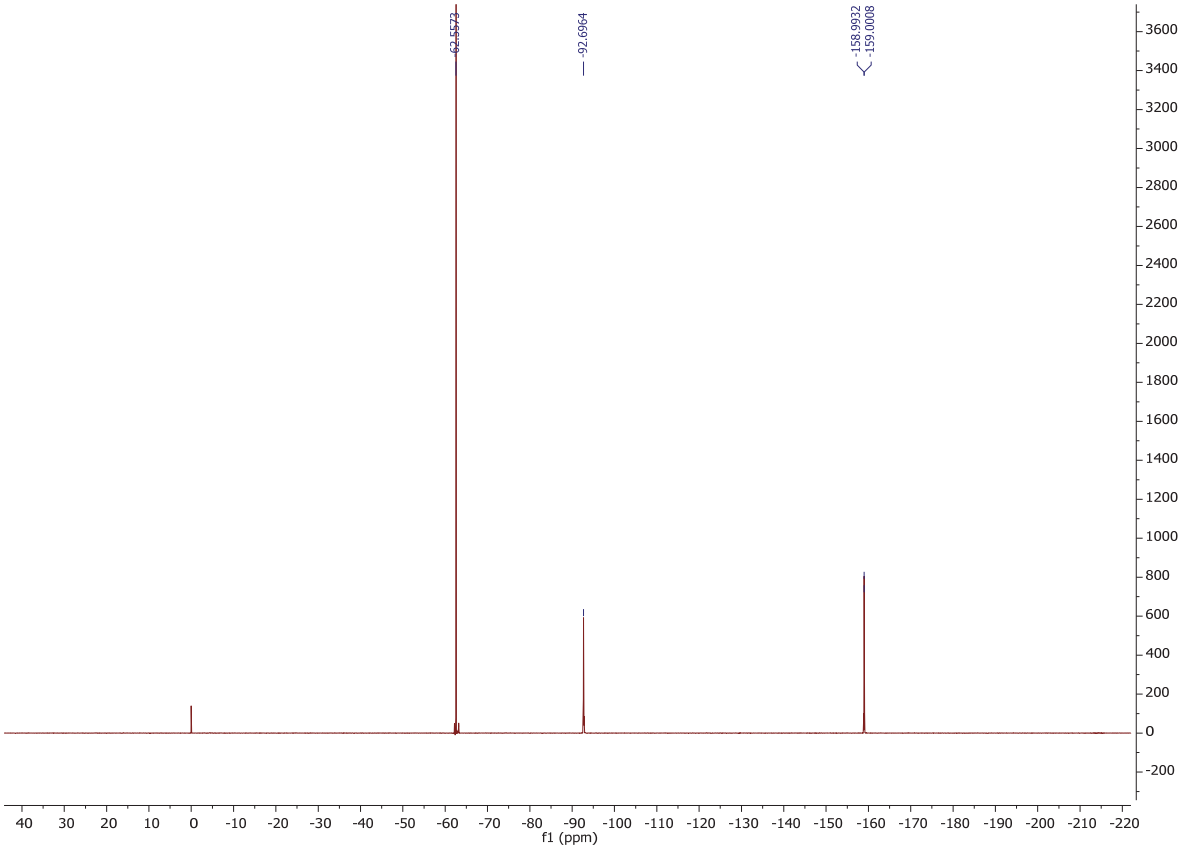

*Figure S2 ^{19}F NMR spectrum of **1***

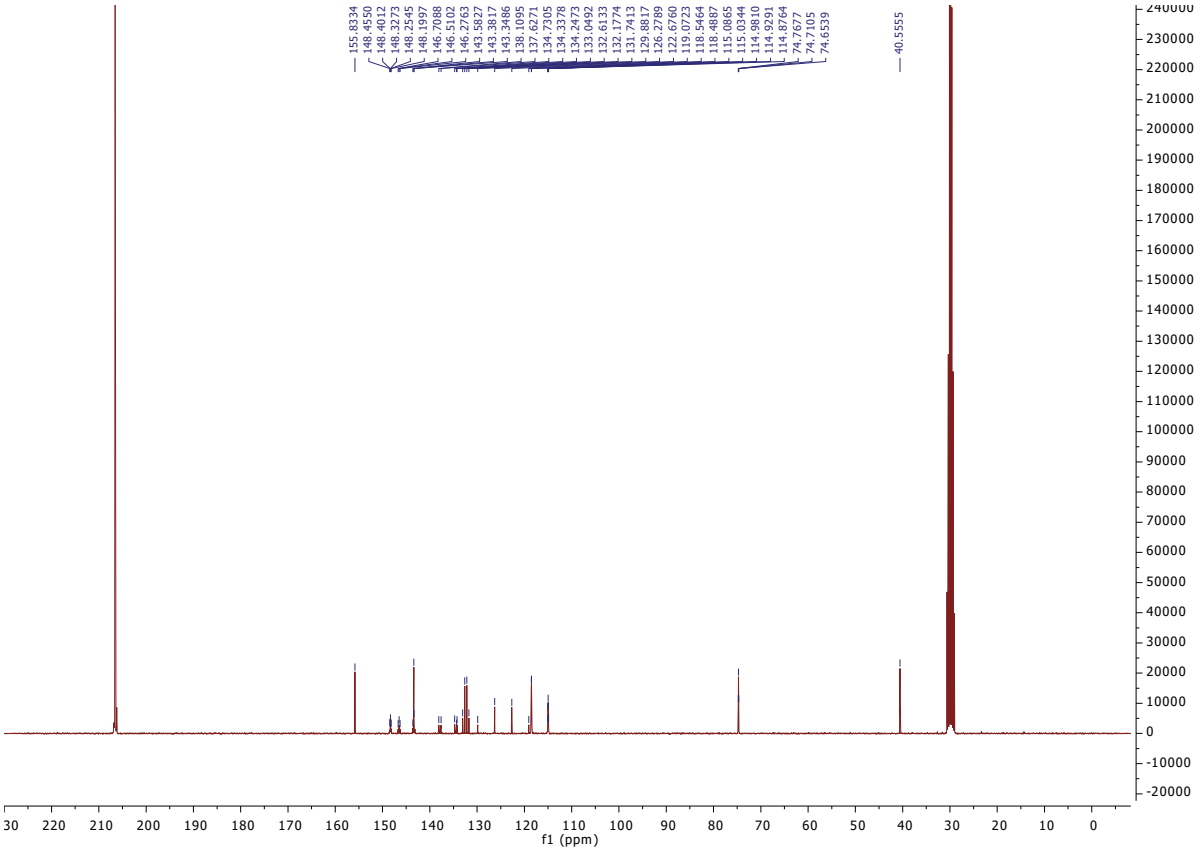

*Figure S3 ^{13}C NMR spectrum of **1***

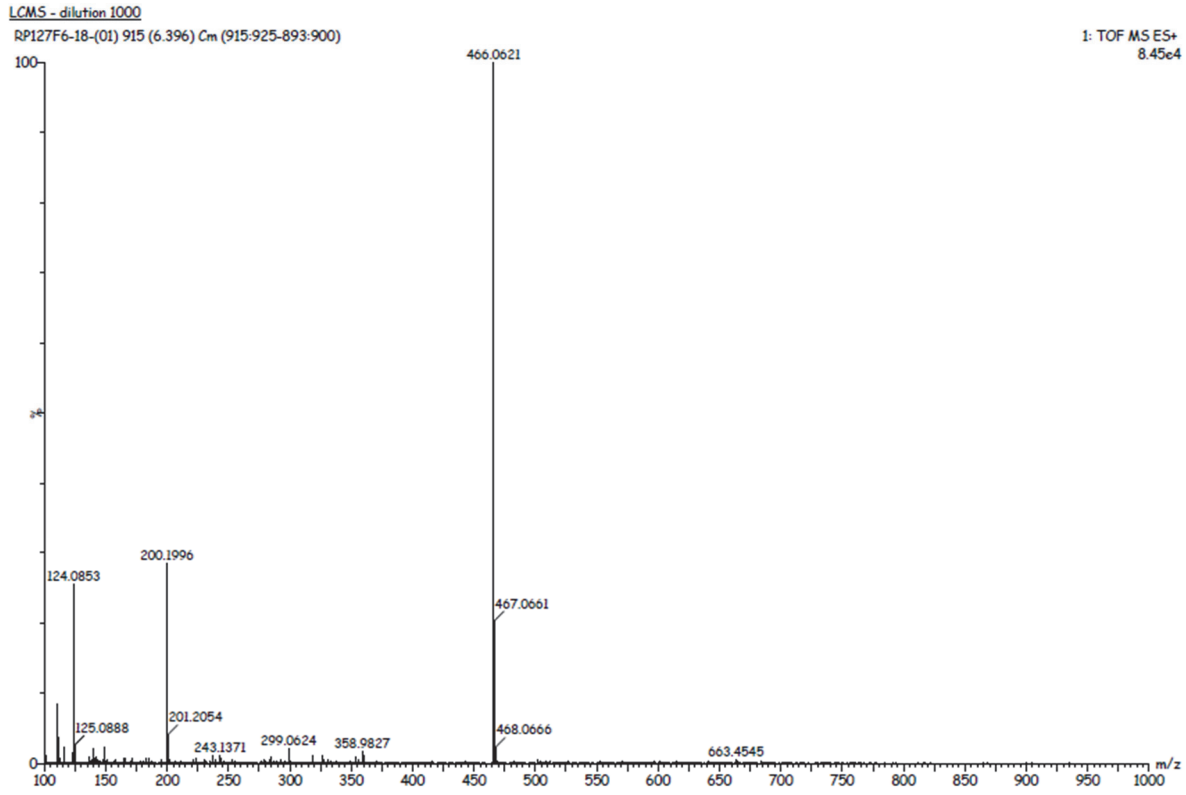

*Figure S4 High resolution mass spectrum of **1***

Preparation of **2i** intermediate :

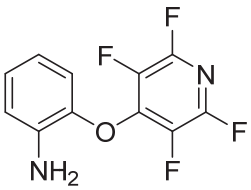

2-aminophenol (250mg, 2.29mmol, 1.0eq), dry K_2CO_3 (333mg, 2.41mmol, 1.05eq) and 23mL of dry acetonitrile were added to a round bottom flask. The reaction mixture was stirred for 15 minutes at rt. Pentafluoropyridine (265µL, 2.41mmol, 1.05eq) was added dropwise to the mixture. The mixture was stirred at rt for 16 hours, then diluted with water and extracted three times with ethyl acetate. Organic layers were gathered, dried over $MgSO_4$, filtered and solvent was evaporated under reduced pressure. The crude product was purified by flash chromatography (eluent: Cyclohexane/EtOAc 95/5) affording 510mg of the desired 2-((perfluoropyridin-4-yl)oxy)aniline **2i** as an orange liquid. Yield : 86%.

^{1}H NMR (300 MHz, Acetone d6, TMS): *δ* (ppm) 7.02-6.89 (m, 3H), 6.59 (t, m, 1H, $^3J_{H-H}$ = 6 Hz), 4.92 (large s, 2H, -NH_2).

^{19}F NMR (282 MHz, Acetone d6, $CFCl_3$): *δ* (ppm) -91.5 to -91.7 (m, 2F), -157.0 to -157.2 (m, 2F).

^{13}C NMR (75 MHz, Acetone d6, TMS): *δ* (ppm) 146.8-146.4 (m, 1C), 146.8-143.0 (large d, m, 2C, $^1J_{C-F}$ = 222 Hz), 144.1 (s, 1C), 139.7 (s, 1C), 138.9-135.0 (large d, m, 2C, $^1J_{C-F}$ = 257 Hz), 127.0 (s, 1C), 117.8 (s, 1C), 117.7 (s, 1C), 117.2 (s, 1C).

HRMS (ESI+- TOF) m/z [M+H]+: calculated for $C_{11}H_7N_2OF_4$ 259.0495, found 259.0493.

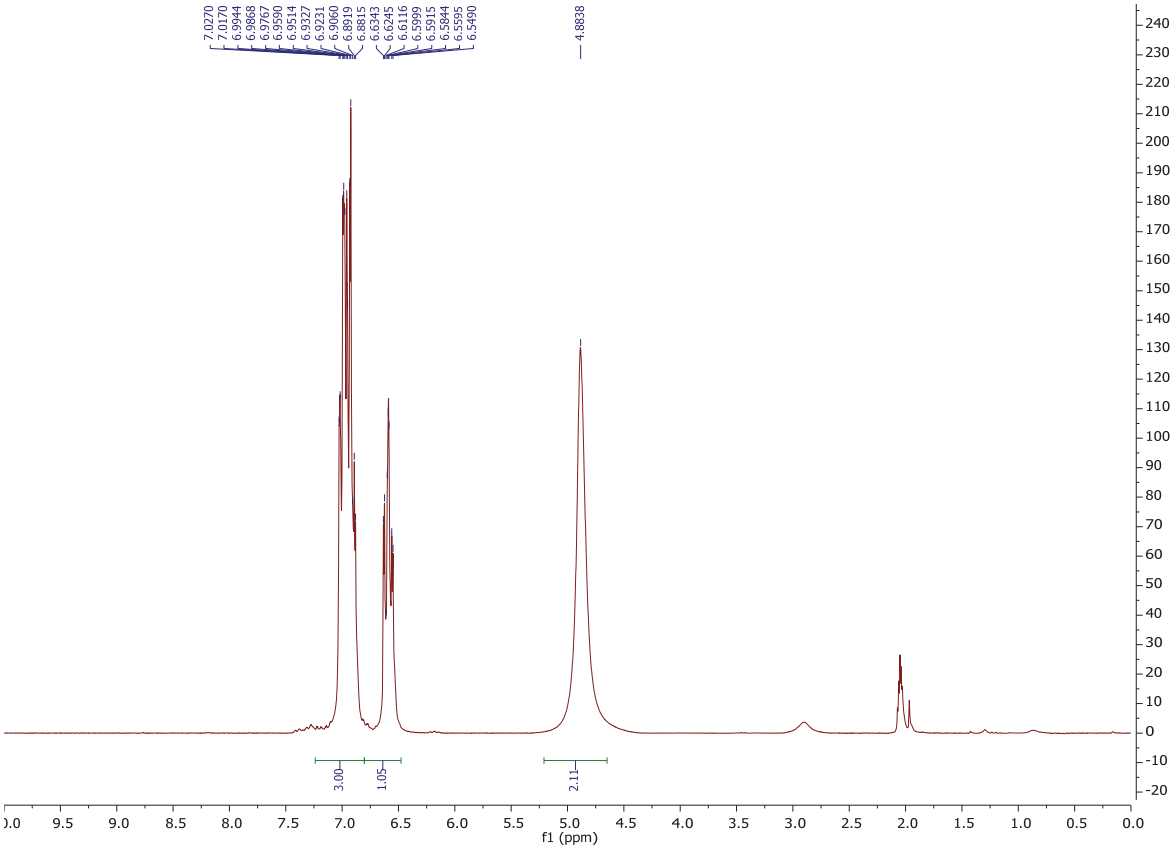

*Figure S5 ^{1}H NMR spectrum of **2i***

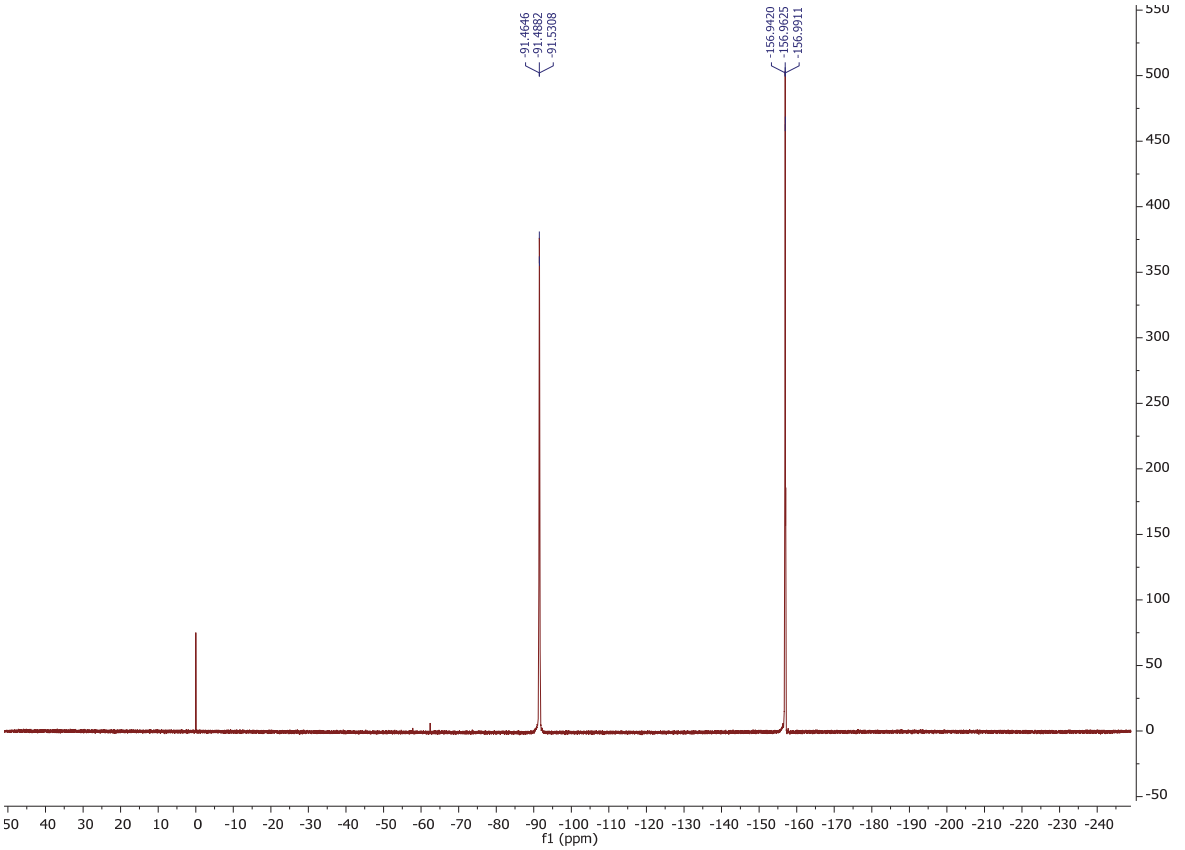

*Figure S6 ^{19}F NMR spectrum of **2i***

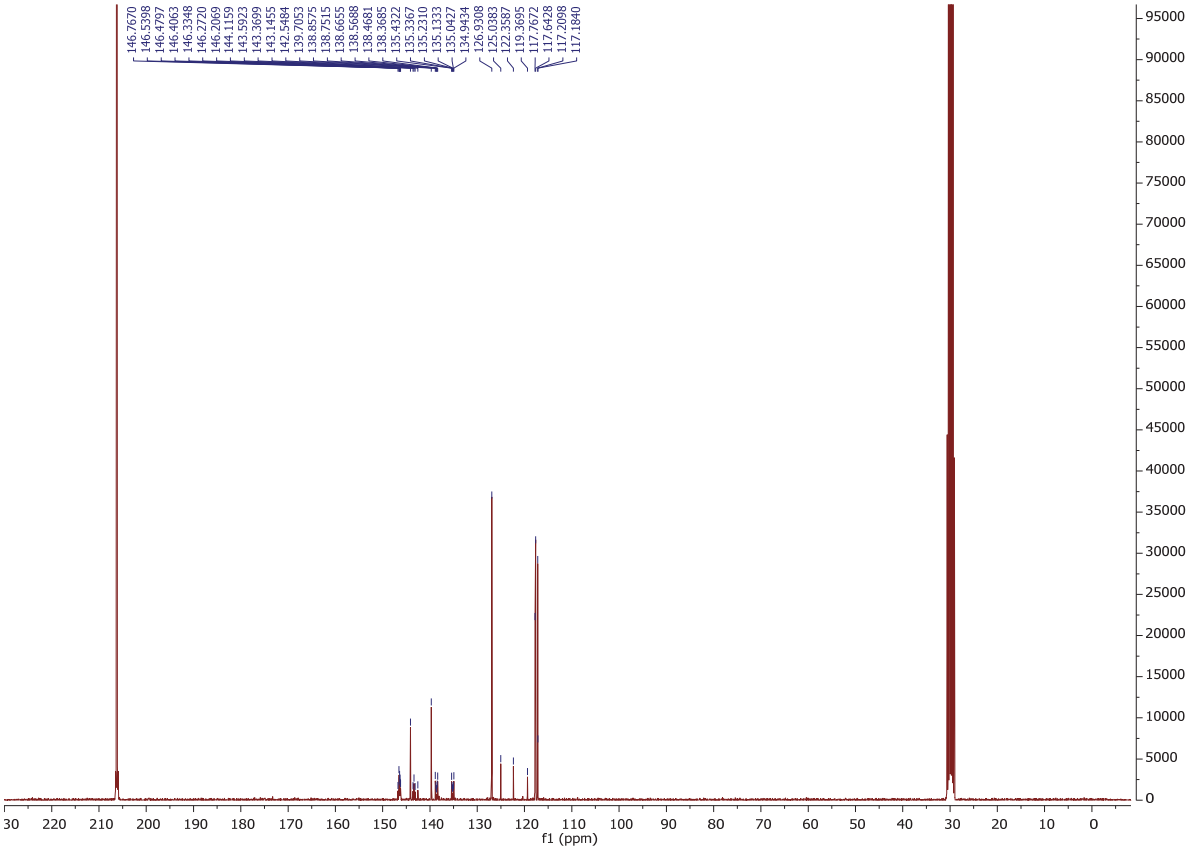

*Figure S7 ^{13}C NMR spectrum of **2i***

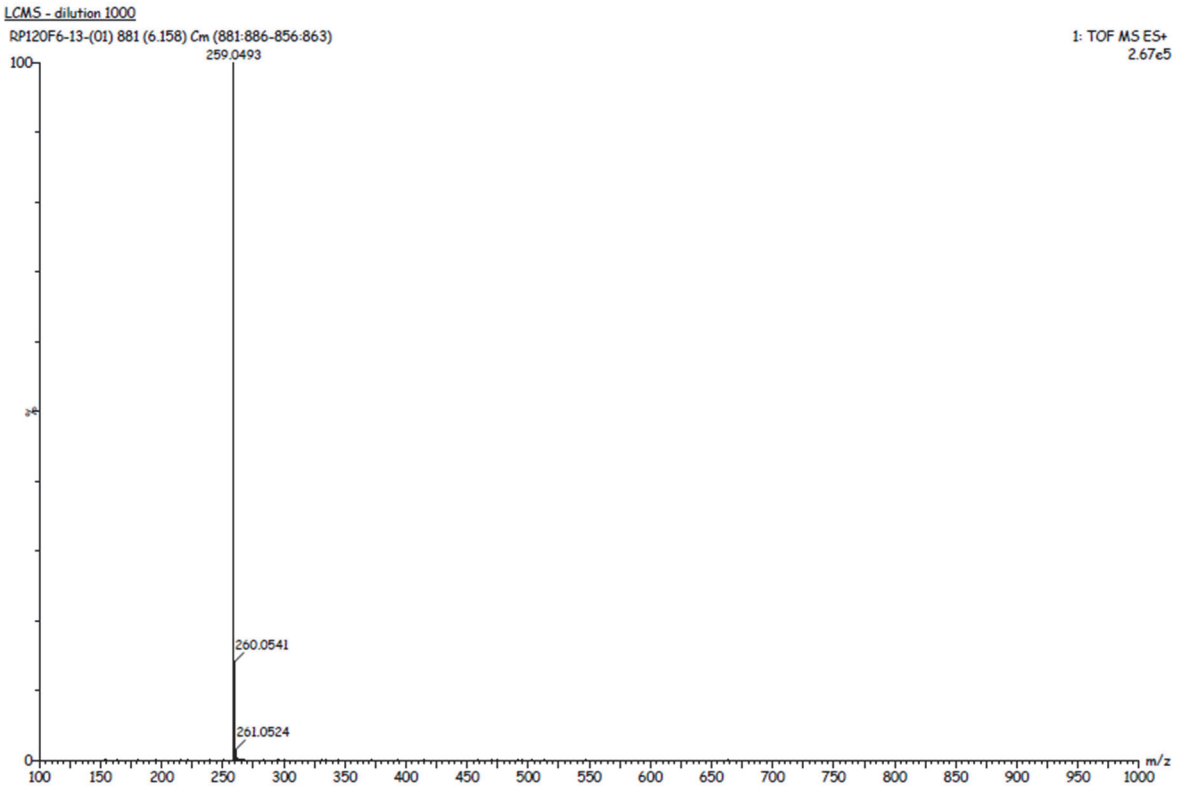

*Figure S8 High resolution mass spectrum of **2i***

Preparation of **2**

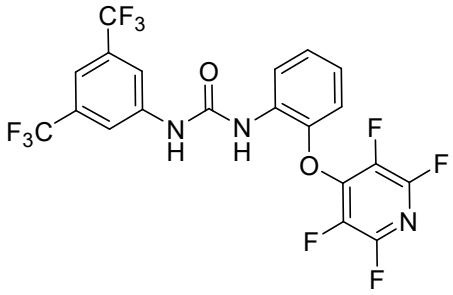

2-((perfluoropyridin-4-yl)oxy)aniline **2i** (106mg, 0.41mmol, 1.04eq) and 1 mL of dry DMF were added to a flask under Argon atmosphere. 3,5-bis(trifluoromethyl)phenyl isocyanate (68µL, 0.39mmol, 1.0eq) was added dropwise. The mixture was stirred for 16 hours at rt. Water was added and the mixture was extracted three times with ethyl acetate. Organic layers were gathered, washed with brine, dried over $MgSO_4$, filtered and the solvent was removed under reduced pressure. The crude product was purified by two subsequent flash Chromatographies (eluent 1 : Cyclohexane/ethyl acetate 9/1 and eluent 2 : gradient Cyclohexane/EtOAc 98/2 to 9/1) to afford 158 mg of desired 1-(3,5-bis(trifluoromethyl)phenyl)-3-(2-((perfluoropyridin-4-yl)oxy)phenyl)urea **2** as a white solid. Yield: 75%.

^{1}H NMR (300 MHz, Acetonitrile d3, TMS): δ (ppm) 8.21 (d, 1H, $^3J_{H\text{-}H}$ = 8 Hz), 8.09 (s, 1H), 8.07 (s, 2H), 7.78 (s, 1H), 7.64 (s, 1H) 7.27 (m, 1H), 7.06 (m, 2H).

^{19}F NMR (282 MHz, Acetonitrile d3, $CFCl_3$): δ (ppm) -62.3 (s, 6F, -C*F*$_3$), -90.1 to -90.2 (m, 2F), -155.6 to 155.7(m, 2F).

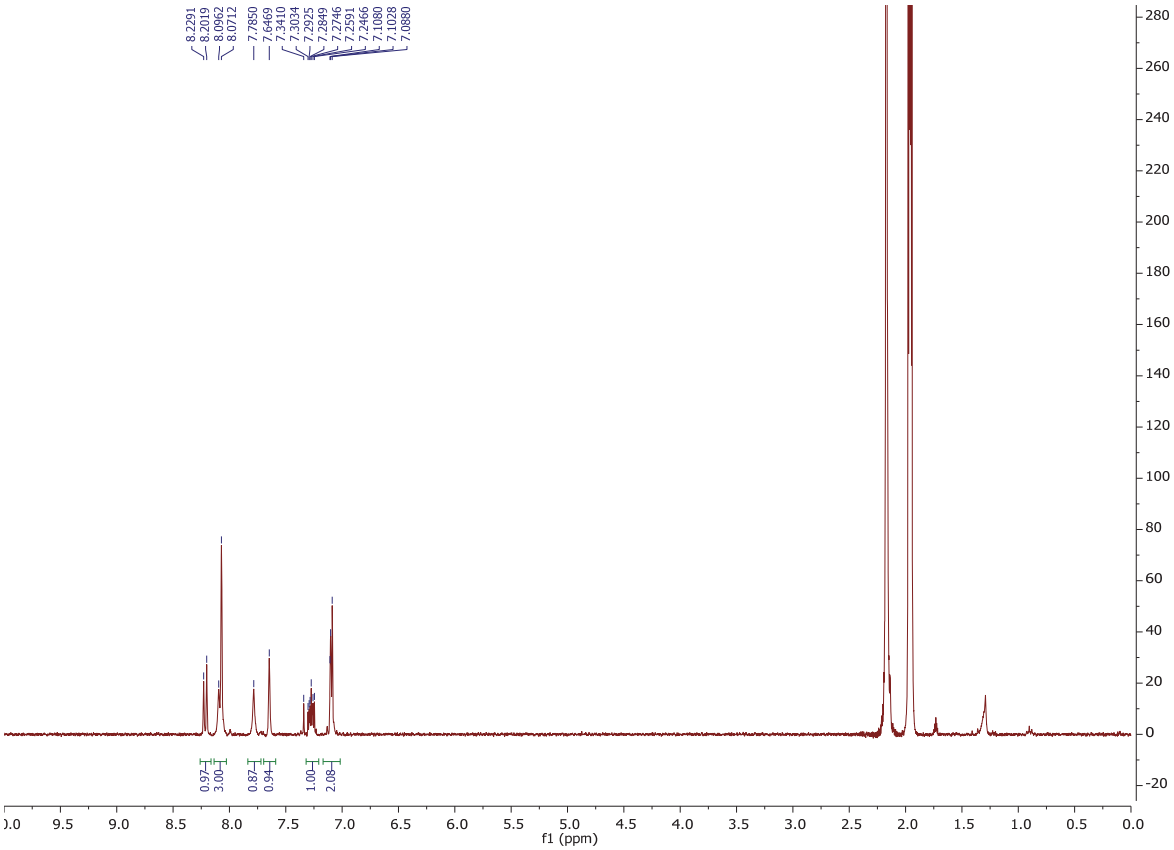

*Figure S9 [1]H NMR spectrum of **2***

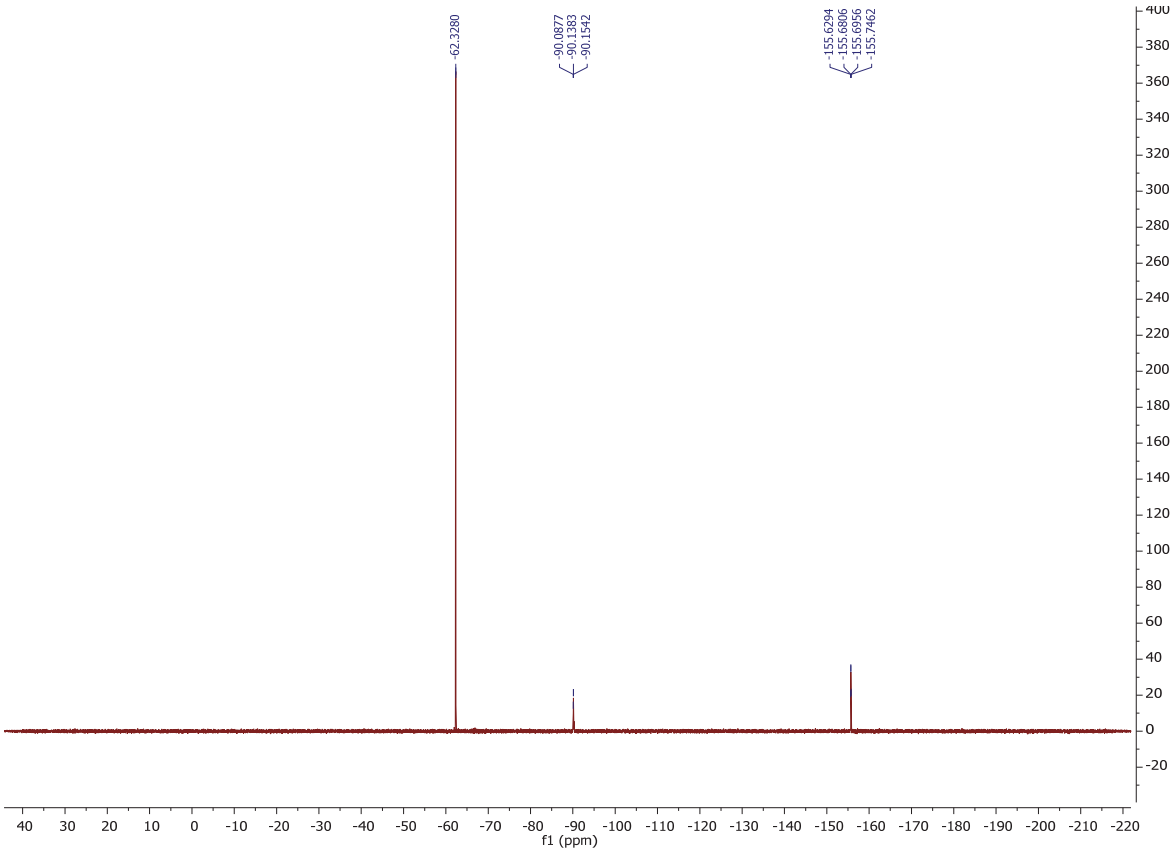

*Figure S10 [19]F NMR spectrum of **2***

Preparation of intermediate **3i**

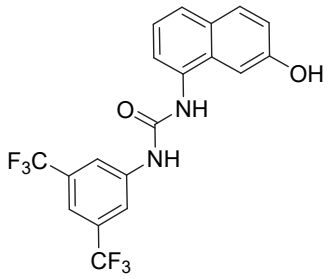

In a round-bottom flask, 8-amino-2-naphthol (100 mg, 0.6 mmol, 1eq) was dissolved in ACN (3 mL). The isocyanate (92.1 µL, 0.6 mmol, 1eq) was added dropwise at 0°C. The reaction mixture is strirred for 16 hours. After no further evolution of the reaction, the reaction mixture was diluted with ethyl acetate (5 mL) and H_2O (10 mL). The aqueous layer was extracted with ethyl acetate (3x10 mL). The combined organic layers were dried over $MgSO_4$, filtered and concentrated under reduced pressure. The crude product was purified by column chromatography (PE/EtOAc, 70/30) to afford 124 mg of brown product. Yield: 50%.

^{1}H NMR (200 MHz, Acetone d6, TMS): δ (ppm) 9.01 (s, 1H), 8.73 (s, 1H), 8.24 (bs, 3H), 7.82 (m, 2H), 7.63 (m, 2H), 7.42 (d, 1H, $^4J_{H\text{-}H}$ = 2.5 Hz), 7.29 (t, 1H, $^3J_{H\text{-}H}$ = 8.24 Hz), 7.18 (dd, 1H, $^4J_{H\text{-}H}$ = 8.63, $^4J_{H\text{-}H}$ = 2.28).

^{19}F NMR (282 MHz, Acetone d6, $CFCl_3$): δ (ppm) -62.50 (m, CF_3).

^{13}C NMR (75 MHz, Acetone d6, TMS): δ (ppm) 156.6, 154.1, 143.2, 132.9, 132.5 (q, 2C, $^2J_{C\text{-}F}$ = 33.9 Hz), 131.0, 130.1, 124.5 (q, 2C, $^1J_{C\text{-}F}$ = 272 Hz), 125.9, 122.7, 122.3, 119.2, 119.0 (m, 1C), 115.4 (quint, $^3J_{C\text{-}F}$ = 4 Hz), 108.5, 104.5.

HRMS (ESI$^+$- TOF) m/z [M+H]$^+$: calculated for $C_{19}H_{13}N_2O_2F_6$: 415.0881, found : 415.0896.

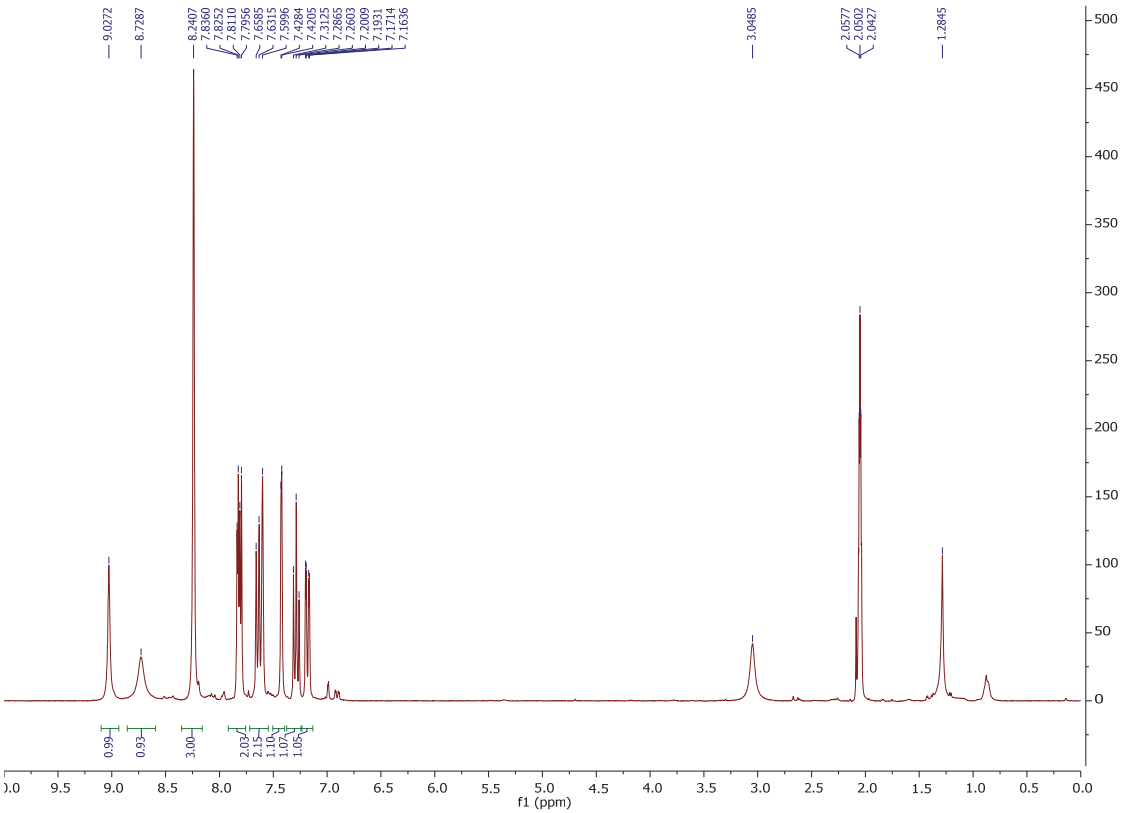

*Figure S11 ^{1}H NMR spectrum of **3i***

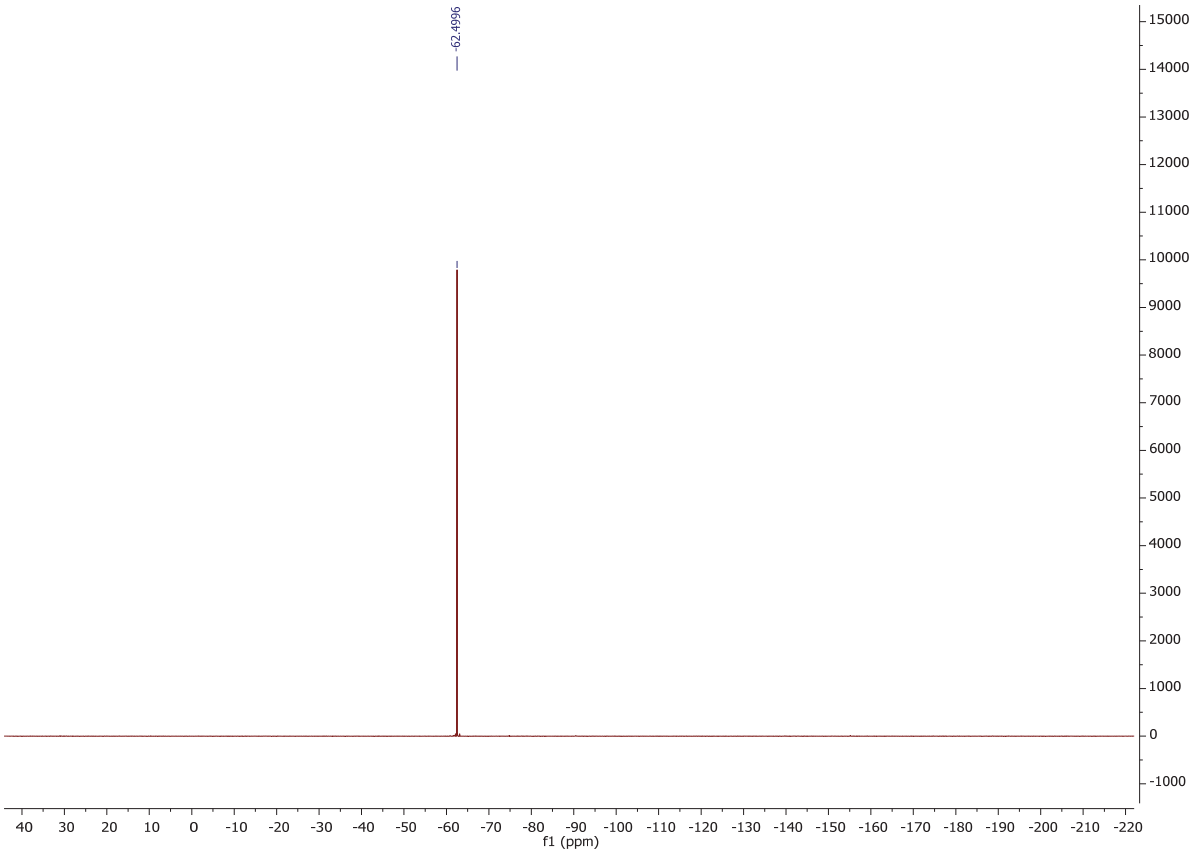

*Figure S12 ^{19}F NMR spectrum of **3i***

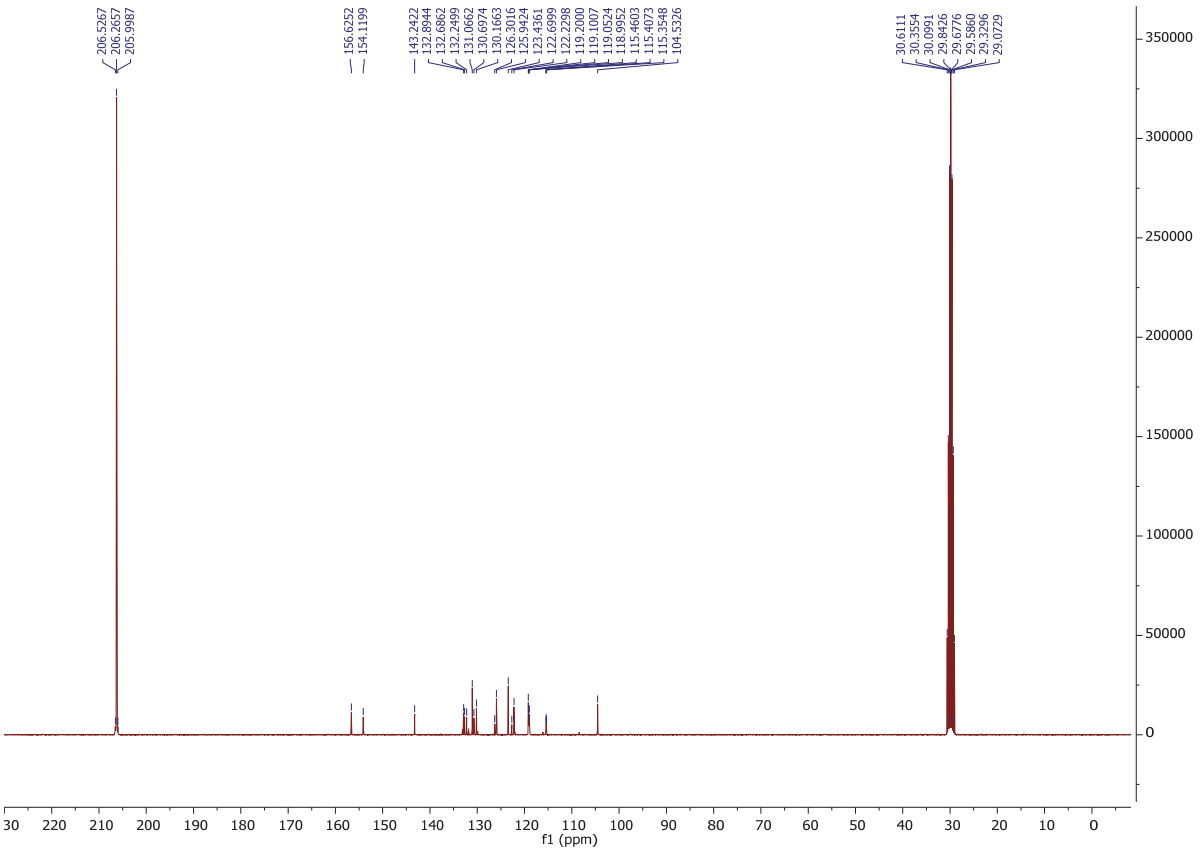

*Figure S13 ^{13}C NMR spectrum of **3i***

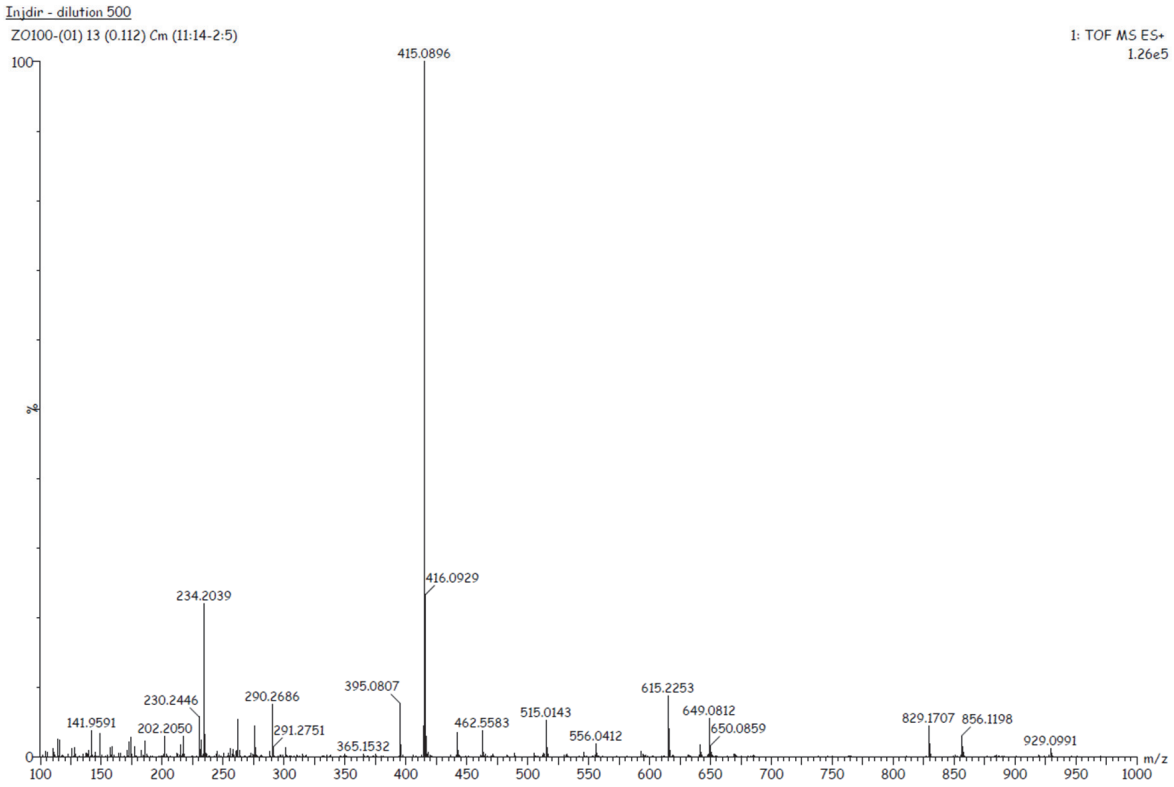

*Figure S14 High resolution mass spectrum of **3i***

Preparation of **3**

In a round-bottom flask, compound **3i** (83 mg, 0.2 mmol, 1eq) and K_2CO_3 (27.6 mg, 0.2 mmol, 1eq) were dissolved in ACN (2 mL) under an argon atmosphere. Pentafluoropyridine (338 mg, 0.2 mmol, 1 eq.) was added. The mixture was then diluted with ethyl acetate and H_2O (3x5 mL). The aqueous layer was extracted with ethyl acetate (3x10 mL). The organic layers were combined, dried over $MgSO_4$, filtered, and concentrated under reduced pressure. The crude product was purified by chromatography (petroleum ether/EtOAc, 80/20) to afford 38 mg of a white powder. Yield: 34%.

^{1}H NMR (200 MHz, Acetone d6, TMS): δ (ppm) 8.94 (s, 1H), 8.40 (s, 1H), 8.20 (s, 2H), 8.07 (d, 2H, $^{3}J_{H-H}$ = 8 Hz), 7.97 (m. 2H), 7.81 (d, 1H, $^{3}J_{H-H}$ = 8 Hz), 7.61 (s, 1H), 7.53 (m, 2H).

^{19}F NMR (282 MHz, Acetone d6, $CFCl_3$): δ (ppm) -62.51 (m, 6F), -90.50 (m, 2F), -155.21 (m, 2F).

^{13}C NMR (75 MHz, Acetone d6, TMS): δ (ppm) 155.0, 153.9, 145.1 (d, m, 2C $^{1}J_{C-F}$ = 239 Hz), 145.2 (m, 1C), 143.1, 137.5 (d, m, 2C, $^{1}J_{C-F}$ = 255 Hz), 134.5, 132.8, 132.6 (q, 2C, $^{2}J_{C-F}$ = 34 Hz), 132.1, 192.6, 125.9, 124.5 (q, 2C $^{1}J_{C-F}$ = 274 Hz), 123.0, 119.1 (m, 1C), 117.8, 115.6 (quint, 1C $^{3}J_{C-F}$ = 4 Hz), 108.8.

HRMS (ESI^{+}- TOF) m/z [M+H]$^{+}$: calculated for $C_{24}H_{12}N_3O_2F_{10}$: 564.0770, found : 564.0780.

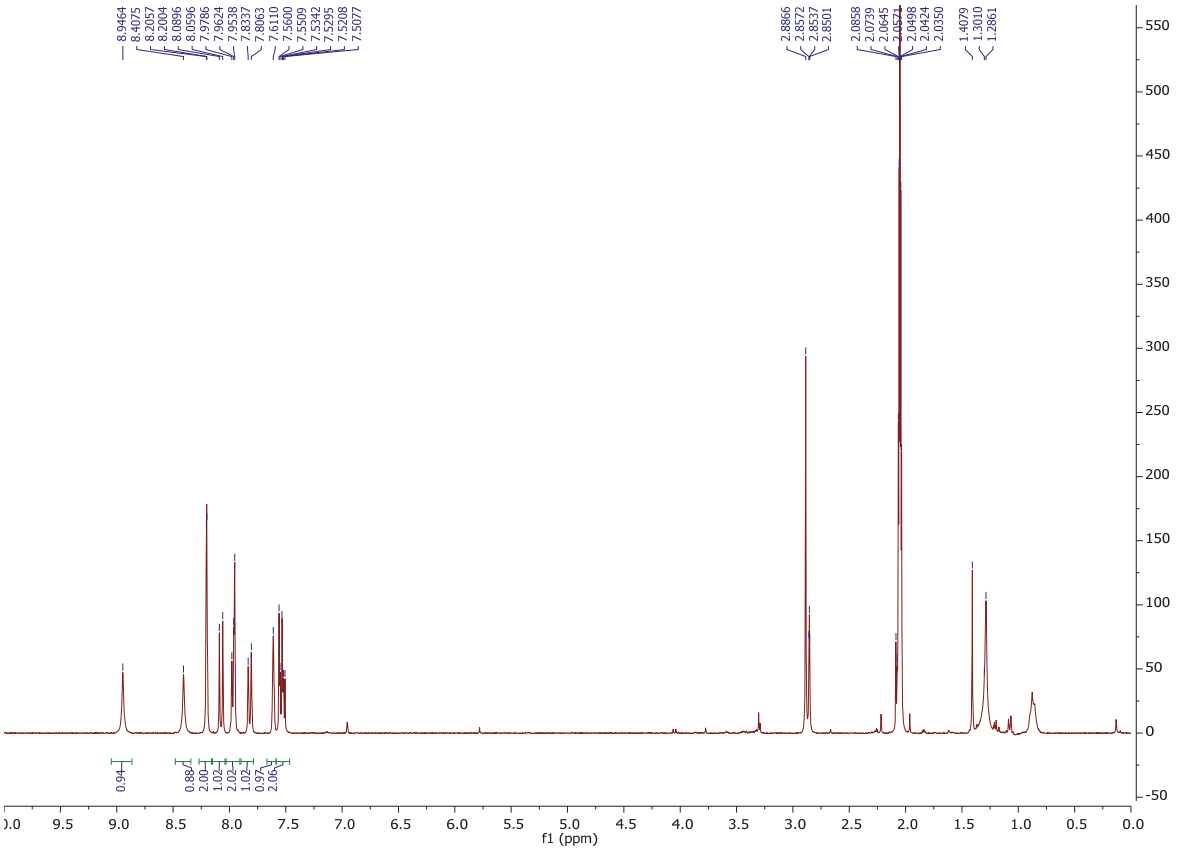

*Figure S15 ^{1}H NMR spectrum of **3***

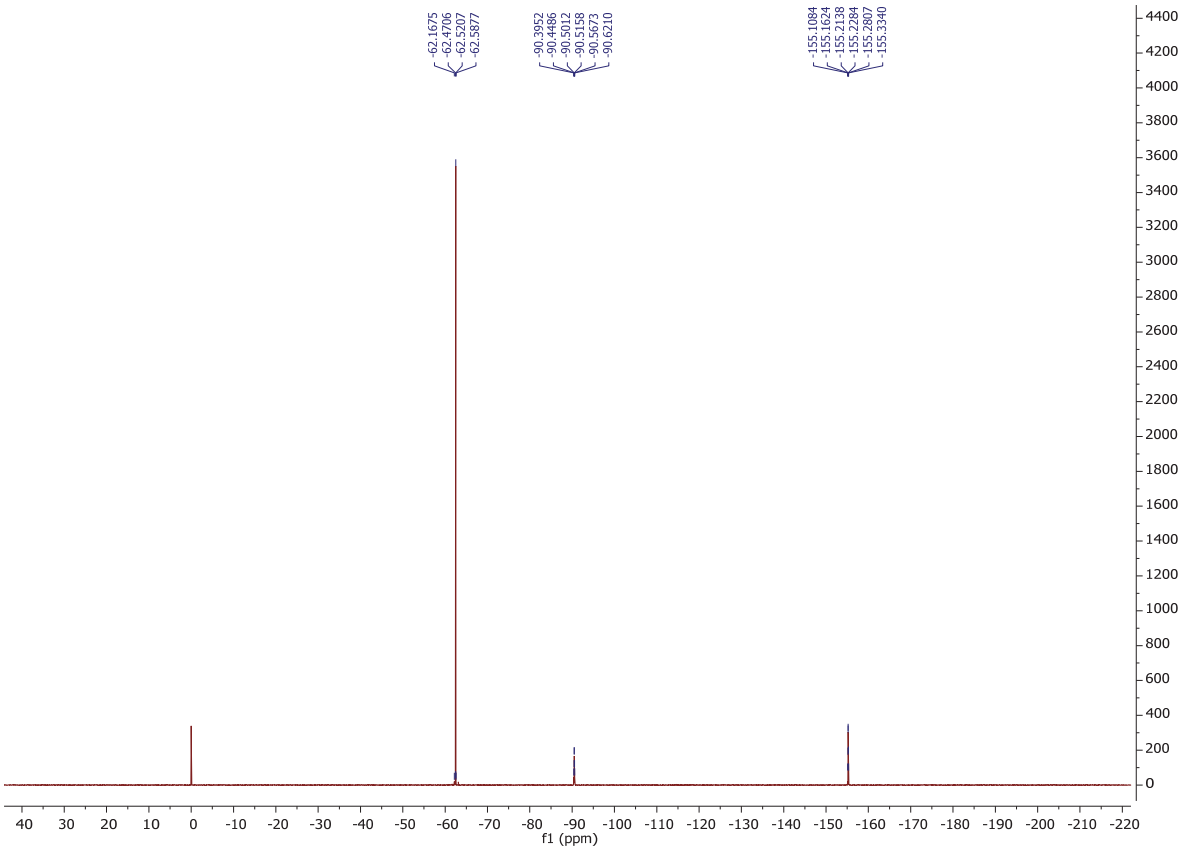

*Figure S16 ^{19}F NMR spectrum of **3***

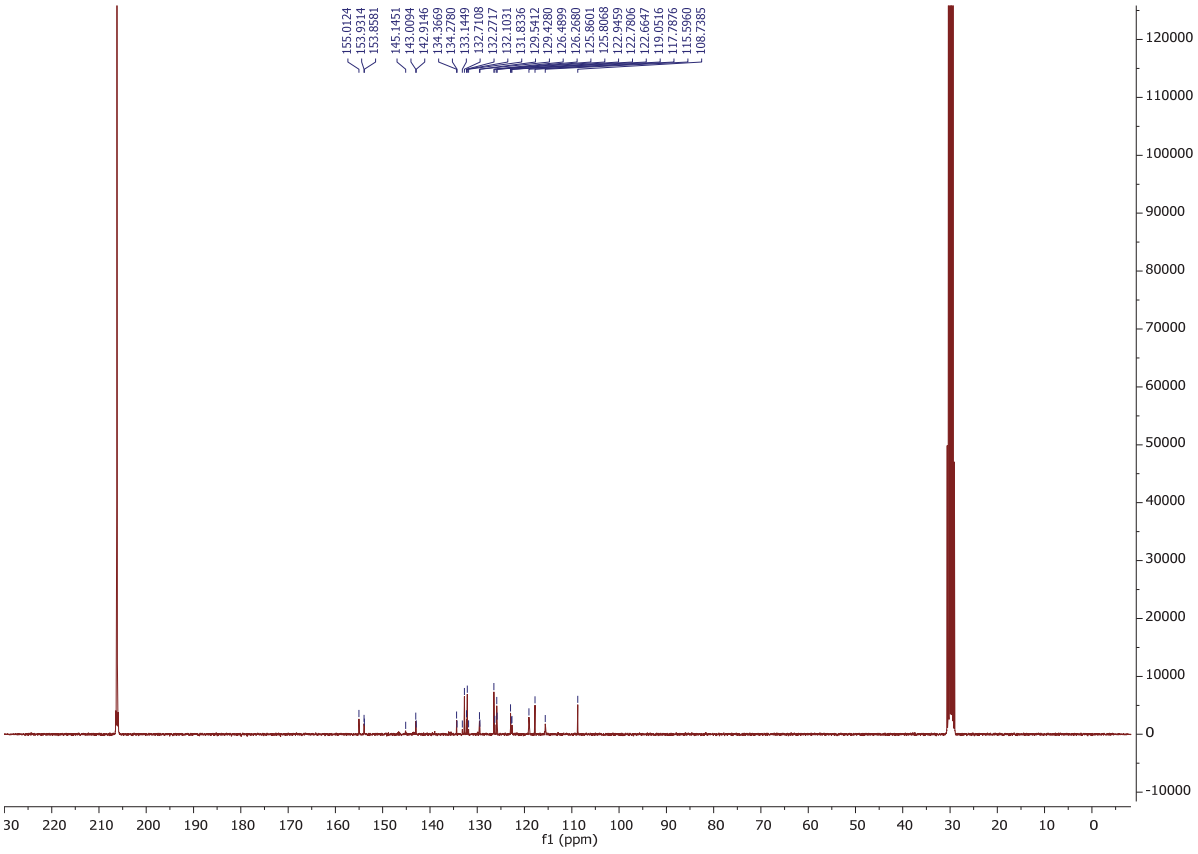

*Figure S17 ^{19}F NMR spectrum of **3***

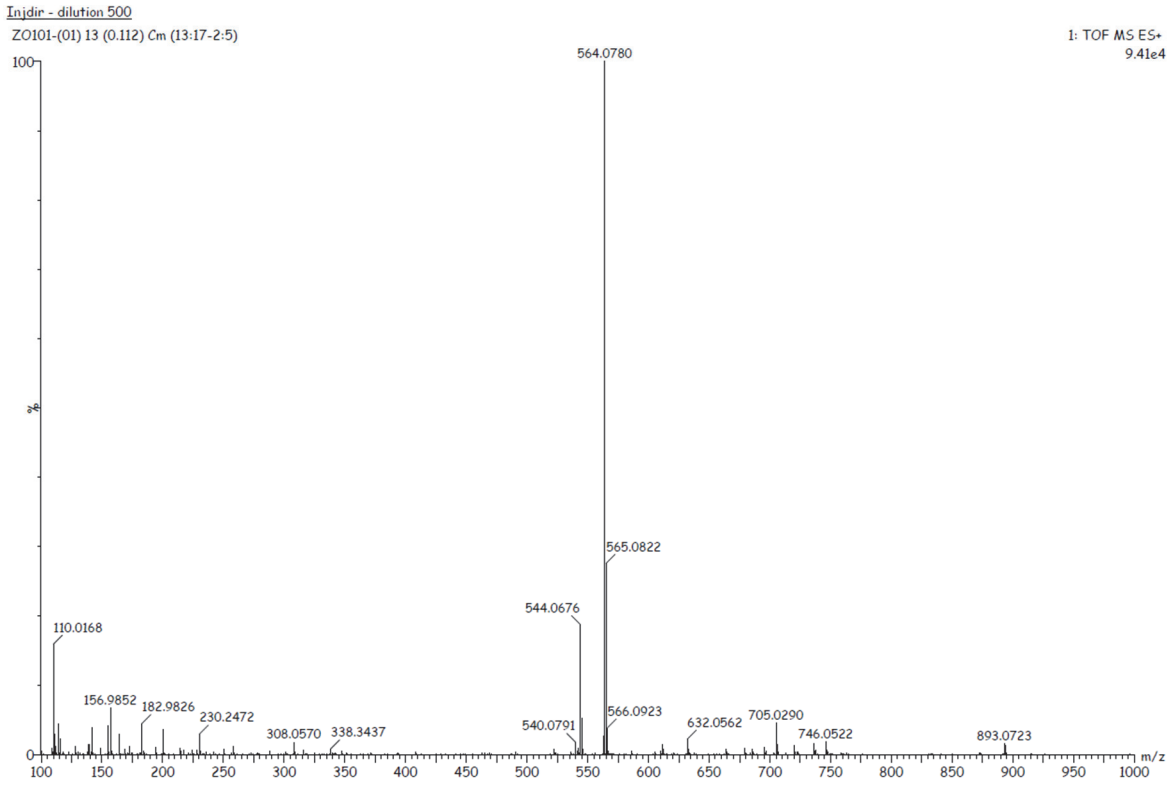

*Figure S18 High resolution mass spectrum of **3***

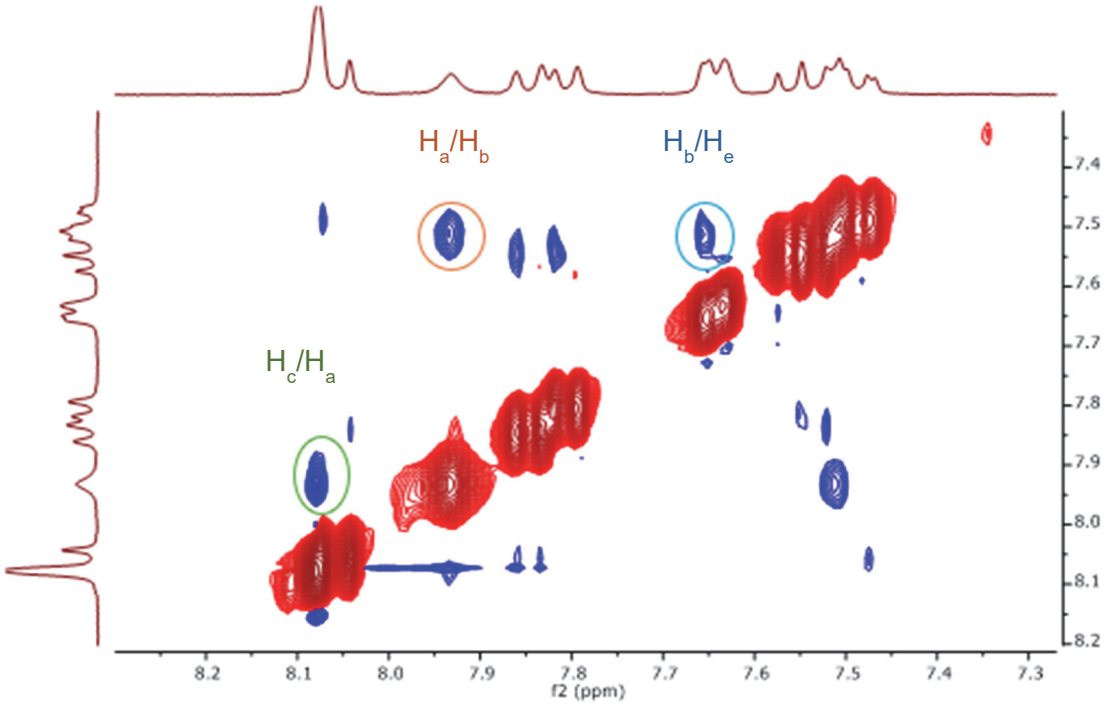

*Figure S19 NOESY spectrum of **3***

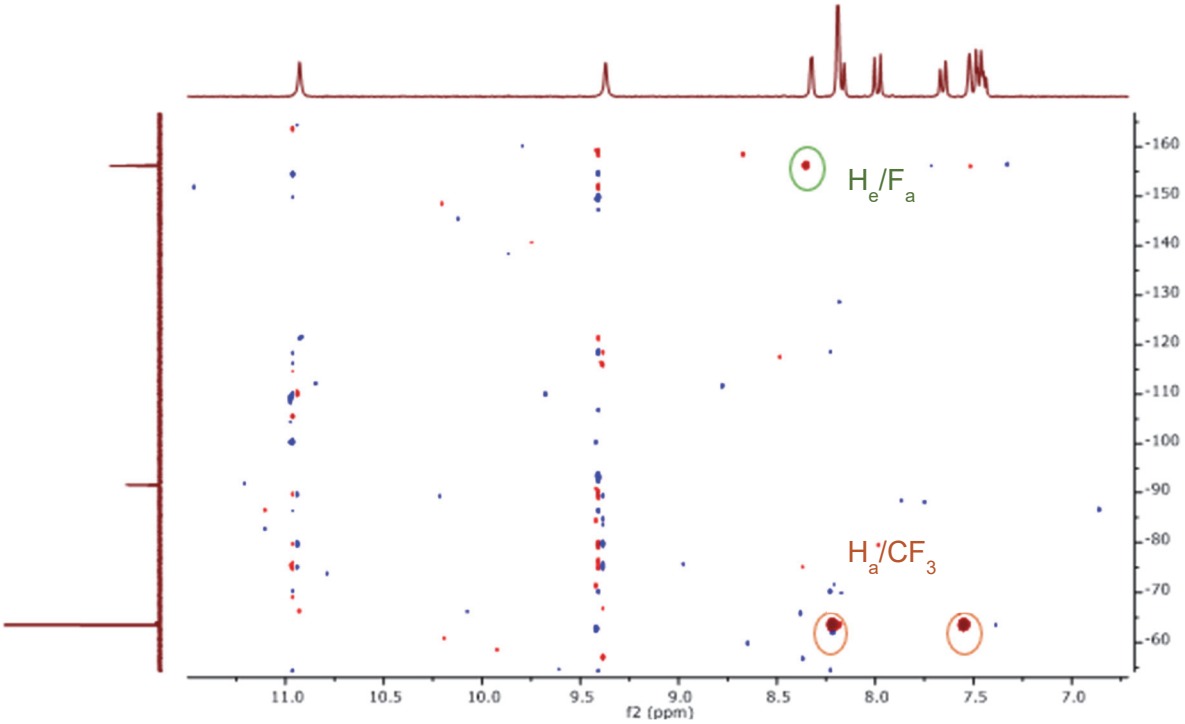

*Figure S20 HOESY spectrum of **3***

3. Mass spectrometry Analysis:

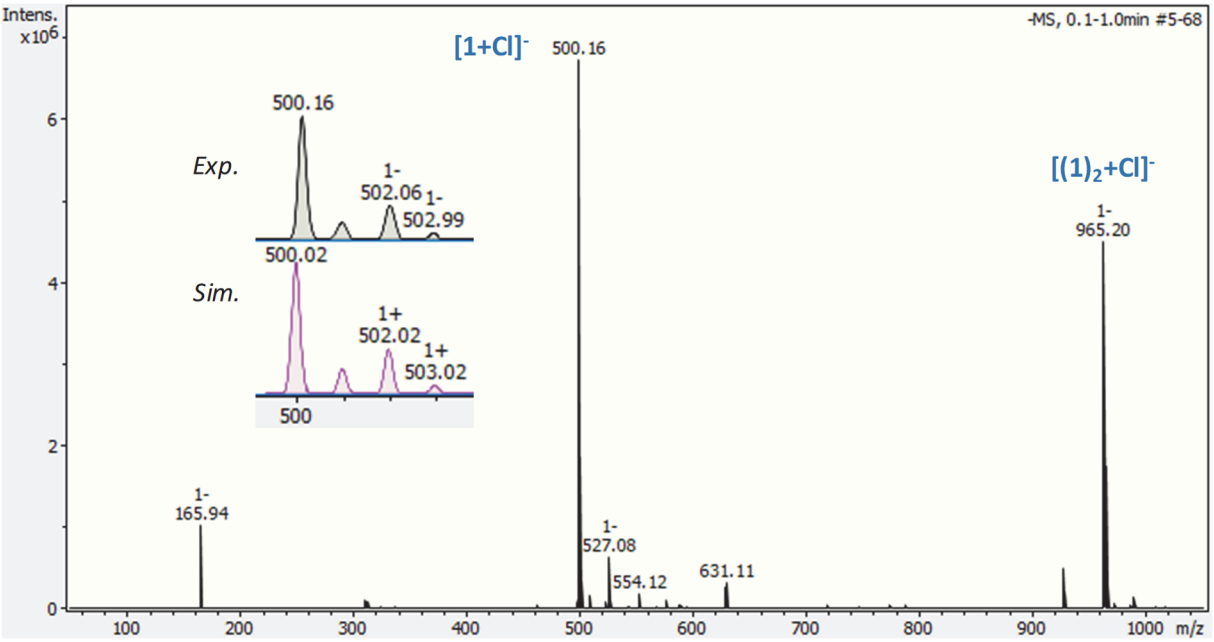

*Figure S21 Negative-ion electrospray mass spectrum of an equimolar mixture of **1**/NBu_4Cl (10^{-5}M) in a 90/10 ACN/water solution*

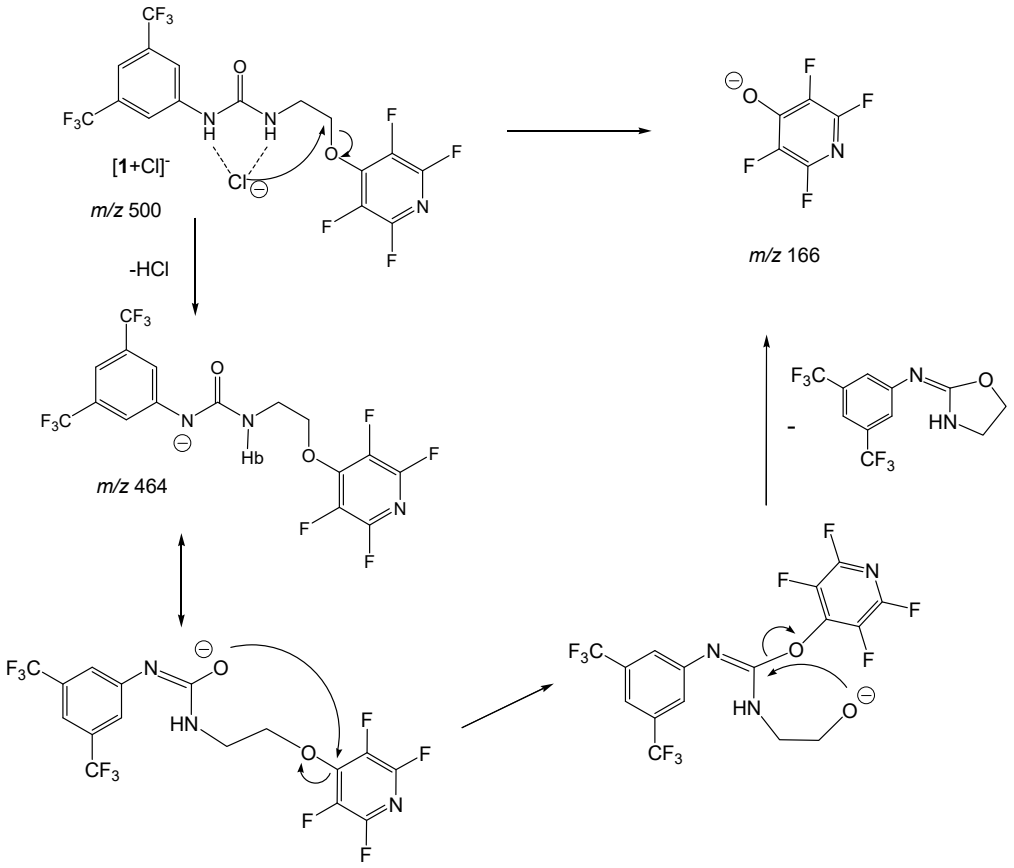

*Figure S22 Possible mechanisms of fragmentation associated with the CID spectrum of [**1**+Cl]⁻*

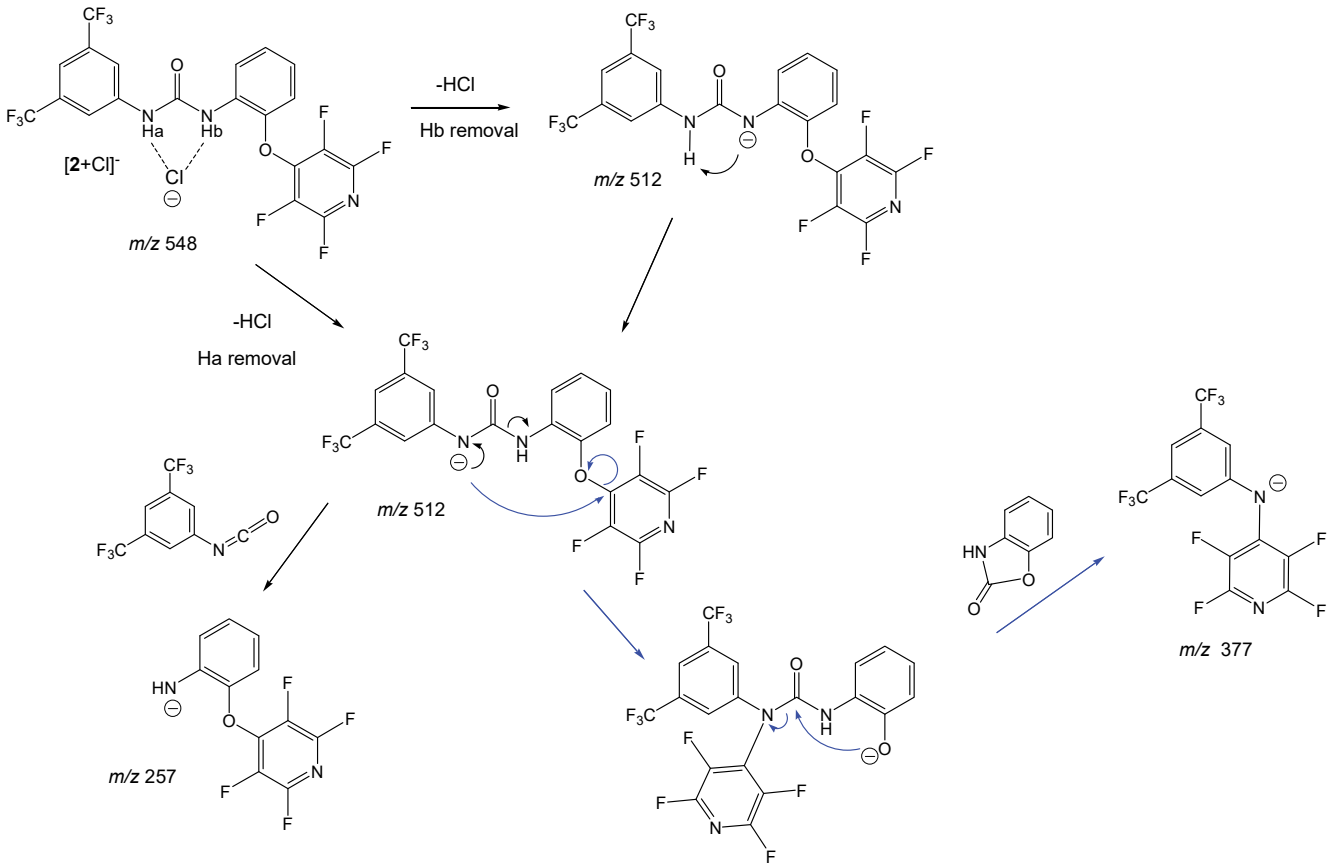

*Figure S23 Possible mechanisms of fragmentation associated with the CID spectrum of [**2**+Cl]⁻*

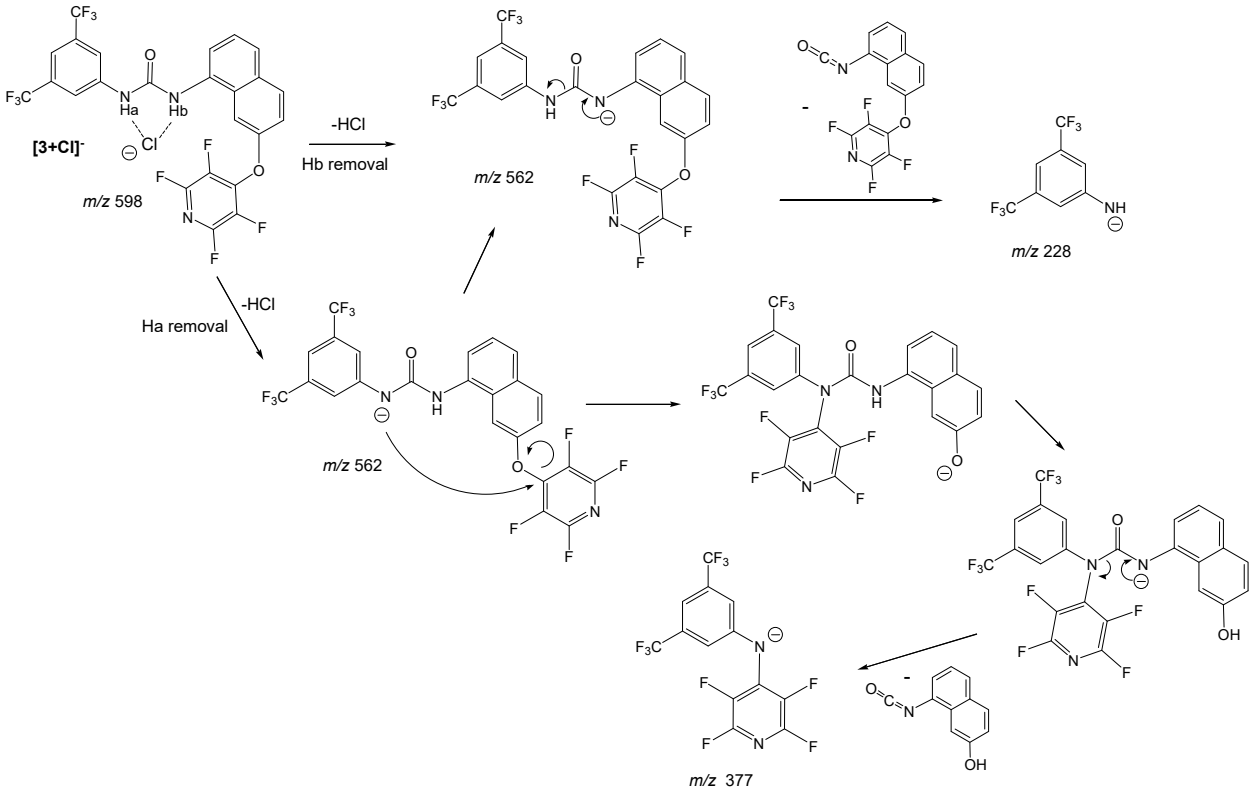

Figure S24 Possible mechanisms of fragmentation associated with the CID spectrum of [3+Cl]⁻

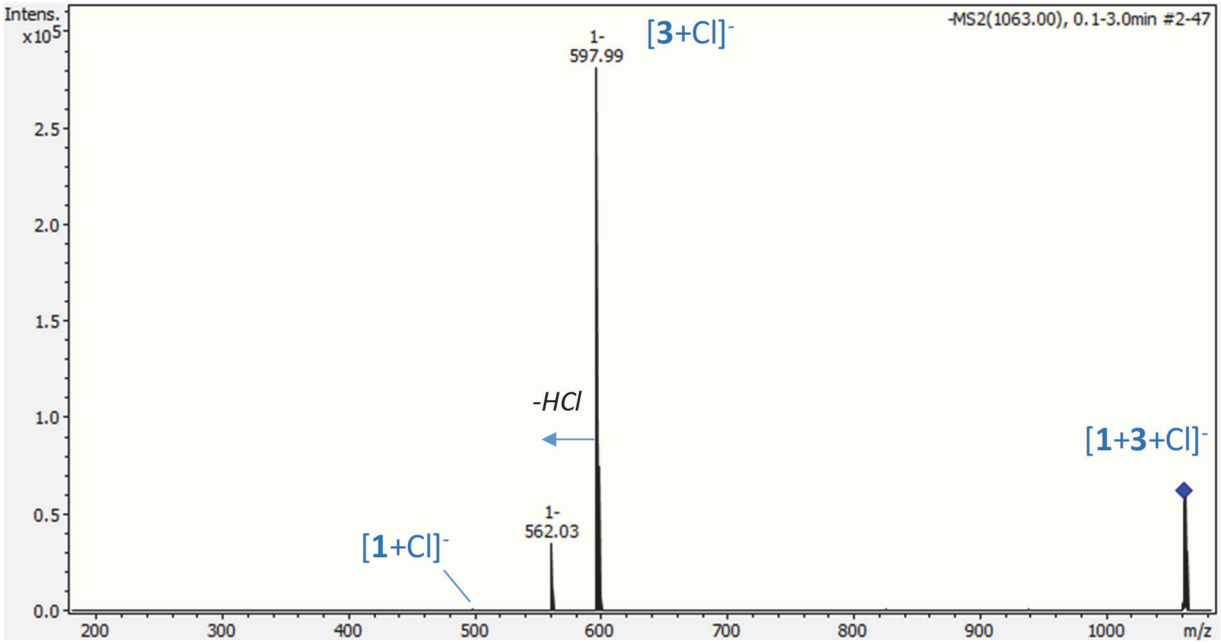

*Figure S25 Low-energy CID spectra of the [**1**+**3**+Cl]⁻ heterodimer (m/z 1063) recorded on a 3D quadrupole ion trap at an excitation amplitude of 0.50V*

4. DFT Analysis:

4.1 Interaction energies calculation :

Table S1 Interaction energies calculation at APFD/aug-cc-pVDZ (ZPE correction included)

receptor + Cl$^-$ ⟶ [**receptor**+Cl]$^-$

	$E_{complex}$ (Hartree)	E_{ligand} (Hartree)	E_{Cl^-} (Hartree)	E_{int} (kJ/mol)	BSSE (kJ/mol)
[**1**+Cl]$^-$	-2387.11321	-1926.86685	-460.173093	-192.4	2.9
[**2a**+Cl]$^-$	-2539.41082	-2079.15716	-460.173093	-211.5	
[**2b**+Cl]$^-$	-2539.41130	-2079.15241	-460.173093	-225.6	2.7
[**3**+Cl]$^-$	-2692.90489	-2232.63921	-460.173093	-243.1	3.1

$$\Delta E_{int,vacuum} = E_{complex,vacuum} - E_{ligand,vacuum} - E_{ion,vacuum}$$

4.2 Correlation HB binding energies / HB distances

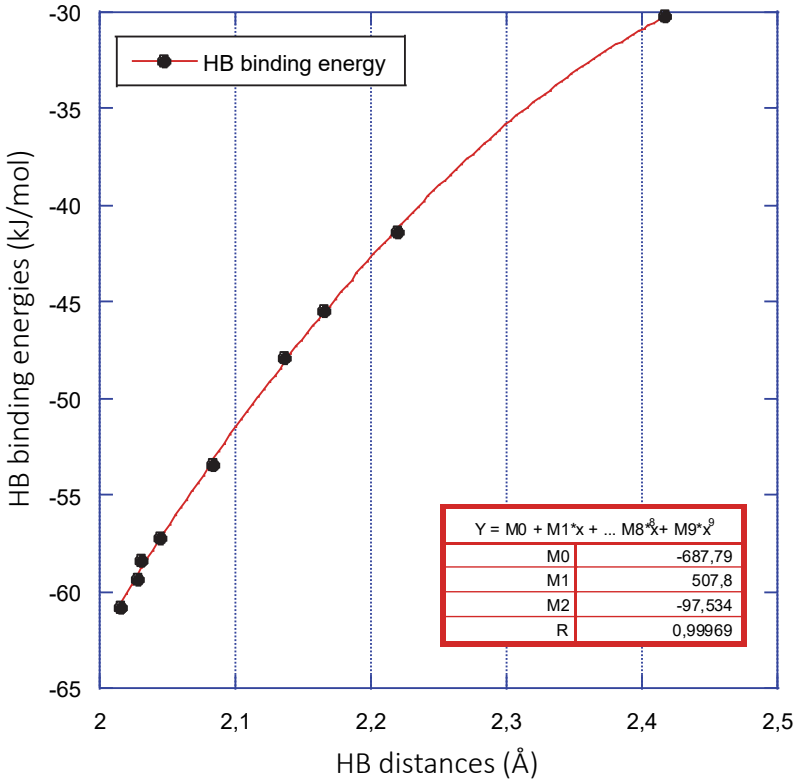

Figure S26: correlation between the hydrogen bond binding energies at the bond critical points and the hydrogen bond distances, computed for all the Cl$^-$/receptor complexes, at the APFD/aug-cc-pVDZ level.

4.3 N-H bond length evolution in function of the receptor

In order to give some additional information about the N-H bond length evolution, we have compared the evolution of both N_a-H_a and N_b-H_b bonds for different systems, urea being used as reference. The different structures considered are given below. Data are summarized in the associated table.

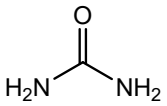

Urea

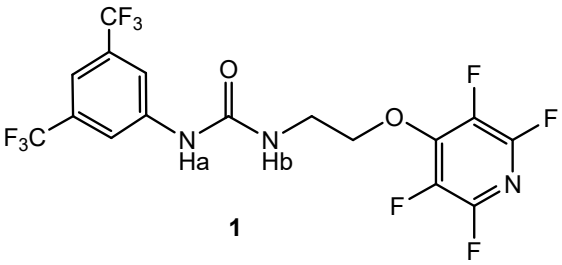

1

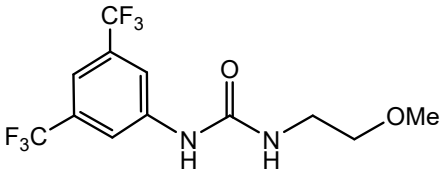

1-OMe

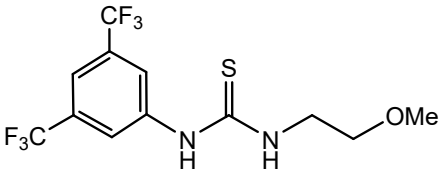

1S-OMe

Distances given in Å

M	Neutral		$[\mathbf{M}+Cl]^-$		$\Delta(N_a\text{-}H_a)$	$\Delta(N_b\text{-}H_b)$
	N_a-H_a	N_b-H_b	N_a-H_a	N_b-H_b		
Urea	1.011	1.011	1.030	1.030	0.019	0.019
1	1.011	1.011	1.044	1.034	0.033	0.023
[**1**+F]$^-$	1.011	1.011	1.098	1.041	0.087	0.030
1-OMe	1.010	1.010	1.045	1.031	0.035	0.021
1S-OMe	1.012	1.012	1.048	1.037	0.036	0.025

Two distinct effects can be observed. First, the influence of the “bis-CF3” withdrawing group can be evidenced by comparing **urea** with **1-OMe** structures. With urea, one observes a N-H bond elongation of 0.019 Å. Adding the withdrawing group clearly strengthen the two hydrogen bonds and more especially the one involving H_a, resulting in greater N_a-H_a bond elongation. Replacing oxygen of the carbonyl group by sulfur (**1S-OMe**), induces further elongation of N-H bonds, more pronounces for N_b-H_b. Finally, comparison between the methoxy form and the entire receptor shows a slight reduction of the HB strength involving Hb, because of the establishment of an interaction between chloride and the tetrafluoropyridine ring. N-H bond elongation is, as expected, much more pronounced with fluoride.

4.4 Relevant bond distances for receptors and ionic complexes

*Table S2 Comparison of selected bond distances in receptors **1-3** and their associated chloride complexes*

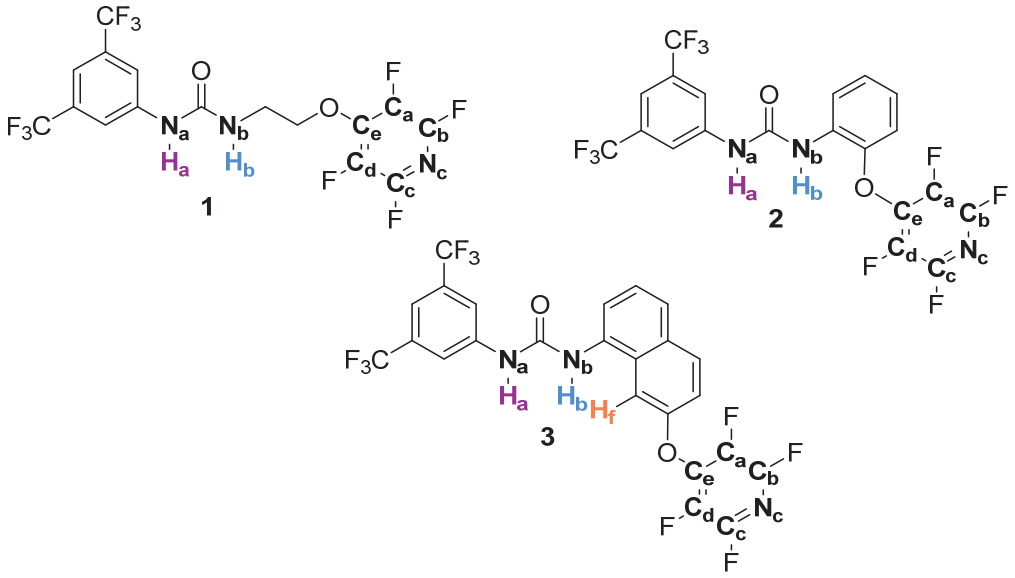

	Fragment contribution								
Entry	Urea	H-bond[a]	**1**	[**1**+Cl]$^-$	**2**	[**2a**+Cl]$^-$	[**2b**+Cl]$^-$	**3**	[**3**+Cl]$^-$
1		N_a-H_a	1.011	1.044	1.010	1.045	1.046	1.009	1.042
2		N_b-H_b	1.011	1.034	1.010	1.043	1.036	1.009	1.028
3		H_a-Cl	--	2.045	--	2.028	2.015	--	2.030
4		H_b-Cl	--	2.136	--	2.083	2.165	--	2.220
	Arom. C-H	H-bond							
5		C-H_f	--	--	--	--	--	1.088	1.095
6		H_f-Cl	--	--	--	--	--	--	2.417
7	anion-π	Cl-centroïd	--	3.409	--	4.203	3.631	--	3.291
8		C_a-Cl	--	3.956	--	5.135	3.537	--	3.565
9		C_b-Cl	--	3.825	--	4.974	4.109	--	3.518
10		N_c-Cl	--	3.602	--	4.302	4.429	--	3.559
11		C_c-Cl	--	3.377	--	3.612	4.180	--	3.548
12		C_d-Cl	--	3.465	--	3.729	3.631	--	3.581
13		C_e-Cl	--	3.778	--	4.546	3.258	--	3.548

4.5 Structure of deprotonated receptors

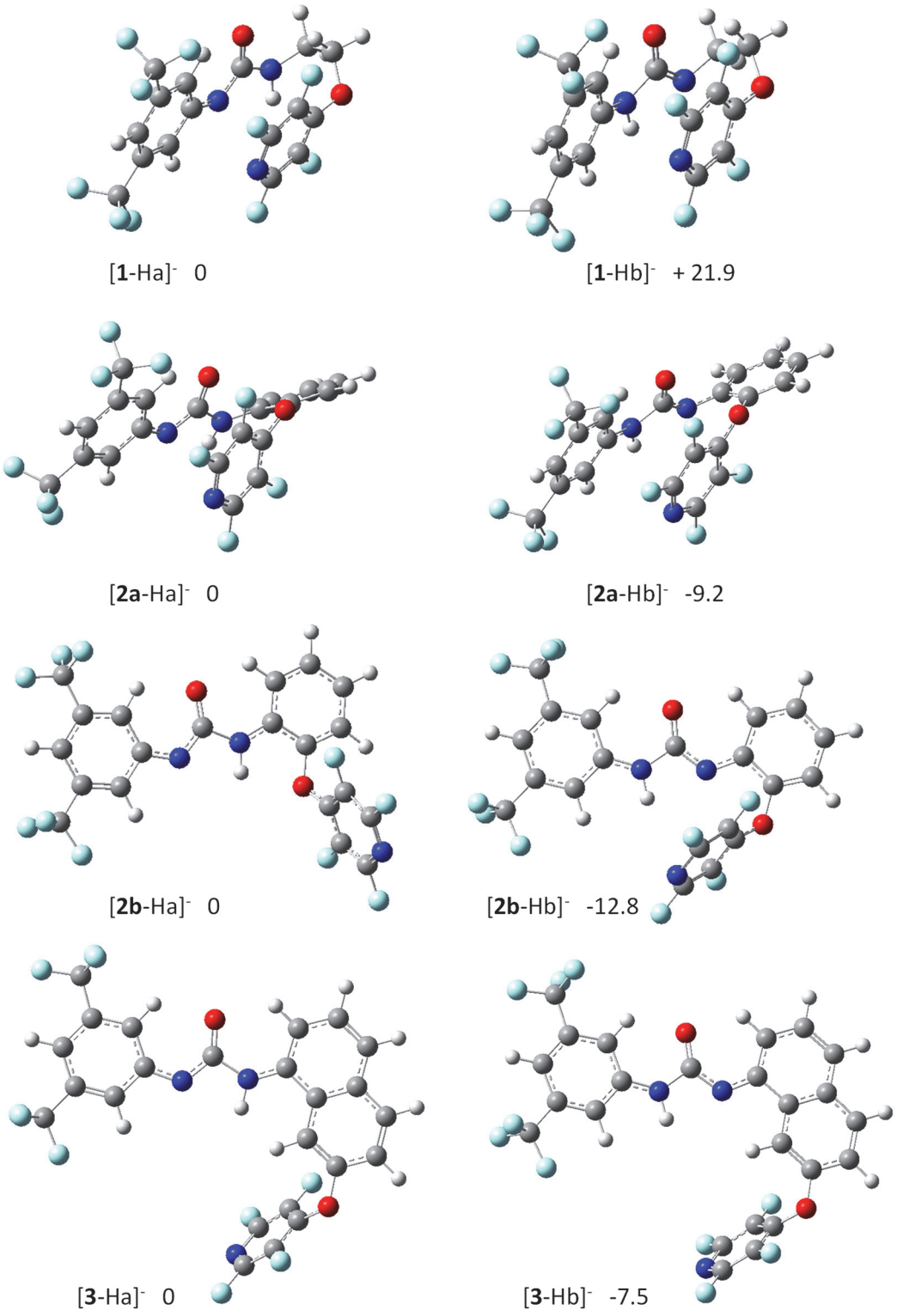

Figure S25 structure of deprotonated receptors arising from the removal of either Ha of Hb. Relative energies at the APFD/aug-cc-pvdz level given in kJ/mol.

4.6 Cartesian coordinates and thermodynamics data

Table S3 Computational data associated with the complexes studied, obtained at the APFD/aug-cc-pVDZ

Structure	E+ZPE (Hartree)	ΔE (kJ mol^{-1})	H°$_{298}$ (Hartree)	ΔH°$_{298}$ (kJ mol^{-1})	G°$_{298}$ (Hartree)	ΔG°$_{298}$ (kJ mol^{-1})
Neutral receptors						
1a	-1926.853342	+35.5	-1926.82444	+38.0	-1926.921076	+17.8
1b	-1926.866845	0	-1926.838924	0	-1926.927873	0
2a	-2079.157163	0	-2079.126547	0	-2079.222754	0
2b	-2079.152411	+12.5	-2079.121672	+12.8	-2079.222511	+0.6
3	-2232.639211	–	-2232.605619	–	-2232.713039	–
Deprotonated receptors						
[**1**-Ha]$^-$	-1926.350235	0	-1926.322449	0	-1926.413577	0
[**1**-Hb]$^-$	-1926.341897	+21.9	-1926.314176	+21.7	-1926.404097	+24.9
[**2a**-Ha]$^-$	-2078.646895	+9.2	-2078.616737	+9.6	-2078.712646	+9.7
[**2a**-Hb]$^-$	-2078.650413	0	-2078.620391	0	-2078.716322	0
[**2b**-Ha]$^-$	-2078.646248	+12.8	-2078.615869	+12.9	-2078.715576	+12.1
[**2b**-Hb]$^-$	-2078.651111	0	-2078.620783	0	-2078.720187	0
[**3**-Ha]$^-$	-2232.132630	+7.5	-2232.099563	+10.1	-2232.205606	-1.9
[**3**-Hb]$^-$	-2232.444287	0	-232.135504	0	-2232.204863	0
[**receptor**+Cl]$^-$ complexes						
[**1**+Cl]$^-$	-2387.11321	–	-2387.083213	–	-2387.180742	–
[**2a**+Cl]$^-$	-2539.410818	+1.3	-2539.378733	+0.3	-2539.478996	+8.8
[**2b**+Cl]$^-$	-2539.411302	0	-2539.378859	0	-2539.482333	0
[**3**+Cl]$^-$	-2692.904892	–	-2692.869988	–	-2692.978383	–

40

1a

C	0.00000000	0.00000000	0.00000000
N	0.00000000	0.00000000	1.39683156
C	1.16385808	0.00000000	-0.77694803
C	1.09664630	-0.05458481	2.24217162
H	-0.91449258	-0.03381137	1.82372813
C	-1.25029312	0.01379197	-0.63787563
C	1.05250587	0.01787719	-2.16668935
H	2.13714027	-0.01722022	-0.29602804
N	0.76222605	0.00564824	3.57640842
O	2.25330902	-0.16680165	1.86080517
C	-1.32744471	0.03149968	-2.02326354
H	-2.16888075	0.01688009	-0.04972799
C	2.33436832	0.02672738	-2.96110514
C	-0.17758342	0.03284345	-2.81223281
C	1.81416836	0.00781872	4.56999662
H	-0.15014066	0.34063177	3.84857619
C	-2.67583518	-0.00753579	-2.69276704
F	3.10269071	-1.04773962	-2.67265312
F	3.07838876	1.12252954	-2.68501451
F	2.11711293	0.01734905	-4.29194822
H	-0.24400246	0.04938073	-3.89732008
C	2.51246058	1.35797405	4.64628209
H	2.54403535	-0.76626366	4.30686793
H	1.37844210	-0.24988289	5.54309041
F	-3.65802567	0.46840785	-1.89455070
F	-3.02388742	-1.27280733	-3.02822475
F	-2.69562854	0.71778700	-3.83010729
O	3.48884051	1.23118949	5.69203095
H	3.00597853	1.58260535	3.69281407
H	1.80228858	2.15929288	4.89121120
C	4.51325895	2.08679753	5.75905009
C	4.55807384	3.39678976	5.25874814
C	5.65735954	1.64253211	6.44071322
C	5.71586482	4.14370419	5.44730089
F	3.50245270	3.94453744	4.63161496
C	6.74296947	2.49500325	6.56767383
F	5.68314858	0.40748739	6.94994491
N	6.77920522	3.71536450	6.08097513
F	5.74677776	5.38729480	4.96278042
F	7.82595613	2.06079165	7.21406786

40

1b

C	0.00000000	0.00000000	0.00000000
C	0.00000000	0.00000000	1.39916611
N	1.17137544	0.00000000	-0.76748145
C	-1.21359137	-0.10260193	2.07529818
H	0.93715325	0.05748411	1.94267674
C	-1.21891623	-0.04713337	-0.69037817
C	2.42492371	-0.37444557	-0.30490714
H	1.02167447	-0.07076461	-1.76458244
C	-1.20147686	-0.08197895	3.58248504
C	-2.42792096	-0.17937565	1.40477183
C	-2.41095612	-0.14012790	0.01236219
H	-1.23600325	-0.05055171	-1.78006638
N	3.23821002	-0.90011359	-1.28429688
O	2.78458314	-0.25650186	0.85841460
F	-2.24331713	-0.76048614	4.10645147
F	-1.28165518	1.18662048	4.05464759
F	-0.07296475	-0.61702118	4.09105761
H	-3.36492583	-0.27306939	1.94939969
C	-3.72215927	-0.24088000	-0.72144243
C	4.44346258	-1.59566423	-0.86969523
H	2.77808134	-1.29395322	-2.09422995
F	-4.34826184	-1.40834257	-0.45939563
F	-4.57131031	0.74690867	-0.35251756
F	-3.57475422	-0.15764212	-2.06103925
C	4.15552542	-2.78265619	0.05128323
H	4.95365774	-1.92837153	-1.78115805
H	5.10607448	-0.89774957	-0.34127588
O	3.12498110	-3.61208908	-0.53355392
H	3.85182783	-2.43639464	1.04200703
H	5.03900134	-3.42467018	0.14332024
C	1.85617382	-3.43042601	-0.13223107
C	0.86499062	-3.25537947	-1.10590162
C	1.41522425	-3.47849028	1.19798933
C	-0.46433835	-3.17216330	-0.71991765
F	1.21714030	-3.13579030	-2.39802316
C	0.05338052	-3.35694488	1.45530934
F	2.28193969	-3.67077312	2.19812037
N	-0.86381711	-3.22322957	0.52740845
F	-1.39753397	-3.01453116	-1.66252272
F	-0.35903850	-3.39501831	2.72053938

41
[**1**+Cl]$^-$

C	0.00000000	0.00000000	0.00000000
N	0.00000000	0.00000000	1.37513308
C	1.15762247	0.00000000	-0.79289813
C	1.08657994	0.14968374	2.21583433
H	-0.92701641	0.03629940	1.85292781
C	-1.26128926	0.01356463	-0.63394537
C	1.03592237	0.01677929	-2.18238719
H	2.13095436	-0.00331258	-0.31025061
N	0.69218309	0.30394704	3.51512153
O	2.26764584	0.16401202	1.85904361
C	-1.34255473	0.02834056	-2.01627873
H	-2.16293771	0.02741463	-0.02077245
C	2.30455193	0.01623166	-2.98711052
C	-0.19819356	0.03058772	-2.81963279
C	1.63233985	0.78323026	4.48832499
H	-0.32453973	0.32937775	3.70248286
C	-2.67853253	0.02939160	-2.70245995
F	3.09409976	1.08086291	-2.70110286
F	3.05960108	-1.08715387	-2.74922641
F	2.08217927	0.04835057	-4.32352099
H	-0.27534791	0.04525766	-3.90399703
C	2.01605677	2.24214553	4.26242006
H	1.18599417	0.66220263	5.48364994
H	2.55655973	0.18722110	4.44406076
F	-2.78761993	1.04772822	-3.59596731
F	-2.87523812	-1.11237683	-3.41960085
F	-3.71655857	0.13778529	-1.85336193
O	0.89902412	3.13185313	4.46719775
H	2.44879169	2.37007640	3.26526823
H	2.74328204	2.56835931	5.01657604
C	-0.10444821	3.21194219	3.57673315
C	-1.38649801	3.43831891	4.09223433
C	-0.00380955	3.18953468	2.17708033
C	-2.45122506	3.61400011	3.22290642
F	-1.56921946	3.47414842	5.41874184
C	-1.15496105	3.35518346	1.42120821
F	1.17920944	3.02520529	1.56095098
N	-2.34588557	3.58430597	1.91610634
F	-3.66319957	3.84864293	3.73565959
F	-1.04111761	3.31742293	0.08573402
Cl	-2.40983845	0.23752298	3.24811022

45

2a

C	0.00000000	0.00000000	0.00000000
C	0.00000000	0.00000000	1.39676732
N	1.16830186	0.00000000	-0.77349941
C	-1.21913981	-0.05123902	2.07349955
H	0.93728692	0.01640350	1.94350371
C	-1.22072661	-0.02856108	-0.69166758
C	2.42962668	-0.36607117	-0.32926926
H	1.00371297	-0.06770585	-1.76800394
C	-1.17019456	-0.08326060	3.57967030
C	-2.43391013	-0.08938918	1.40513342
C	-2.41442480	-0.07267833	0.00992308
H	-1.23735923	-0.04137294	-1.78137095
N	3.30530937	-0.63758527	-1.36391716
O	2.74381572	-0.48248966	0.84132559
F	-0.53685459	-1.18914562	4.02934455
F	-0.49624750	0.98047348	4.07533267
F	-2.39868388	-0.07162058	4.13653733
H	-3.37425692	-0.13477473	1.94953499
C	-3.72943106	-0.12258267	-0.72205637
C	4.52971123	-1.30670562	-1.15771929
H	3.05423271	-0.41762405	-2.31722903
F	-4.42713827	-1.23724061	-0.41220270
F	-4.51545712	0.93044082	-0.39527362
F	-3.57881261	-0.10399615	-2.06322805
C	5.70027637	-0.77097885	-1.69985369
C	4.60986545	-2.53505995	-0.47960036
C	6.92409679	-1.41888435	-1.56247673
H	5.63492575	0.18406212	-2.22320995
C	5.83624857	-3.16882714	-0.30815845
O	3.54216441	-3.16828169	0.13727475
C	6.99288905	-2.61674129	-0.85042770
H	7.82337184	-0.97899767	-1.99397955
H	5.85953600	-4.10696817	0.24545518
C	2.30904286	-3.20555456	-0.39325558
H	7.94725014	-3.12718208	-0.71851075
C	1.22802612	-3.19558933	0.49722789
C	2.00893272	-3.29532139	-1.75843791
C	-0.06061266	-3.23024661	-0.02134867
F	1.44023423	-3.12343068	1.80607837
C	0.67470517	-3.30694971	-2.14149497
F	2.98531556	-3.33598500	-2.67528330
N	-0.33434707	-3.27585257	-1.30553009
F	-1.08988674	-3.18941676	0.82167324
F	0.39090087	-3.34359143	-3.44883517

46
[**2a**+Cl]$^-$

C	1.09096200	0.01376400	-1.08519300
N	-0.20847600	0.32676300	-1.42192300
C	1.56046000	-1.28951200	-0.86575900
C	-1.29851200	-0.51699000	-1.34543400
H	-0.44856500	1.34097800	-1.49063200
C	1.98063400	1.09698800	-0.92439800
C	2.88714300	-1.48296400	-0.48100800
H	0.87873600	-2.12781200	-0.97534200
N	-2.47619100	0.19177800	-1.42126500
O	-1.24676600	-1.73519600	-1.20123500
C	3.29211800	0.86530600	-0.54529900
H	1.61362500	2.11227000	-1.07635300
C	3.33725300	-2.89646200	-0.24159400
C	3.77207800	-0.42696000	-0.31384800
C	-3.70421600	-0.36256200	-1.05082200
H	-2.39877100	1.22463500	-1.54481600
C	4.25088300	2.00912600	-0.37670300
F	4.63793100	-2.97862300	0.13051500
F	3.20572400	-3.66619600	-1.35311200
F	2.61644800	-3.50621100	0.72810900
H	4.80129300	-0.59482900	-0.00672400
C	-4.81670100	-0.18488400	-1.88043600
C	-3.90318900	-1.02929600	0.17290500
F	4.86406800	1.98159900	0.83455200
F	5.25276700	1.96242800	-1.29931900
F	3.66924700	3.21672000	-0.49739600
C	-6.07033900	-0.68500600	-1.53853700
H	-4.66470400	0.35322800	-2.81661600
C	-5.14344200	-1.56392100	0.50540800
O	-2.90142800	-1.25829700	1.10334700
C	-6.23100300	-1.39622300	-0.34852300
H	-6.91711800	-0.53188800	-2.20927500
H	-5.24099400	-2.09124400	1.45441300
C	-1.97684400	-0.32344000	1.39857900
H	-7.20298300	-1.80996000	-0.07568500
C	-2.20977200	1.05443600	1.47409700
C	-0.69276100	-0.77478200	1.72785400
C	-1.15517700	1.88750000	1.82925200
F	-3.42521900	1.55175800	1.22641400
C	0.27002500	0.16491300	2.06383500
F	-0.41105800	-2.07818400	1.71433000
N	0.05234700	1.45785700	2.11560300
F	-1.38273500	3.19303100	1.94377900
F	1.50367300	-0.26022800	2.36272600
Cl	-1.47199700	3.09051500	-1.56143500

45

2b

N	-1.25147500	0.02901400	-0.25583200
C	-0.53299300	1.21631500	-0.27042500
C	-2.63246000	-0.12926400	-0.12249200
N	0.82065700	0.99334800	-0.41650700
O	-1.04255800	2.31909500	-0.16541200
H	-0.73444300	-0.83218500	-0.35850300
C	-3.52882800	0.93496900	0.02527200
C	-3.12531900	-1.44419100	-0.13843400
C	1.83482200	1.95101200	-0.48513800
H	1.14919900	0.04157300	-0.50130200
C	-4.89054100	0.66265200	0.15416600
H	-3.16213700	1.95644600	0.04032900
C	-4.48542600	-1.68159900	-0.00602000
H	-2.44227900	-2.28706800	-0.25008400
C	1.65100200	3.33641900	-0.39192300
C	3.14139000	1.47117500	-0.65607300
C	-5.81679700	1.84111500	0.32007300
C	-5.39252700	-0.63219400	0.14130100
C	-5.00997800	-3.09171300	-0.07311100
C	2.75093800	4.19030800	-0.46694300
H	0.64795200	3.72808300	-0.25607800
C	4.23712300	2.31577700	-0.74313100
O	3.26428400	0.08216500	-0.79927900
F	-5.70550200	2.70708500	-0.71255500
F	-5.53290700	2.53787500	1.44436000
F	-7.11201200	1.47319500	0.39535200
H	-6.45747800	-0.82457100	0.24684900
F	-4.05111300	-4.00995000	0.17972600
F	-5.51007800	-3.37402400	-1.29954200
F	-6.00784400	-3.29864500	0.81193300
C	4.04149400	3.69251700	-0.64050800
H	2.58845700	5.26571600	-0.38825100
H	5.23279700	1.89615600	-0.89030600
C	4.31859100	-0.52523100	-0.20952100
H	4.89483000	4.36761900	-0.70367900
C	5.05590800	-1.45120000	-0.95051700
C	4.67475300	-0.33410300	1.13162500
C	6.10204000	-2.11763100	-0.32066300
F	4.75505900	-1.67895200	-2.23016500
C	5.75077100	-1.05600200	1.63395100
F	3.98195700	0.50817300	1.90116400
N	6.44216600	-1.92219300	0.93082500
F	6.81144600	-3.00090800	-1.02192200
F	6.10055900	-0.87694000	2.90722800

46

[**2**b+Cl]$^-$

N	0.00000000	0.00000000	0.00000000
C	0.00000000	0.00000000	1.37642466
C	1.09322758	0.00000000	-0.83931756
C	1.15337099	0.03267168	2.17569003
C	-1.26446135	-0.03056141	2.00552287
H	-0.93167520	-0.04002578	-0.47428416
N	0.68083037	0.03250635	-2.15632352
O	2.26501669	-0.01888706	-0.46867873
C	1.02486801	0.03658473	3.56523441
H	2.13032097	0.05233696	1.70151060
C	-1.35203626	-0.02623630	3.38776846
H	-2.16266926	-0.05847158	1.38731559
C	1.47883907	-0.08246009	-3.27744720
H	-0.34540156	0.05722648	-2.29865327
C	2.28991752	0.07307640	4.37601332
C	-0.21158864	0.00785841	4.19648251
C	-2.69028592	-0.05801786	4.07002265
C	2.86383684	-0.32510671	-3.27262870
C	0.85033749	0.02161661	-4.53285159
F	3.08763316	-0.99472730	4.12486815
F	3.03607364	1.17362220	4.10722596
F	2.06002196	0.07857850	5.71083807
H	-0.29381253	0.01121257	5.28065704
F	-2.81553202	-1.14288549	4.88079413
F	-2.87080083	1.02560974	4.87248742
F	-3.72711402	-0.08753642	3.21307502
C	3.55785692	-0.47624721	-4.47183208
H	3.37328515	-0.39815895	-2.31654079
C	1.53850145	-0.12685362	-5.72688437
O	-0.50118788	0.38127544	-4.56074723
C	2.90918628	-0.38693299	-5.70413698
H	4.63154676	-0.67004174	-4.43601870
H	0.99023752	-0.02737670	-6.66451442
C	-1.43342747	-0.53221095	-4.87550979
H	3.46040141	-0.50660512	-6.63753197
C	-2.62672201	-0.05356702	-5.42714206
C	-1.34471209	-1.91325301	-4.66349270
C	-3.63331579	-0.95519937	-5.72721415
F	-2.77951465	1.25527017	-5.65321871
C	-2.42778275	-2.70399614	-5.01937728
F	-0.26348266	-2.46314464	-4.09984051
N	-3.54262629	-2.25184505	-5.54109629
F	-4.77335892	-0.49253784	-6.26128210
F	-2.33973125	-4.02655825	-4.81816978
Cl	-2.44292428	-0.14765662	-1.80202106

```
50
 3
 C                  0.00000000    0.00000000    0.00000000
 N                  0.00000000    0.00000000    1.39629899
 C                  1.16294565    0.00000000   -0.77830321
 C                  1.10053565    0.00040151    2.24306029
 H                 -0.91676036   -0.01375576    1.81940330
 C                 -1.25177512    0.00244630   -0.63639941
 C                  1.04941881    0.00304580   -2.16819860
 H                  2.13678824   -0.00034406   -0.29859901
 N                  0.73043847    0.02605149    3.57311101
 O                  2.25617080   -0.01555826    1.85650747
 C                 -1.33047416    0.00699777   -2.02137762
 H                 -2.16968872    0.00621144   -0.04729228
 C                  2.32976914    0.01390489   -2.96467229
 C                 -0.18135716    0.00610437   -2.81194965
 C                  1.60286975   -0.02046502    4.67555276
 H                 -0.25304419    0.06936585    3.79505195
 C                 -2.67723898   -0.04200818   -2.69361837
 F                  3.11946179   -1.03711713   -2.64723830
 F                  3.05328713    1.13097155   -2.72210052
 F                  2.11129767   -0.03815798   -4.29456828
 H                 -0.24964698    0.01227160   -3.89704178
 C                  2.79419930   -0.71936530    4.64120317
 C                  1.19394003    0.64777283    5.87009051
 F                 -3.67198136    0.38186258   -1.88353230
 F                 -2.99215294   -1.30313849   -3.07484298
 F                 -2.71163958    0.72138321   -3.80623514
 C                  3.60538315   -0.80202969    5.79260250
 H                  3.10275370   -1.20751351    3.72040561
 C                  0.02358424    1.44713017    5.93242582
 C                  2.00114550    0.50963219    7.04071972
 C                  3.21317961   -0.22001272    6.97619917
 H                  4.54278607   -1.35667519    5.73738859
 C                 -0.35055527    2.01957828    7.12367221
 H                 -0.56044347    1.64821987    5.03568121
 C                  1.57059019    1.12992966    8.24342170
 H                  3.82762361   -0.30746784    7.87321819
 C                  0.41064530    1.86287612    8.29934544
 O                 -1.46096983    2.84516511    7.26108754
 H                  2.18318542    1.01463672    9.13876155
 H                  0.07312976    2.33967689    9.21876491
 C                 -2.41574029    2.83478670    6.30871367
 C                 -2.80384376    4.04845176    5.73596540
 C                 -3.10692945    1.68267766    5.90787578
 C                 -3.83611994    4.04232884    4.80228787
 F                 -2.18857627    5.17901935    6.07882092
 C                 -4.10586344    1.81342906    4.95154705
 F                 -2.80497031    0.49192188    6.43260362
 N                 -4.46286370    2.95651214    4.41562696
 F                 -4.20809385    5.19662332    4.25266380
 F                 -4.74969815    0.71534167    4.54744863
```

51

[**3**+Cl]$^-$

H	0.00000000	0.00000000	0.00000000
N	0.00000000	0.00000000	1.04187612
C	1.23192299	0.00000000	1.65718711
C	-1.24192168	0.00494183	1.64555191
C	1.43225829	0.00151684	3.04642015
C	2.35983334	-0.00158576	0.80646160
N	-2.23835356	0.00578560	0.68934955
O	-1.42213427	0.00806106	2.86079732
C	2.73310253	0.00194870	3.55165992
H	0.57209429	0.00243459	3.70930797
C	3.63569154	-0.00101465	1.34514544
H	2.20918392	-0.00333423	-0.27387175
C	-3.61209261	0.01117147	0.89547747
H	-1.88959617	0.00496419	-0.27778846
C	2.89354490	0.00465293	5.04615301
C	3.85015915	0.00083159	2.72703873
C	4.84368502	-0.00147164	0.45155696
C	-4.18897020	0.02279929	2.15945926
C	-4.46359729	0.00347381	-0.26668931
F	2.31175977	-1.07598122	5.62345491
F	2.32077331	1.09304713	5.61828697
F	4.19057876	0.00033483	5.43641401
H	4.85699090	0.00113526	3.13745542
F	5.63565137	-1.08367777	0.67821233
F	5.63133567	1.08554215	0.67190907
F	4.53948296	-0.00566331	-0.85887950
C	-5.59012986	0.02834541	2.31509025
H	-3.54064778	0.02675088	3.02960736
C	-3.94808228	-0.00572030	-1.58946524
C	-5.88233379	0.01023787	-0.07936952
C	-6.43112856	0.02256203	1.22735402
H	-6.00180646	0.03718803	3.32637069
C	-4.81289019	-0.02641845	-2.65651945
H	-2.87168087	0.00501380	-1.79154126
C	-6.72535049	0.00521007	-1.22149556
H	-7.51568450	0.02699753	1.34921066
C	-6.21133259	-0.01579524	-2.49514751
O	-4.37690820	-0.00264598	-3.97958228
H	-7.80641461	0.01175271	-1.06946472
H	-6.85168528	-0.02675621	-3.37699787
C	-3.17168343	-0.53512499	-4.28357689
C	-2.28275509	0.21292176	-5.05519266
C	-2.78784697	-1.83745763	-3.94736174
C	-1.08820946	-0.37506937	-5.44786302
F	-2.58678423	1.46733357	-5.40622025
C	-1.55731430	-2.29773068	-4.39325576
F	-3.59915296	-2.61988620	-3.22570472
N	-0.73751298	-1.59870792	-5.13922639
F	-0.24273839	0.33595498	-6.20328308
F	-1.19270999	-3.54677347	-4.08195910
Cl	-0.46173298	0.01294645	-1.97722933

39

[**1**-Ha]$^-$

C	0.00000000	0.00000000	0.00000000
C	0.00000000	0.00000000	1.39272450
C	1.24704938	0.00000000	2.02720194
C	2.43030929	0.00898904	1.30825953
C	2.44175705	0.02891430	-0.11326474
C	1.17158500	-0.00016204	-0.75253261
N	3.66461853	0.14058256	-0.69754030
C	3.79386976	0.19347728	-2.03580426
N	5.11760354	0.51014602	-2.39828066
C	5.37878782	1.08312926	-3.69181663
C	4.55156258	2.33108795	-4.00294033
O	4.72409928	3.33590064	-2.97246864
C	3.91227541	3.26131448	-1.90260251
C	-1.30968842	-0.05303238	-0.73012105
F	-2.35059235	0.40127937	0.01714638
F	-1.64488533	-1.32514459	-1.09465824
F	-1.31104224	0.67246346	-1.87199977
C	1.27326883	-0.03751599	3.52442118
F	2.48799490	0.23425563	4.05289262
F	0.91319925	-1.26079288	4.01570259
F	0.40195158	0.84553418	4.08260023
H	-0.92528636	0.01061395	1.96316984
H	3.39167008	0.03592481	1.81874330
H	1.13689079	0.00098903	-1.83817631
H	5.66879635	0.85018785	-1.62277370
H	6.45064494	1.31918278	-3.74722066
H	5.15171395	0.34817037	-4.48055090
H	3.49636639	2.05908354	-4.09656222
H	4.89690757	2.81283283	-4.92712582
C	1.78954295	3.28784175	-0.77587748
C	2.51128664	3.29857218	-1.96159686
C	4.47419431	3.21843769	-0.62377669
C	3.64058759	3.21444596	0.48350320
N	2.33272724	3.26278339	0.41758203
F	5.80696332	3.14867184	-0.48352585
F	1.87850849	3.39143472	-3.14097023
F	0.45570998	3.34837742	-0.84160691
F	4.19262964	3.16478946	1.70266969
O	2.95767421	0.03407869	-2.95282623

39

[**1**-Hb]$^-$

C	0.00000000	0.00000000	0.00000000
C	0.00000000	0.00000000	1.39590681
C	1.23740602	0.00000000	2.03381285
C	2.42768761	0.00714271	1.31782442
C	2.41835847	0.02103373	-0.09176451
C	1.16792333	-0.00313263	-0.74877084
N	3.61139832	0.07397371	-0.75740127
C	3.84220551	0.48262187	-2.11702240
N	5.06835610	0.96053326	-2.23100691
C	5.38988207	1.47588375	-3.53260798
C	4.55832871	2.70061327	-3.92212395
O	4.56693922	3.69370506	-2.85668099
C	3.74658004	3.47274576	-1.82297857
C	-1.32581843	-0.03676751	-0.70499679
F	-2.24755761	0.76183892	-0.10691385
F	-1.86553403	-1.29117157	-0.69691131
F	-1.25836539	0.33984208	-1.99578957
C	1.29133043	-0.05364977	3.53177643
F	2.37955415	0.56657359	4.04387910
F	1.33936885	-1.33703260	3.99336306
F	0.20683751	0.51076772	4.11546348
H	-0.92775654	0.01565882	1.96203228
H	3.37787897	0.04268796	1.85106310
H	1.16141343	0.01422903	-1.83561810
H	4.43634751	0.22886972	-0.19294745
H	6.45678069	1.74954730	-3.53939271
H	5.22766293	0.73973909	-4.34866702
H	3.52849564	2.40281342	-4.13984563
H	4.98762997	3.22981811	-4.78325683
C	1.59069639	3.24039727	-0.77398602
C	2.34964462	3.35591754	-1.92995794
C	4.26037745	3.48237477	-0.51746078
C	3.38940368	3.35169010	0.55117460
N	2.08453043	3.24058082	0.44088650
F	5.57573566	3.60698724	-0.31472465
F	1.74613785	3.42052077	-3.12571232
F	0.25785085	3.15531670	-0.89212256
F	3.89726386	3.33056301	1.79705308
O	2.91530586	0.37972404	-2.95573675

43

[**2a**-Ha]$^-$

C	0.00000000	0.00000000	0.00000000
C	0.00000000	0.00000000	1.39124072
C	1.24701056	0.00000000	2.02752220
C	2.43068483	0.00514723	1.30895115
C	2.44112042	0.01357950	-0.11201246
C	1.17314135	-0.00295594	-0.75192318
N	3.66884389	0.08880935	-0.70004447
C	3.78422596	0.09608080	-2.03627096
N	5.13691628	0.33120172	-2.39881047
O	3.81477883	2.37873665	-4.09733631
C	3.58442919	2.77751428	-2.83508446
C	-1.30433359	-0.03685744	-0.74214956
F	-1.33944413	0.82360632	-1.78535654
F	-2.37038419	0.26597440	0.04467909
F	-1.56387633	-1.26958072	-1.26300301
C	1.26828795	-0.03330299	3.52520716
F	2.49486006	0.17640555	4.05497904
F	0.84192543	-1.23243124	4.01947357
F	0.44437921	0.89844214	4.07686578
H	-0.92541377	0.00906867	1.96153353
H	3.39222007	0.02293107	1.81928920
H	1.13585214	-0.00582501	-1.83771245
H	5.81193897	0.21778773	-1.65695178
C	1.97852700	3.26275162	-1.12194600
C	2.25041414	2.83655745	-2.41350994
C	4.55524563	3.20204244	-1.92117315
C	4.14535664	3.58604964	-0.65295632
N	2.89840634	3.62857187	-0.25781952
F	5.85423171	3.24021956	-2.25765344
F	1.26951714	2.48661068	-3.24265895
F	0.70572904	3.32243065	-0.71988037
F	5.08389680	3.96823170	0.22753783
C	6.59750328	1.39235734	-6.21152744
C	7.27209136	0.46405223	-5.41691718
C	6.75731285	0.11718168	-4.17162784
C	5.58007127	0.68782057	-3.66035234
C	4.95424971	1.67357978	-4.45599296
C	5.44006497	1.99187231	-5.72020611
H	6.97221932	1.65891652	-7.20070201
H	8.18707011	-0.01039109	-5.77610710
H	7.25370823	-0.64127831	-3.56339718
H	4.90248604	2.74390238	-6.29835189
O	2.95300293	-0.03224897	-2.95196976

43

[**2a**-Hb]$^-$

C	0.00000000	0.00000000	0.00000000
C	0.00000000	0.00000000	1.39129317
C	1.24036722	0.00000000	2.03123153
C	2.42836481	0.00148742	1.31660150
C	2.41857810	0.00589653	-0.09486555
C	1.17177044	-0.00420328	-0.75039988
N	3.62017984	0.03543343	-0.75304731
C	3.85851698	0.39063835	-2.11731559
N	5.14399982	0.70973744	-2.27354066
O	3.78240766	3.06718440	-3.43700935
C	3.61497996	3.18121728	-2.11776882
C	-1.30195820	-0.01447511	-0.75140745
F	-1.36358303	0.94683684	-1.69788677
F	-2.37662794	0.16376659	0.05770883
F	-1.50223483	-1.19653882	-1.39370392
C	1.26842039	-0.04104522	3.53081791
F	2.46813567	0.30060015	4.05158474
F	0.98636101	-1.28643192	4.00871861
F	0.34851329	0.78525452	4.08667103
H	-0.92606497	0.01309788	1.95963439
H	3.37899526	0.02854457	1.84862236
H	1.15857648	0.01365421	-1.83741148
C	2.08493647	3.25867070	-0.26595635
C	2.30027193	3.13411743	-1.62975183
C	4.62647631	3.40288981	-1.16997190
C	4.26885809	3.49161157	0.16657600
N	3.03974876	3.42553817	0.62121102
F	5.90262255	3.55173480	-1.53925253
F	1.27851668	2.96619554	-2.46921377
F	0.82845920	3.20278588	0.19541186
F	5.24421845	3.67343330	1.07501268
C	6.54598366	2.63069434	-5.77228102
C	7.19527343	1.51096501	-5.24435204
C	6.70048274	0.88508428	-4.10474283
C	5.53716288	1.32332191	-3.43554224
C	4.93535849	2.48737099	-3.97986543
C	5.41264856	3.11745497	-5.12113294
H	6.91853154	3.12616725	-6.67008018
H	8.09201235	1.11828289	-5.72934276
H	7.19956728	0.00830309	-3.68909780
H	4.88415724	3.99993266	-5.48470515
O	2.92406455	0.37247526	-2.93466425
H	4.44982620	0.13997531	-0.18517812

43

[**2b**-Ha]$^-$

C	0.00000000	0.00000000	0.00000000
C	0.00000000	0.00000000	1.39156225
C	1.24814052	0.00000000	2.02706191
C	2.43102974	-0.00046903	1.30724888
C	2.44278065	-0.00000093	-0.11562458
C	1.17327539	0.00007904	-0.75364071
N	3.67345554	0.00013573	-0.69940216
C	3.80573441	-0.00177511	-2.03536520
N	5.19495558	-0.00179312	-2.34706921
O	7.89881032	-0.06522521	-2.37395479
C	8.78907302	0.89376049	-2.09784188
C	-1.30141085	0.00192872	-0.74845014
F	-1.43852555	1.09199449	-1.54819459
F	-2.38679384	-0.00726814	0.06824718
F	-1.43231462	-1.07652972	-1.56462138
C	1.26529616	-0.00992691	3.52511195
F	2.50816335	0.04669662	4.05460669
F	0.68030190	-1.12842119	4.04064720
F	0.57338224	1.03710405	4.05638325
H	-0.92506651	0.00078955	1.96259066
H	3.39325771	-0.00076826	1.81687910
H	1.13603814	0.00063615	-1.83972001
H	5.78019610	-0.01741118	-1.52445245
C	8.67076716	2.24975132	-2.44718796
C	9.67878655	3.12134889	-2.05446088
C	10.84142778	1.51335610	-1.01091374
C	9.91761276	0.53554777	-1.34626279
F	9.56930136	4.41121532	-2.39423910
F	7.61173153	2.70234285	-3.11909703
F	11.92109338	1.16131294	-0.30048217
F	10.09414773	-0.73686276	-0.97426305
N	10.73604712	2.77543610	-1.35693399
C	5.81003435	-0.01339829	-3.56689015
C	7.21884827	-0.01039953	-3.61331766
C	5.14710769	-0.01634408	-4.81399337
C	7.94515692	-0.01904424	-4.79375431
C	5.87063228	-0.01254490	-6.00232766
C	7.26884852	-0.01293477	-6.01359543
H	4.06036841	-0.01264333	-4.80225168
H	5.32321726	-0.01012565	-6.94718661
H	7.82559833	-0.01668986	-6.95108099
H	9.03566441	-0.03116769	-4.74855324
O	2.96891833	-0.00267668	-2.95456044

43

[**2b**-Hb]$^-$

C	0.00000000	0.00000000	0.00000000
C	0.00000000	0.00000000	1.39207619
C	1.24150910	0.00000000	2.03207673
C	2.42985211	-0.00106018	1.31798015
C	2.42029180	-0.00156298	-0.09596666
C	1.17202540	-0.00017235	-0.75108434
N	3.62010754	-0.00557501	-0.74973818
C	3.89610107	0.01942250	-2.14930199
N	5.22372163	0.00976731	-2.31179138
O	7.93118620	-0.01703703	-2.34595548
C	7.56660372	0.70020877	-1.28070213
C	-1.30252403	0.02581299	-0.75095893
F	-1.48634952	1.19633079	-1.41261752
F	-2.37921123	-0.12856104	0.05949320
F	-1.37759967	-0.95322860	-1.68378177
C	1.26206707	-0.04047562	3.53260101
F	2.48266887	0.20330410	4.05666748
F	0.87080546	-1.25249790	4.01248760
F	0.41185383	0.86626565	4.07958049
H	-0.92603275	0.00178002	1.96104908
H	3.38130026	0.00331699	1.85008660
H	1.15914267	0.00290138	-1.83826754
C	7.15124681	2.04180977	-1.29241692
C	6.87604420	2.66305389	-0.08586074
C	7.42916974	0.85595847	1.11318756
C	7.73093175	0.11597202	-0.01734487
F	6.45490228	3.93722847	-0.10551374
F	7.00389718	2.70303743	-2.44481005
F	7.56731716	0.27579510	2.31811167
F	8.13905365	-1.15692450	0.08206066
N	7.00701473	2.09978192	1.09551230
C	5.80541556	0.07205357	-3.54303845
C	7.22410744	0.10605147	-3.55420552
C	5.19277196	0.11426269	-4.82111816
C	7.98657363	0.15621769	-4.70656760
C	5.95190643	0.16955312	-5.98866417
C	7.34867551	0.18765558	-5.95021619
H	4.10665733	0.09646361	-4.85991225
H	5.43734475	0.19745925	-6.95241773
H	7.93670015	0.22797426	-6.86833966
H	9.07400983	0.16897707	-4.62031302
O	2.95860214	0.04728189	-2.96308658
H	4.46071803	-0.01570895	-0.18946589

49

[**3**-Ha]$^-$

C	0.00000000	0.00000000	0.00000000
C	0.00000000	0.00000000	1.40530712
C	1.16992180	0.00000000	2.13551101
C	2.40888847	0.00156699	1.45077858
C	2.44012387	0.00441270	0.01806860
C	1.19737522	0.00086654	-0.71808444
C	3.63705393	-0.00245183	2.16361608
C	4.85223308	0.00664260	1.52015693
C	4.85999507	0.01636470	0.11516643
C	3.70371779	0.00321486	-0.62543515
O	6.12643394	-0.02956959	-0.48999161
C	6.34194018	0.70133262	-1.59471176
C	5.95573188	2.04126986	-1.75652177
C	6.31231101	2.69419982	-2.92936510
N	7.00911972	2.14676913	-3.89815513
C	7.38363303	0.89848338	-3.74795532
C	7.08308295	0.12647527	-2.63378155
F	8.09760881	0.34815575	-4.73528200
F	7.49290018	-1.14249583	-2.54082039
F	5.95128176	3.97141580	-3.08133263
F	5.28847408	2.68143869	-0.79342783
N	1.24740629	-0.00098338	-2.08559720
C	0.19766932	-0.01714589	-3.04923097
O	-0.98847249	-0.02164064	-2.68095777
N	0.75902480	-0.02515210	-4.27065317
C	-0.00758197	-0.04459606	-5.39641697
C	0.70089191	-0.05308330	-6.63034621
C	0.04332139	-0.07528632	-7.84866952
C	-1.35479866	-0.08957542	-7.93015511
C	-2.05751731	-0.08034766	-6.72916577
C	-1.42538895	-0.05849325	-5.48641900
C	0.81420068	-0.08319362	-9.13347998
C	-3.55869803	-0.09591181	-6.73996733
F	0.52509136	0.99524561	-9.91521348
F	0.52675921	-1.17292896	-9.90036273
F	2.15509398	-0.08102693	-8.96234678
F	-4.07080279	-1.18198849	-6.10352605
F	-4.08325109	-0.10919238	-7.99278786
F	-4.09349222	0.98645757	-6.11663011
H	-0.92847512	-0.00161377	-0.56447269
H	-0.96208363	-0.00036266	1.92267161
H	1.16099916	-0.00141122	3.22648483
H	3.60161772	-0.00720404	3.25475771
H	5.79628078	0.00961241	2.06432958
H	3.78774379	-0.00682314	-1.71193485
H	2.14502819	-0.00324030	-2.54276846
H	1.78876149	-0.04189064	-6.58543163
H	-1.86471559	-0.10699221	-8.89010301
H	-2.00605194	-0.05215225	-4.56791609

49
[**3**-Hb]$^-$

C	0.00000000	0.00000000	0.00000000
C	0.00000000	0.00000000	1.40726157
C	1.16683163	0.00000000	2.14569864
C	2.40881032	-0.00037641	1.46335692
C	2.42958675	0.00056388	0.03334701
C	1.19796985	0.00172321	-0.73493341
C	3.64500763	-0.00450854	2.16344183
C	4.85271090	0.00000544	1.50157585
C	4.84124305	0.00323177	0.09577523
C	3.67768840	-0.00738752	-0.63062999
O	6.10609111	-0.04966863	-0.53106448
C	6.28653806	0.64773189	-1.65752222
C	5.87794922	1.97718696	-1.85920111
C	6.19182626	2.58985586	-3.06482087
N	6.86893348	2.01930766	-4.03543375
C	7.26764993	0.78343723	-3.84682173
C	7.01096851	0.05015729	-2.69753876
F	7.96129867	0.20524470	-4.83641538
F	7.44326511	-1.21001852	-2.57355264
F	5.80553714	3.85662792	-3.25487008
F	5.23103360	2.64832539	-0.90502682
N	1.34704032	0.00714063	-2.09130732
C	0.29030163	-0.00644065	-2.91361447
O	-0.93459762	-0.02944931	-2.70583428
N	0.76876512	0.00900086	-4.25994372
C	0.07226638	-0.00356394	-5.43443650
C	0.80287983	0.01574790	-6.64606848
C	0.14842530	0.00182936	-7.86776469
C	-1.24561714	-0.03043090	-7.95405551
C	-1.95728082	-0.04807852	-6.75794459
C	-1.33554322	-0.03546598	-5.51242172
C	0.92914139	0.02320898	-9.14958855
C	-3.46060976	-0.08427617	-6.77695310
F	0.63008632	1.10976857	-9.90967905
F	0.65887502	-1.05838060	-9.92776501
F	2.26726488	0.03933645	-8.96195582
F	-3.95324055	-1.18685017	-6.16047956
F	-3.97079106	-0.08601858	-8.03367174
F	-4.00611549	0.98169445	-6.14161023
H	-0.93880476	-0.00081015	-0.54650315
H	-0.96300224	0.00030627	1.92547357
H	1.15065993	-0.00036709	3.23721720
H	3.62597492	-0.00657847	3.25547126
H	5.80341788	0.00193118	2.03500701
H	3.66912037	-0.01851694	-1.72031860
H	1.89211420	0.04194930	-6.61667949
H	-1.74979659	-0.04107827	-8.91694501
H	-1.90328159	-0.04966276	-4.58524930
H	1.77729933	0.02943016	-4.30900061

4.7 Calculations at the B3LYP(GD3-BJ)/6-311++G(d,p) level

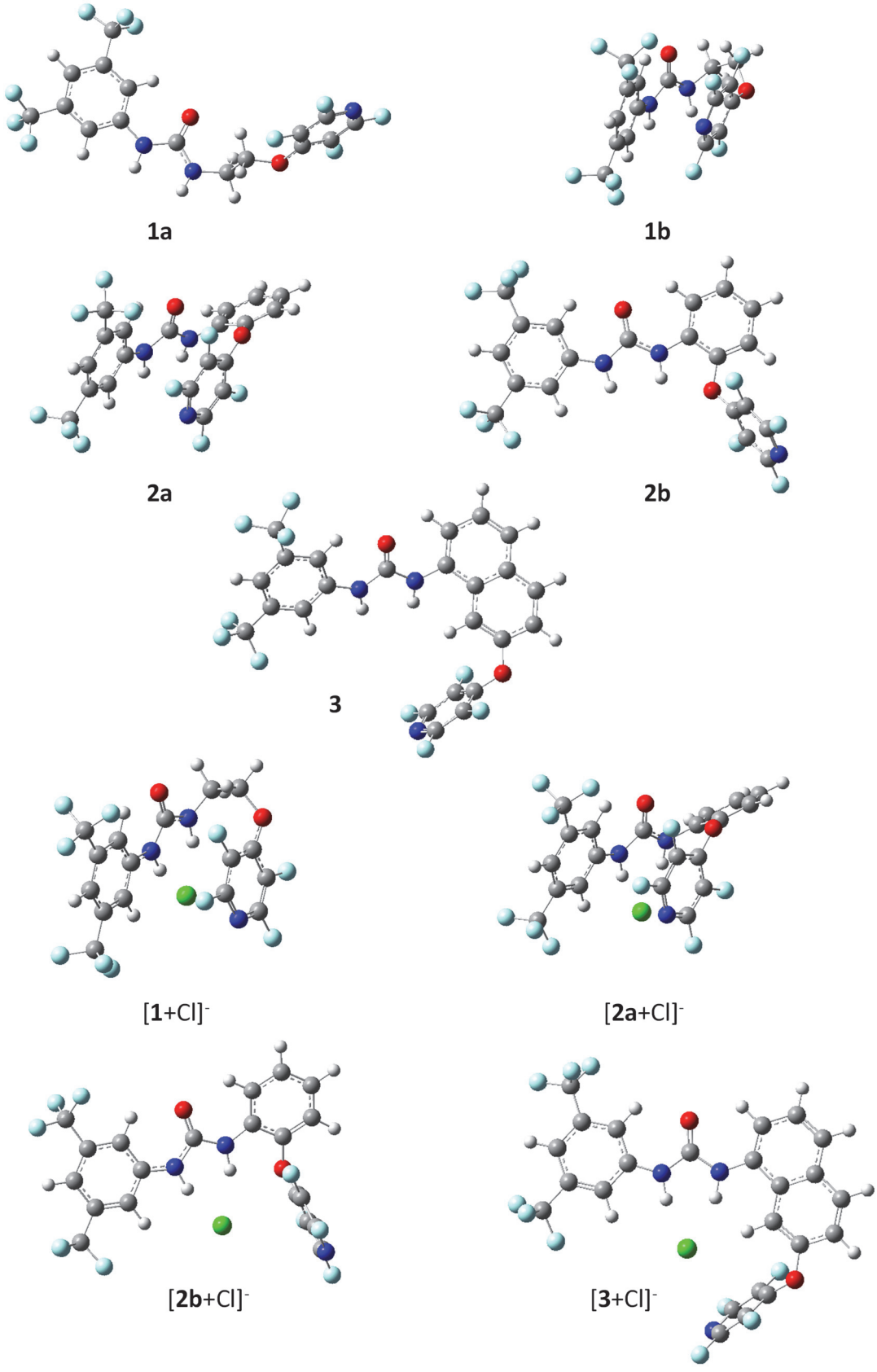

Figure S26 Structure of neutral receptors and associated complexes obtained at the B3LYP(GD3-BJ)/6-311++G(d,p) level.

Table S4 Computational data associated with the structures studied, obtained at the B3LYP(GD3-BJ)/ 6-311++G(d,p) level

Structure	E+ZPE (Hartree)	ΔE (kJ mol^{-1})	H°$_{298}$ (Hartree)	ΔH°$_{298}$ (kJ mol^{-1})	G°$_{298}$ (Hartree)	ΔG°$_{298}$ (kJ mol^{-1})
Neutral receptors						
1a	-1928.655927	+25.7	-1928.626797	+28.3	-1928.723393	+11.7
1b	-1928.665706	0	-1928.637565	0	-1928.727840	0
2a	-2081.110947	0	-2081.080154	0	-2081.177399	+9.3
2b	-2081.110656	+0.8	-2081.079656	+1.3	-2081.180959	0
3	-2234.756364	–	-2234.722578	–	-2234.830076	–
[receptor+Cl]$^-$ complexes						
[**1**+Cl]$^-$	-2389.043203	–	-2389.013008	–	-2389.110807	–
[**2a**+Cl]$^-$	-2541.493089	+12.0	-2541.460784	+11.4	-2541.561744	+18.9
[**2b**+Cl]$^-$	-2541.497673	0	-2541.465115	0	-2541.568929	0
[**3**+Cl]$^-$	-2695.151672	–	-2695.116445	–	-2695.226086	–

Table S5 Interaction energies calculation at the B3LYP(GD3-BJ)/6-311++G(d,p) level (ZPE correction included)

	$E_{complex}$ (Hartree)	E_{ligand} (Hartree)	E_{Cl^-} (Hartree)	$E_{int.}$ (kJ/mol)
[**1**+Cl]$^-$	-2389.043203	-1928.665706	-460.303727	-193.7
[**2a**+Cl]$^-$	-2541.493089	-2081.110947	-460.303727	-205.8
[**2b**+Cl]$^-$	-2541.497673	-2081.110656	-460.303727	-218.7
[**3**+Cl]$^-$	-2695.151672	-2234.756364	-460.303727	-243.1

$$\Delta E_{int,vacuum} = E_{complex,vacuum} - E_{ligand,vacuum} - E_{ion,vacuum}$$

5. Bibliography

[1] H. E. Gottlieb, V. Kotlyar, A. Nudelman, *J. Org. Chem.* **1997**, *62*, 7512–7515.
[2] J. Contreras-García, E. R. Johnson, S. Keinan, R. Chaudret, J.-P. Piquemal, D. N. Beratan, W. Yang, *J. Chem. Theory Comput.* **2011**, *7*, 625–632.
[3] H. S. Rzepa, Script for creating an NCI surface as a JVXL compressed file from a (Gaussian) cube of total electron density
[4] E. F. Pettersen, T. D. Goddard, C. C. Huang, G. S. Couch, D. M. Greenblatt, E. C. Meng, T. E. Ferrin, *J. Comput. Chem.* **2004**, *25*, 1605–1612.
[5] R. Plais, G. Gouarin, A. Gaucher, V. Haldys, A. Brosseau, G. Clavier, J. Salpin, D. Prim, *ChemPhysChem* **2020**, *21*, 1249–1257.